INHIBITION OF GLI1 AND GLI2 AS A TARGETED THERAPY FOR BLADDER CANCER

by

PETER ANDREW RAVEN

B.Sc., The University of British Columbia, 2002
M.Sc., The University of British Columbia, 2006

A DISSERTATION SUBMITTED IN PARTIAL FULFILLMENT OF
THE REQUIREMENTS FOR THE DEGREE OF

DOCTOR OF PHILOSOPHY

in

THE FACULTY OF GRADUATE AND POSTDOCTORAL STUDIES

(Experimental Medicine)

THE UNIVERSITY OF BRITISH COLUMBIA

(Vancouver)

June 2018

The following individuals certify that they have read, and recommend to the Faculty of Graduate and Postdoctoral Studies for acceptance, the dissertation entitled:

Inhibition of Gli1 and Gli2 as a targeted therapy for bladder cancer

submitted by Peter Raven in partial fulfillment of the requirements for

the degree of Doctor of Philosophy

in Experimental Medicine

Examining Committee:

Alan So, Experimental Medicine
Co-supervisor

Michael Cox, Experimental Medicine
Co-supervisor

Christopher Ong, Experimental Medicine
Supervisory Committee Member

Marcel Bally, Interdisciplinary Oncology
University Examiner

Yuzhuo Wang, Interdisciplinary Oncology
University Examiner

Additional Supervisory Committee Members:

Ralph Buttyan, Experimental Medicine
Supervisory Committee Member

Abstract

The sonic hedgehog (SHH) signaling pathway has been shown to play an integral role in the maintenance and progression of bladder cancer (BCa). Smoothened inhibitors are currently used in the clinic for treatment of some skin cancers, however they have not been evaluated in BCa and SHH inhibition may be an efficacious strategy for BCa treatment. I assessed an in-house human BCa tissue microarray comprising non-invasive, invasive and lymph node metastasized transitional cell carcinoma and found that the transcription factors downstream of SHH, Gli1 and Gli2, were increased in more aggressive tumors. A panel of BCa cell lines show that two invasive lines, UM-UC-3 and 253J-BV, both express these transcription factors but differ in other parameters in the SHH pathway. UM-UC-3 produces greater quantities of SHH ligand, is less responsive in viability to pathway stimulation by recombinant human SHH or SAG, and less responsive to inhibition by a variety of molecules including the Smoothened inhibitors cyclopamine and SANT-1. 253J-BV, on the other hand, was highly responsive to these manipulations and appears more representative of canonical SHH signaling while UM-UC-3 resembles non-canonical autocrine signaling. To overcome this variability I utilized a Gli1 and Gli2 antisense oligonucleotide (ASO) to bypass pathway mechanics and target the transcription factors directly. UM-UC-3 decreased in viability due to both ASOs but 253J-BV was only affected by Gli2 ASO. IC50s were in the nanomolar range. To evaluate *in vivo* efficacy I developed a murine intravesical orthotopic human bladder cancer (mio-hBC) model for the establishment of non-invasive urothelial cell carcinomas. In this model I pre-treat the bladder with poly-L-lysine for 15 minutes, followed by intravesical instillation of luciferase–transfected human UM-UC-3 cells. Cancer cells are quantified by bioluminescent imaging. Tumors grew to 541.6±0.75 fold (Mean±SE) initial size after 40 days and were confirmed to reflect patient samples by a response to mitomycin C. Treatment of these tumors with Gli2 ASO resulted in decreased tumor size, growth rate and Gli2 mRNA and protein expression. These results validate this model and support the conclusion that Gli2 ASO may be a promising new targeted therapy for BCa.

Lay Summary

Bladder cancer progression has been linked to a signaling pathway, sonic hedgehog, normally involved in embryo development. Drugs to inhibit this pathway are effective in skin cancer but have not been tested in bladder cancers. I analyzed patient tumors and found that markers for active sonic hedgehog signaling, Gli1 and Gli2, are increased in aggressive tumors. Using two invasive bladder cancer cell lines, UM-UC-3, 253J-BV I found that these cells use SHH to grow but UM-UC-3 is difficult to inhibit using currents drugs while 253J-BV responds to drug treatment similar to skin cancer. Therefore, I tested a new therapy, an antisense oligonucleotide (ASO) that targets the Gli1 and Gli2 proteins. Gli2 ASO was effective at treating both cell lines. I developed a mouse model for bladder cancer and found that Gli2 ASO reduce tumor size here as well. This therapy may be a promising new treatment for bladder cancer.

Preface

This thesis was written by me with extensive review by my committee, Dr. Alan So, Dr. Michael Cox, and Dr. Claudia Chavez-Munoz.

Chapter 1. This chapter contains a table (Table 1.1) reproduced from Rimkus et al. [1] with additions by me.

Chapter 2 and 3. Bladder cancer tissue microarrays (TMAs) were compiled from patients at the Urology Clinic at Vancouver General Hospital under Consent Version 9.3 as part of the GU Biobanking protocol of The University of British Columbia by Dr. Peter Black and Dr. Alan So. All experiments were designed by me and Dr. Alan So and performed by me and the co-op student Summer Lysakowski under my direct supervision. The antisense oligonucleotides were provided by Ionis Pharmaceuticals Inc. (Carlsbad, CA, USA). The results have been prepared and have been reviewed by the legal team at Ionis Pharmaceuticals. These chapters will be submitted by me as a manuscript entitled "Inhibition of Gli1 and Gli2 with antisense-oligonucleotides: A novel therapy for the treatment of bladder cancer".

Chapter 4. All animal procedures were performed according to the guidelines of the Canadian Council on Animal Care (CCAC). The protocol was approved by the Animal Care Committee of the University of British Columbia (Protocol No. A15-0073). Experiments were designed by me and Dr. Alan So and were performed by me and Dr. Igor Moskalev. Dr. Yoshi Matsui instilled tumor cells and measured tumors in the growth curves in Figure 4.8. The instillation procedure is a modified form of the one developed in the Vancouver Prostate Centre by Hadaschik et al. [2]. These results have been submitted by me as a manuscript entitled "Development of a next generation murine intravesical orthotropic human bladder cancer (mio-hBC) model" and is currently under revision.

Table of Contents

Abstract ... iii
Lay Summary ... iv
Preface ... v
Table of Contents ... vi
List of Tables ... ix
List of Figures ... x
List of Abbreviations ... xi
Acknowledgements ... xvi
Dedication ... xvii
Chapter 1: Introduction ... 1
1.1 Bladder cancer ... 1
1.2 Diagnosis ... 10
1.3 Treatment ... 10
1.4 SHH in development ... 13
1.5 SHH mechanism ... 15
1.6 SHH signaling in cancer ... 20
1.7 Inhibition of SHH signaling ... 22
1.8 SHH in bladder cancer ... 25
1.9 Hypotheses and objectives ... 27
Chapter 2: Assessment of Gli1 and Gli2 activation in bladder cancer ... 30
2.1 Introduction ... 30
2.2 Materials and methods ... 31
2.2.1 Cell lines ... *31*
2.2.2 Assessment of secreted sonic hedgehog protein ... *32*
2.2.3 Western blot ... *33*
2.2.4 Tissue microarray ... *34*
2.2.5 Immunofluorescent staining ... *35*
2.2.6 Viability and invasion assays ... *36*
2.2.7 Drug treatment ... *37*
2.2.8 Gli2 plasmid transfection ... *37*

2.2.9 Statistical analysis *38*

2.3 Results 39

2.3.1 SHH pathway activity is highly variable between cell lines *39*
2.3.2 253J-BV but not UM-UC-3 respond to SHH ligand and smoothened agonist. *45*
2.3.3 Direct over-expression of Gli2 did not affect cell viability *49*

2.4 Discussion 49

2.5 Conclusion *55*

Chapter 3: Inhibition of Gli1 and Gli2 by antisense oligonucleotides to treat bladder cancer 57

3.1 Introduction 57

3.2 Materials and methods 58

3.2.1 Cell culture *58*
3.2.2 Western blot *58*
3.2.3 Drug treatment *59*
3.2.4 Viability and cell cycle analysis *60*
3.2.5 Statistical Analysis *61*

3.3 Results 61

3.3.1 UM-UC-3 cells are resistant to pathway inhibition *61*
3.3.2 SHH ligand inhibition is not an effective treatment strategy *62*
3.3.3 Smoothened inhibition is largely effective in 253J-BV but not UM-UC-3. ..... *67*
3.3.4 Gli antisense oligonucleotide at low concentration effectively inhibits both cell lines *69*

3.4 Discussion 73

3.5 Conclusion 78

Chapter 4: Development of a murine intravesical orthotropic human bladder cancer (mio-hBC) model 80

4.1 Introduction 80

4.2 Materials and methods 82

4.2.1 Animals *82*
4.2.2 Cell culture *85*
4.2.3 Luciferase transfection of bladder cancer cell lines *85*
4.2.4 Animal drug treatment *86*
4.2.5 Tumor imaging *87*
4.2.6 Tissue harvesting *87*
4.2.7 Immunohistochemistry *88*
4.2.8 In vivo assessment of Gli ASOs *89*
4.2.9 Quantitative PCR *90*

4.2.10 Statistical analysis *91*
4.2.11 Experimental design *91*
4.3 Results 93
4.3.1 Luciferase transfected bladder cell lines showed linear luminesce with cell number *93*
4.3.2 UM-UC-3-luc tumors grow quickly with poly-L-lysine pretreatment *93*
4.3.3 Tumor gross appearance by ultrasound corroborates bioluminescent activity *97*
4.3.4 This bladder tumor model recapitulates patient tumors *99*
4.3.5 Most bladder cancer cell lines had insufficient tumor growth when intravesically instilled in mice *102*
4.3.6 Gli2 ASO reduced tumor growth in vivo *105*
4.4 Discussion 108
4.5 Conclusion 115
Chapter 5: General discussion and conclusions 117
5.1 Rationale 117
5.2 SHH pathway variability 118
5.3 Inhibition 121
5.4 Animal model 122
5.5 Limitations and future directions 125
5.5.1 SHH function in bladder cancer *125*
5.5.2 SHH inhibition *130*
5.5.3 Genetic variability *132*
5.5.4 mio-hBC model *133*
5.6 Conclusion 134
Bibliography 136

List of Tables

Table 1.1. Sonic hedgehog pathway inhibitors and targets ……..…23
Table 4.1. Tumor engraftment using poly-L-lysine pre-treatment ……...…97

List of Figures

Figure 1.1. Structure of the bladder……..….3
Figure 1.2. Bladder tumor stages……..….6
Figure 1.3. General schematic of the sonic hedgehog pathway ……...…17
Figure 2.1. SHH is active in patient samples and UC cell lines ……...…41
Figure 2.2. Primary cilia are only found in UM-UC-3 cells ……...….43
Figure 2.3. Only 253J-BV responds to SHH ligand ……...…46
Figure 2.4. Smoothened activation has larger effect on 253J-BV cells ……..…48
Figure 2.5. Overexpression of Gli2 did not increase cell viability …….....50
Figure 3.1. SHH pathway was targeted at a variety of locations…….63
Figure 3.2. SHH pathway inhibition by a panel of small molecule inhibitors ……...64
Figure 3.3. SHH ligand inhibition has a small effect on UC cells ……...66
Figure 3.4. Smoothened inhibition was much more effective in 253J-BV cells ……...68
Figure 3.5. Gli2 ASO reduces viability and increases apoptosis in both UC cell lines ….71
Figure 3.6. Gli2 ASO blocks upstream SHH pathway inhibition ……...74
Figure 4.1. Schematic of the murine intravesical orthotopic human bladder cancer (mio-hBC) model ……...…83
Figure 4.2. Cell Luminescence is linear with cell number ……94
Figure 4.3. Poly-L-lysine pre-treatment resulted in larger and more consistent tumor growth ……...…96
Figure 4.4. Growth in UM-UC-3-luc tumors visualized by bioluminescent imaging and small animal ultrasound ……..…98
Figure 4.5. Hematoxylin and eosin (H&E) staining of normal mouse bladder and bladder containing UM-UC-3-luc tumors ……...…….100
Figure 4.6. UM-UC-3-luc tumors respond to intravesical mitomycin C ……...…101
Figure 4.7. Histology of mitomycin C treated tumors ……...…103
Figure 4.8. Many bladder cancer cell lines were unsuitable for an intravesical model ...104
Figure 4.9. Gli2 ASO reduces tumor growth *in vivo* ……107
Figure 5.1. BCa cell lines respond in growth to GANT-61 and HPI-1……..…129

List of Abbreviations

ABC - Adenosine triphosphate binding cassette

ADH7 - Alcohol dehydrogenase 7

AKT - AKT serine/threonine kinase 1, Protein kinase B

ANOVA - Analysis of variance

ASO - Antisense oligonucleotide

AUA - American Urological Association

BBN - N-butyl-N-(4-hydroxybutyl) nitrosamine

BCa - Bladder cancer

BCG - Bacillus Calmette-Guérin

BCL2 - B-cell lymphoma 2

BMI1 - B lymphoma Mo-Murine leukemia virus insertion region 1 homolog (mouse)

BMP4 - Bone morphogenetic protein 4

BOC - Brother of CDO

BOK - BCL2 family apoptosis regulator

BrdU - 5-bromo-2'-deoxyuridine

CAM - Calcium/calmodulin dependent

Cas9 - CRISPR-associated protein-9 nuclease

CDK - Cyclin dependent kinase

CDKN2A - Cyclin dependent kinase inhibitor 2A

CDO - CAM-related/downregulated by oncogenes

CIS - Carcinoma *in situ*

CRISPR - Clustered regularly interspaced short palindromic repeats

CSC - Cancer stem cell

CUA - Canadian Urological Association

DAB - 3,3'-Diaminobenzidine

DAPI - 4',6-diamidino-2-phenylindole

Dbx - Developing brain homeobox

DHH - Desert hedgehog

DMSO - Dimethyl sulfoxide

DNA - Deoxyribonucleic acid

DRAL - Down-regulated in rhabdomyosarcoma LIM protein

Dyrk1 - Dual specificity tyrosine phosphorylation regulated kinase 1

EGFR - Epidermal growth factor receptor

EORTC - European Organization for Research and Treatment of Cancer

FDA - Food and drug administration

FGFR3 - Fibroblast growth factor receptor 3

ELISA - Enzyme-linked immunosorbent assay

EMT - Epithelial-mesenchymal transition

EPHA7 - Ephrin receptor A7

EtOH - Ethanol

FITC - Fluorescein isothiocyanate

FOXM1 - Forkhead box M1

GAPDH - Glyceraldehyde-3-phosphate dehydrogenase

GAS1 - Growth arrest specific 1

Gli - Glioma-associated oncogene family zinc finger

GSK3β - Glycogen synthase kinase 3 beta

H&E - Hematoxylin and eosin

H19 - Imprinted maternally expressed transcript

HEPES - 4-(2-hydroxyethyl)-1-piperazineethanesulfonic acid

HER2 - Human epidermal growth factor receptor 2

HH - Hedgehog

HIP - Hedgehog interacting protein

HRP - Horse radish peroxidase

IC_{50} - Half maximal inhibitory concentration

IGF - Insulin-like growth factor

IHH - Indian hedgehog

Irx - Iroquois homeobox

Ki67 - Antigen identified by monoclonal antibody Ki-67

Kif7 - Kinesin family member 7

K-ras - Kirsten rat sarcoma viral oncogene homolog

MIBC - Muscle invasive bladder cancer

mio-hBC - Murine intravesical orthotopic human bladder cancer

MLH2 - MutL (E. coli) homolog 2 (cancer, nonpolyposis type 2)

mRNA - Messenger ribonucleic acid

MSH2 - MutS (E. coli) homolog 2 (colon cancer, nonpolyposis type 1)

MSH9 - MutS protein homolog 6

mTOR - mechanistic target of rapamycin kinase

MTS - 3-(4,5-dimethylthiazol-2-yl)-5-(3-carboxymethoxyphenyl)-2-(4-sulfophenyl)-2H-tetrazolium

MTSS1 - Metastasis suppressor 1

MYC - V-myc avian myelocytomatosis viral oncogene homolog

Myod/Myf - Myogenic differentiation

N-cad - Cadherin 2, type 1, N-cadherin, neuronal-cadherin

Nanog - Nanog homeobox

Nkx - Homeobox gene Nkx

NMDA - N-Nitrosodimethylamine

NMIBC - Non-muscle invasive bladder cancer

OSF2 - Osteoblast specific transcription factor 2

p53 - Tumor protein p53

PARP - Poly(ADP-ribose) polymerase

Pax - Paired box protein

PBS - Phosphate buffered saline

PCR - Polymerase chain reaction

PD1 - Programmed cell death 1

PD-L1 - Programmed death-ligand 1

PDX - Patient derived xenograft

PI3K - Phosphatidylinositol-4,5-bisphosphate 3-kinase catalytic subunit delta

PKA - Protein kinase A

PKC-α - Protein kinase C alpha

PMS2 - Postmeiotic segregation increased 1 homolog 2, mismatch repair system component

PTCH - Patched

PTEN - Phosphatase and tensin homolog

PTHR1 - Parathyroid hormone 1 receptor

qPCR - Quantitative polymerase chain reaction

RAC1 - Ras-related C3 botulinum toxin substrate 1

RB - Retinoblastoma

Ren - Renin

RHOA - Ras homolog family member A

rhSHH - recombinant human sonic hedgehog

RIPA - Radioimmunoprecipitation assay

RNA – Ribonucleic acid

RPMI - Roswell Park Memorial Institute

SAG - Smoothened agonist

SCC - Squamous cell carcinoma

SCID - Severe combined immunodeficiency

SCR - Scrambled sequence nucleotide

SDS-PAGE - Sodium dodecyl sulfate–polyacrylamide gel electrophoresis

SHH - Sonic hedgehog

SHHat - Sonic hedgehog acyltransferase

siRNA – Short interfering RNA

Smad - Mothers against decapentaplegic homolog 1

SMO - Smoothened

Sox 2 - Sex determining region Y box 2

SPP1 - Secreted phosphoprotein 1

SUFU - Suppressor of fused

TBST - Tris-buffered saline plus tween

TCC - Transitional cell carcinoma

TGF-β - Transforming growth factor beta

TMB - Tetramethylbenzidine

TSC1 - Tuberous sclerosis complex subunit 1

Tunel - Terminal deoxynucleotidyl transferase dUTP nick end labeling

TUR - Transurethral resection

TURBT - Transurethral resection of bladder tumor

UC - Urothelial carcinoma

VEGF - Vascular endothelial growth factor

Wnt - Wingless-type mouse mammary tumor virus integration site

Zeb - Zinc finger E-box binding homeobox

Acknowledgements

I would like to thank my supervisor Dr. Alan So for his learned guidance, critical feedback and tireless support throughout my degree. I would also like to thank my co-supervisor Dr. Michael Cox for always being available to guide me through the complexities of completing a PhD and for pushing me to excel. Thank you to Dr. Claudia Chavez-Munoz for ensuring that my work is thorough, well written and scientifically sound. A special thanks to my committee members, Dr. Ralph Buttyan and Dr. Christopher Ong for their esteemed input and critical analysis. I would like to thank the co-op student Summer Lysakowski without whose impressive molecular biology skills I would not have been able to acquire as much of the high quality data presented here. Thank you to Dr. Igor Moskalev for his tutelage and mentorship in everything relating to animal studies. My thanks to the Canadian Institute of Health Research and Vancouver Prostate Centre for funding this project. I would also like to thank the Experimental Medicine Program, Department of Urology, The University of British Columbia and the Vancouver Prostate Centre for affording me this opportunity and for contributing to my success. A very special thanks to my wife Anna, son Max and family and friends for enduring my long journey to becoming a doctor of philosophy.

Dedication

To my wife Anna and my son Max for supporting me throughout my studies.

Chapter 1: Introduction

The cell signaling pathway, sonic hedgehog, plays a fundamental role in many malignancies and is essential for embryogenesis and possibly tumorigenesis. Current treatments for bladder cancer do not specifically target tumor cells and thus can result in significant side effects. Bladder cancer also offers a unique opportunity to treat tumors directly by intravesical instillation without exposure to surrounding tissues or off-target organs as is the case in systemic therapy. Hence, there is a strong need for a more specific, targeted intravesical therapy for urothelial carcinoma. Therefore, I hypothesize that sonic hedgehog pathway activation, specifically activation of the transcription factors Gli1 and Gli2, is responsible for growth and progression of bladder cancer, and as such can be inhibited by a targeted therapy. The following introduction will outline the background and rational for this project and provide the basis for this hypothesis.

1.1 Bladder cancer

Bladder cancer (BCa) affects 1 in 27 men (3.8%) and 1 in 84 women (1.2%) in Canada and has the 8th highest mortality rate [3]. Worldwide it is the 6th most common malignancy [4]. BCa is initially diagnosed at many stages and appears as a non-invasive tumor on the surface of the bladder lumen in 70% of cases, as an invasive tumor that has grown into the muscular section of the bladder wall in 30% of cases with associated metastatic disease in 7% of cases [5]. Of the non-invasive tumors, clinically termed non-muscle invasive bladder cancer (NMIBC), 80% will recur following treatment such as tumor resection and 20-30% of these tumors will advance to an invasive phenotype (termed muscle–invasive bladder

cancer; MIBC). Invasive disease has the potential for metastases and need for radical therapies such as radical cystectomy or chemo-radiation. In addition to the risk this disease poses, a substantial cost is associated with the treatment of BCa. Data from 2001 in the United States shows a single patient can cost $96,000-$187,000 from diagnosis through follow up [6]. BCa is the fifth most costly form of cancer in the United States with $3,700,000,000 spent on treatment each year and is the most costly form of cancer worldwide [4]. Calculations of the cost of each type of treatment are still underway [7]. Given the impact of this disease and the high cost of current treatments new therapies are desperately needed.

In order to understand the natural history of BCa progression it is necessary to understand the tissue structure of the bladder (Figure 1.1). The bladder is a muscular reservoir situated behind the pubic symphysis from which it is separated by perivesical fatty tissue. Two ureters enter the underside of the bladder at the interureteric bar at the top of the trigone, a triangular region above and behind the urethral opening. Internally, a layer of epithelium, called mucosa, is loosely attached to underlying muscularis propria except in the region of the trigone in which it is tightly attached and smooth [8]. This allows the mucosa to expand laterally during bladder filling and fold during emptying. Directly interior to the muscle is a layer of stromal cells consisting of fibroblasts and extracellular matrix, on top of which is the lamina propria separating the mucosa, otherwise known as urothelium, from the stroma. Interior to the lamina propria is the first cell layer of the urothelium, the basal cells, which are responsible for cell proliferation and maintenance of the other urothelial cells. Epithelial stem cells reside in the basal layer and are responsible for the continued

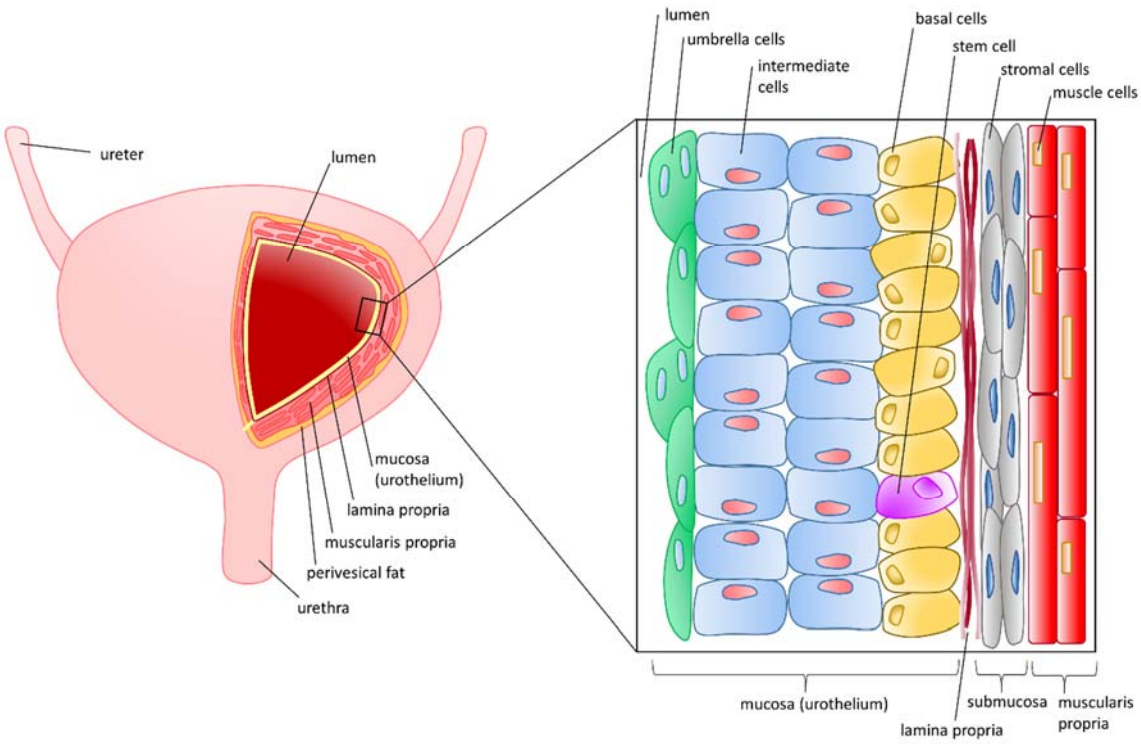

Figure 1.1. Structure of the bladder. Starting at the lumen and moving outward through the bladder wall, the urothelium consists of three cell layers; umbrella cells, intermediate transient amplifying cells and basal cells. Stem cells responsible for regenerating the urothelium are found in the basal cell layer. The lamina propria underlies the basal cell layer and separates the urothelium from stromal and muscle cells underneath.

replacement of the urothelium [9]. They give rise to a series of intermediate, transient amplifying cells, with limited proliferative ability. Facing the lumen are the tightly bound, poly-nucleate, umbrella cells responsible for preventing urine solutes from diffusing into the blood [9].

BCa arises from various cellular origins and exhibits differing phenotypes as a result [10]. These include squamous cell carcinoma, adenocarcinoma, small cell carcinoma and sarcoma or rhabdomyosarcoma. Most commonly (approximately 90%) BCa is transitional cell carcinoma (TCC), also known as urothelial cancer (UC) [11]. Within TCC there are both non-invasive and invasive stages and two different growth patterns, papillary and the flat growing carcinoma *in situ* (CIS). In addition, tumors are graded as low or high dependent on the degree of cellular differentiation and the likelihood of a tumor to progress. Low grade papillary or non-invasive tumors grow into the lumen from the urothelium and rarely progress to penetrate the lamina propria. Conversely, high grade tumors may progress to grow into an invasive phenotype to penetrate the lamina propria and enter the muscle layer of the bladder.

The degree to which TCC has invaded and its grade is determined after resection through a transurethral approach using an instrument called a resectoscope. After the tumor is resected, the pathologic stage is assessed: no tumor (T0), carcinoma *in situ* (Tis), tumor in the urothelium (Ta), invasion of the stroma (T1), invasion of the muscle (T2), invasion of the perivesicular fat (T3a), invasion through the bladder wall (T3b) and invasion of nearby

organs (T4). Tumor staging is often accompanied by lymph node staging to assess the presence of metastases (Figure 1.2).

Disease management is based on the classification of NMIBC as low or high risk using the European Organization for Research and Treatment of Cancer (EORTC) risk calculator [12]. High risk includes NMIBC with T1 tumors, high-grade tumors, CIS and multiple, recurrent and >3 cm tumors. High risk tumors have a 45% chance of progression within 5 years and so are managed with more radical treatment. When progression occurs or patients present with MIBC the European Association of Urology has developed guidelines to evaluate survival that combine patient age, activity level, the Charlson Comorbidity Index and other prognostic indicators such as tumor location and molecular markers (discussed later in this document; [13, 14]. In addition to the EORTC, there are other risk stratification systems for NMIBC that include the Canadian Urological Association (CUA) and the American Urological Association (AUA) systems. The AUA system, for example, utilizes a low, intermediate and high risk system with similar criteria as the EORTC system. By using any of these systems treatment is recommended that reflects the severity of risk (see section 1.3).

In order to improve the way patient disease is managed new classifications for risk of recurrence and progression have been pursued. Recently, BCa has been classified by gene signatures rather than pathological appearance. Biochemical analysis of invasive and non-invasive TCC tumors have found distinct pathway differences. Papillary NMIBC are in many cases characterized by aberrant fibroblast growth factor receptor 3 signaling, while

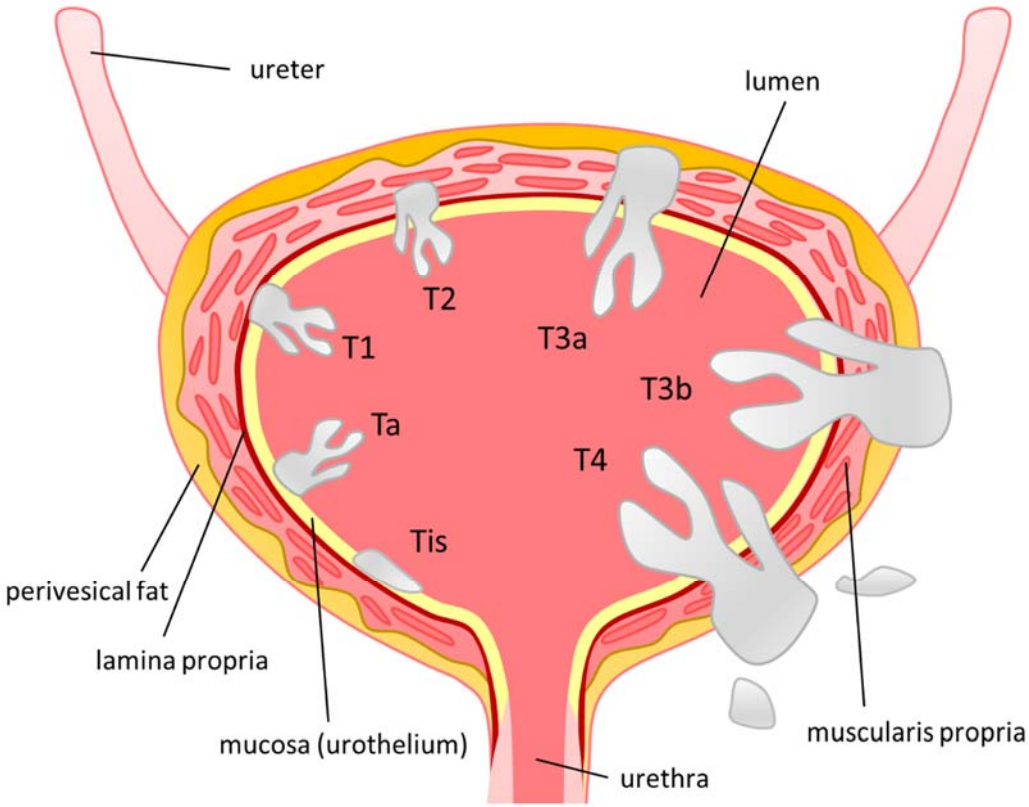

Figure 1.2. Bladder tumor stages. No tumor (T0), carcinoma *in situ* (Tis), tumor in the urothelium (Ta), invasion of the stroma (T1), invasion of the muscle (T2), invasion of the perivesicular fat (T3a), invasion through the bladder wall (T3b) and invasion of nearby organs (T4).

flat invasive tumors have mutations in p53, Pten, and Rb and growth mediated by accompanying stromal and inflammatory interactions [9].

A variety of institutions have attempted to classify BCa by mRNA expression or cell surface markers. In 2010 Lindgren et al. looked at gene expression and genomic mutations in three bladder data sets and distinguished two groups MS1 and MS2 with the dominant characteristic of MS2 being mutational instability [15]. They validated this profile using pathology data and were able to distinguish between muscle invasive and non-muscle invasive tumors. This study demonstrated that molecular typing may be useful in determining tumor characteristics and treatment regimes. Later stratifications further divided the MS1 and MS2 groups into SCC-like/Urobasal B, infiltrated Mesechymal, Genomivally Unstable, Urobasel, Infiltrated epithelial and variant [16, 17]. Volkmer et al. [18] analyzed a subset of markers from a set of BCa gene expression data sets and validated these markers by xenograft studies. They then applied their classifier to large sets of BCa patients from other groups. Three sub-types were identified according to differentiation, Basal, Intermediate, and Differentiated with the Basal subtype showing poor survival.

The Cancer Genome Atlas Research Network [19] has identified four clusters (I-IV) of BCa with differing gene expression patterns and gene mutations. Cluster I represented papillary type tumors with FGFR3 overexpression. Luminal breast and urothelial markers were identified in Clusters I and II. Cluster III had high epithelial gene expression and stem cell markers and these markers were low in Cluster IV. Choi et al. [20] used previously established breast cancer profiles to screen MIBC data sets. They found remarkable

similarity with breast cancer and 3 distinct groups, an aggressive basal group, a luminal group showing FGFR3 expression, and a drug resistant p53-like group (similar to p53 gene mutated cancers). In consensus with this classification are the basal and luminal subtypes identified by Damrauer et al. [21] from microarray datasets of high grade MIBC. In addition, Rebouissou et al. [22] using a panel of 40 genes were able to find a basal-like subset of bladder tumors displaying high epidermal growth factor receptor expression. This subset could be matched to BCa cell lines and toxin induced [N-butyl-N-(4-hydroxybutyl) nitrosamine or BBN] *in vivo* models. A meeting report of BCa taxonomy [23] has summarized these findings and found consensus in 4 cell markers for the basal type of BCa but a larger consensus on how the various studies and data sets align and what these classifications mean for diagnosis and treatment are still ongoing.

Geographically BCa rates vary by region. Incidence is highest in Northern Europe, Southern Europe, and North America [4] in comparison to other regions of the world. The incidence rate in the more developed world is more than twice that of the less developed world. The reasons for this difference are likely due to a greater prevalence the factors that will be discussed below.

Increased BCa incidence is related to internal factors associated with genetic mutations and gene deletions involved in BCa progression. For example, a family history of BCa increases the risk of acquiring BCa two-fold [24] and a history or hemolymphopoietic cancer can significantly increase BCa risk. Interestingly, a history of other cancers is not associated with a risk of BCa. This hereditary component may be due to inherited genetic

mutations such as in FGFR3 and genes that bioactivate and detoxify carcinogens [4]. People with Lynch Syndrome (mutations in mismatch repair genes MLH1, MSH2, MSH6 and PMS2) are also at a much higher risk of developing BCa [25]. Related to genetics, race has been postulated to be a risk factor for BCa with higher incidence, more severe tumor at presentation and reduced survival in African Americans [26].

External factors such as cigarette smoking and exposure to second hand smoke are linked to higher BCa cancer risk. Cigarette smoke creates b-naphthylamine and polycyclic aromatic hydrocarbons that are excreted by the kidneys and affect the urinary system. Tobacco varieties high in these carcinogens and smoke inhaled into the lungs rather than the mouth increase BCa risk. In addition, cessation of smoking after treatment can improve disease specific and overall survival [4, 27]. Occupational exposure to carcinogens such as arsenic, benzidine, 4-aminobiphenyl,2-naphthylamine, 4-chloro-o-toluidine, polycyclic aromatics, hydrocarbons, and chlorinated hydrocarbons is highly associated with BCa. These compounds are commonly found in dyes, paints, and metal and petroleum products. As such, risks have been associated with careers in printing and farming [4].

In addition to carcinogens, some medical treatments that result in cell damage such as radiation beam therapy for prostate cancer, cyclophosphamide for lymphoma and hypoglycemic medication for diabetes are also linked to increased risk of BCa [4]. Conversely, not receiving medical treatment for recurrent exposure to the parasitic trematode *Schistosoma mansoni* or *Schistosoma haematobium* can result in chronic inflammation and squamous cell carcinoma in the bladder [28].

1.2 Diagnosis

BCa is currently diagnosed with cystoscopy followed by histological analysis after transurethral resection of bladder tumor (TURBT) or biopsy. Imaging techniques such as positron emission technology, computerized tomography and magnetic resonance imaging can also be used to determine the size and location of tumors [29]. In addition, a variety of urinary markers have been developed for BCa prognosis that utilize the cell fraction of urine containing detached tumor cells or the cell-free fraction containing diagnostic proteins. One example is urine cytology which has become standard and has been reported to have high specificity but low sensitivity [29]. Other biomarker tests including BTA Stat, BTA Track, NMP22 BladderCheck, NMP22 Bladder cancer test and UroVysion have similar limitations and as such cystoscopy remains the gold standard.

1.3 Treatment

Upon detection of a bladder tumor by cystoscopy, TURBT is performed after which tissue is analyzed for tumor stage and grade [30]. Briefly, the tumor is scraped from the urothelium, removed through the urethra, and staged by a pathologist. Various protocols have been employed and evaluated for safety [30], mainly to prevent irrigation fluid from entering the bloodstream in the case of bladder perforation (TUR syndrome)[31]. In many case improvements in surgical technique and visualization systems result in better tumor excision and clinical outcomes [32]. Despite tumor resection, recurrences are approximately 80%.

To improve the efficacy of resection adjuvant intravesical instillation of Bacillus Calmette-Guerin (BCG) is performed. BCG refers to a variety of strains of *Mycobacterium bovis* that were attenuated to vaccinate against *Mycobacterium tuberculosis* [33]. The method of action is an induced immune response to BCG in the bladder that concomitantly kills tumor cells following a schedule of 5 or more weekly induction treatments with greater than 2 weekly maintenance treatments [34]. Different strains have been passaged in various institutions; meta-analysis has shown that BCG is more efficacious than chemotherapy at reducing recurrence potentially due to a prolonged immune response following treatment [33]. Unfortunately, some tumors are BCG unresponsive and have high recurrence rates following treatment [34]. In addition potentially significant side effects, including septic shock, can occur if a bladder perforation is present and BCG enters the bloodstream.

An alternative to BCG treatment is chemotherapy. There are a large variety of cytotoxic and cytostatic chemotherapy treatments including but not limited to mitomycin C, epirubicin, doxorubicin, cisplatin, gemcitabine, methotrexate, vinblastine, adriamycin, thiophosphoamide, bexidem, bropirimine and ofloxacin [33]. These treatments can be applied adjuvantly or neoadjuvantly, single or in combination, intravesically or systemically to reduce tumor recurrence [35]. Unfortunately, due to the pan effects of cytotoxic treatments side effects occur as non-target healthy cells are also affected. Once again, tumor recurrence is high despite chemotherapy.

In MIBC radical cystectomy is considered standard of care, comprising the removal of the bladder and prostate in men and the uterus, ovaries and anterior vagina in women. Radical cystectomy and lymph node removal results in a 5-year survival of 60% when the tumor has not exited the bladder but only 10-50% if it has invaded surrounding tissues [36]. Trimodal therapy, involving transurethral resection, chemotherapy and radiation is also another curative option for MIBC. However there are also side effects that follow, such as cystitis, hematuria, enterocolitis, proctitis, and stenosis.

A quickly growing field in cancer treatment is immune therapy. Although immunotherapy in the form of BCG had been in use in BCa treatment since 1976 [37], and other immune-stimulating treatments such as maltose tetrapalmitate are in use [33], an anti-PDL1 monoclonal antibody, atezolizumab, has recently shown a 15% response rate in metatastic BCa patients and is the first new treatment to be approved in over 20 years [38]. PDL1 on the tumor surface binds with PD1 on T-cells suppressing their anti-tumor activity. By inhibiting this interaction T-cells are more effective at destroying cancer cells. This treatment is an effective second line after the failure of chemotherapy in advanced disease. In addition to anti-PDL1 antibodies an anti-PD1 antibody, nivolumab, has been shown to be very effective and has been approved for advanced BCa [38, 39]. Anti-PDL1 and PD1 antibodies are not without risks, some side effects have been reported, including encephalitis, pericardial effusion and neuromuscular disorder [38, 40].

In response to the limited treatment options mentioned previously, many institutions are pursuing agents that target a specific chemical pathway unique to BCa. The advantage of

such a treatment is reduced side effects due to a decrease in off target effects as healthy cells will not be utilizing the target pathway to the same extent as the tumor. High mutational status and abundant gene dysregulation lends BCa to be targeted by these small molecules, or other pathway inhibitors [41]. In addition targeted therapies are often designed for patients who do not respond to chemotherapy or have become resistant to the DNA-damaging modality of chemotherapy function [42]. A recent review of targeting therapies by Aragon-Ching and Trump summarizes these most commonly targeted pathways and the current drugs available [43]. Angiogenesis through VEGF, FGFR, HER2 pathway, EGFR, TSC1, PI3K, RB and CDK function have been evaluated for effectiveness [43]. These drugs target BCa at non-invasive, invasive, and metastatic stages of progression. The utility of these treatments in combination with more traditional chemotherapy is a topic that is currently under investigation [35].

1.4 SHH in development

Hedgehog proteins and their functions have been the subject of a myriad of reviews over the past decade as the complexities of this pathway are slowly being clarified [1, 44-49]. This protein family was first identified in the fruit fly, *Drosophila melanogaster*, as a family of morphogens consisting of Sonic Hedgehog (SHH), Indian Hedgehog (IHH) and Desert Hedgehog (DHH) [50]. SHH was identified through knockout experiments in which bristle patterning was deregulated on the larval cuticle, resulting in a hedgehog appearance [51]. In mammals the three hedgehog ligands have differing functions. SHH is responsible for digit patterning in the limb bud, and floor plate patterning of the neural

tube above the notochord. IHH is responsible for primitive endoderm, bone and cartilage development and desert hedgehog for the development of germ cells and formation of nerve sheaths [44].

SHH has many essential roles in embryogenesis. Early in vertebrate development it is involved in left-right and dorsal-ventral patterning and in the zone of polarizing activity in the limb bud to direct digit differentiation [52]. SHH is later involved in the development of most epithelial tissues. Disruption of the SHH pathway leads to cyclopia, a condition with defects in neural tube patterning, limb malformation, missing ribs and aberrant lung branching, holoprosencephaly, and polydactyly in Pallister-Hall syndrome [51]. In more extreme cases, loss of function mutations in the hedgehog (HH) pathway mediator Smoothened (SMO) are embryologically lethal [53]. Developmental patterning is achieved through the formation of a SHH gradient in which SHH stimulates its own expression at the source and is regulated in its diffusion by lipid interactions and binding to cell surface proteins such as its receptor patched 1 (PTCH) and hedgehog interacting protein (HIP) [54]. In addition to concentration, time of exposure is vital for proper patterning [55]. This is controlled by the upregulation of PTCH in response to SHH stimulation to desensitize the cells and limit SHH exposure [56]. At a cellular level SHH stimulates cell growth, migration and invasion, and self-renewal through downstream targets of the Glis such as BMP4, FGF4 and VEGF, Myod/Myf, Pax, Nkx, Dbx, and Irx to name a few (reviewed by Varjosalo et al. [47]).

Analysis of SHH in bladder development has shown that SHH and other members of the SHH pathway: PTCH, Gli1, Gli 2 and Gli3 (see section 1.5), are essential for proper bladder mesenchymal differentiation [57]. At 14 days of mammalian embryonic growth (as studied in a mouse) the developing bladder is comprised of a SHH positive urothelium, a PTCH and Gli1 positive suburothelial inner mesenchyme, a Gli negative inner mesenchyme and a low PTCH, low Gli1 and high Gli3 expressing outer mesenchyme. Signaling from these layers maintains the SHH gradient and allows for the radial development of the bladder. In addition, detrusor smooth muscle development and regional designation of the lamina propria is determined by high levels of SHH expression [57]. Consistent with other embryologoical patterning, SHH is tightly controlled spatially and temporally for proper bladder development.

In an adult SHH is implicated in maintaining stem cell populations by promoting gene expression of MYC, Bcl2, cyclin D1, cyclin E, IGF2, BMI1, NANOG and Sox 2 [49, 58-61]. This maintenance occurs in granular cell precursors, neuron stem cells, retinal precursor cells, hair follicles, haemopoetic cells, and in regeneration of pancreas, prostate and bladder [62-64]. The role of stem cells in regenerating damaged tissue, especially epithelium, appears to be the major role of SHH after development [65].

1.5 SHH mechanism

In canonical signaling SHH protein is secreted and interacts with lipids in the extracellular space, which determine the ease and distance to which it will diffuse [44]. SHH binds to

the 12 transmembrane domain proteins, Patched 1 (PTCH) or Patched 2 at the base of the primary cilia, a non-motile flagellar organelle on the cell surface (Figure 1.2). Patched 1 (PTCH) is the primary regulator of the SHH pathway. In an unstimulated state, PTCH inhibits the G-coupled, 7 transmembrane domain, receptor protein SMO from translocating from endosomes to the cell surface through a yet unknown mechanism. This mechanism may be through at PTCH-controlled ligand influx or efflux (possibly oxysterols or vitamin D3) which directly binds and inhibits SMO [66, 67]. PTCH may process lyphophorin which in turn modifies the endosome to which SMO is bound and prevents trafficking to the cell surface. Alternatively, PTCH may maintain phosphatidylinositol-4-phosphate at a low level in the cell preventing SMO activation. Although the exact mechanism is unknown, the strength of SMO activation is related to the degree of phosphorylation required to separate the inactive SMO dimer prior to signal activation. How SHH might achieves this is unknown.

Upon Binding of SHH to PTCH, SMO inhibition is removed and SMO translocates up the primary cilia where it is responsible for the activation of the zinc finger transcription factors Gli1, Gli2 and Gli3 through binding the suppressor of fused homologue (SUFU) in the presence of Kif7 and the resulting phosphorylation of the Glis by GSK3B and PKA. Gli1 is a full length protein whose role is to feedback and enhance pathway activity by promoting transcription of PTCH1 and Gli1. Gli2 is the primary positive effector of the SHH pathway (truncated, processing turns on) and GLi3 the primary negative effector (truncated repressor, processing turns off). In the absence of SHH stimulation, Gli proteins are transported up the cilia and anchored by SUFU so that they remain in their repressor

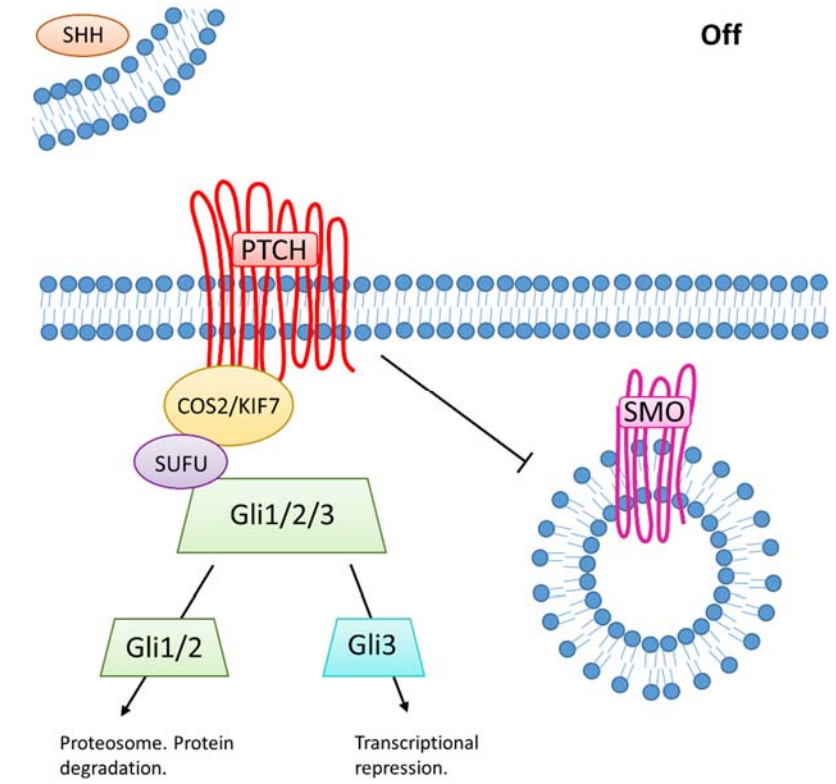
SHH
Off
PTCH
COS2/KIF7
SUFU
Gli1/2/3
SMO
Gli1/2
Gli3
Proteosome. Protein degradation.
Transcriptional repression.

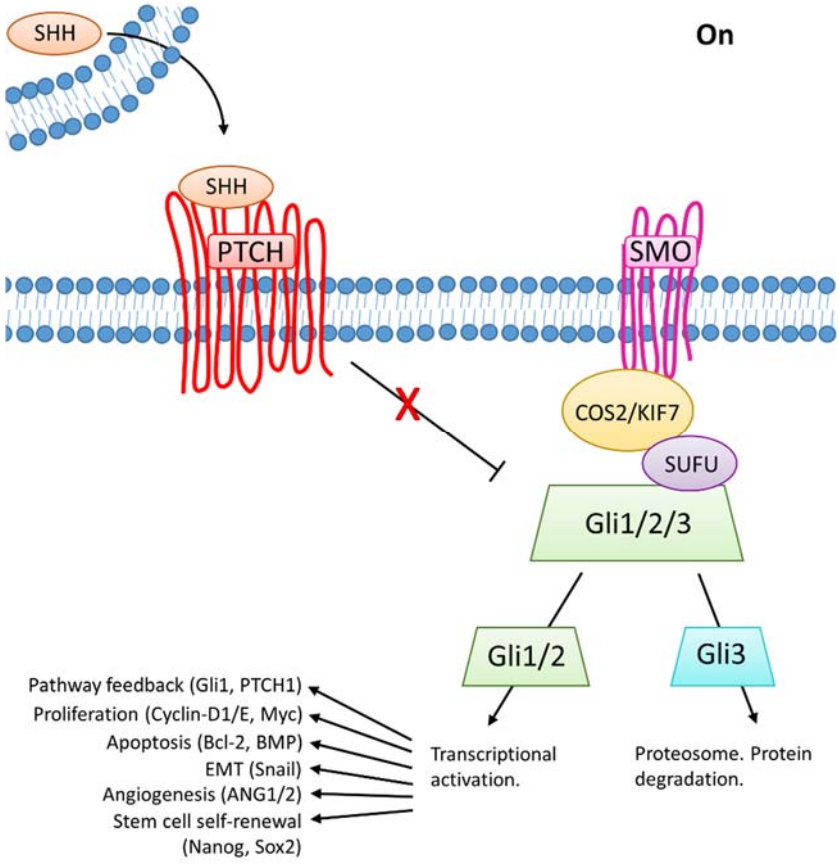
SHH
On
SHH
PTCH
SMO
COS2/KIF7
SUFU
Gli1/2/3
Gli1/2
Gli3
Pathway feedback (Gli1, PTCH1)
Proliferation (Cyclin-D1/E, Myc)
Apoptosis (Bcl-2, BMP)
EMT (Snail)
Angiogenesis (ANG1/2)
Stem cell self-renewal (Nanog, Sox2)
Transcriptional activation.
Proteosome. Protein degradation.

Figure 1.3. General schematic of the sonic hedgehog pathway. In the off state SHH is sequestered in neighboring cells and PTCH represses SMO, preventing it from relocating to the cell surface. As a result, the COS2-SUFU complex binds PTCH and Gli3 is processed into a transcriptional repressor form while Gli1 and 2 are shuttled to the proteome for degradation. Upon SHH ligand binding to PTCH, repression of SMO is alleviated and SMO translocates to the cell membrane. Here it now binds the COS2-SUFU complex and Gli1 and 2 are processed to the transcriptional activator forms while Gli3 is sent to the proteasome for degradation (Gli3 in some instances can act as a transcriptional activator). A wide variety of gene targets involved in cell survival and growth are activated as a result of SHH pathway activity. In canonical signaling this cascade is thought to occur in the primary cilium. PTCH – Patched, SMO – Smoothened, SUFU- Suppressor of Fused, Gli1/2/3 – Glioma-associated oncogene homologue 1/2/3.

forms [68]. Only a small fraction of the total cellular content of SHH pathway proteins is located in the primary cilium at a given time. As such it is still unknown if the cilia is required for SHH signaling [47].

It is important to note again the duality of the Gli transcription factors. All Glis have a c-terminal activating domain but only Gli2 and 3 have an n-terminal repressor domain. The state of SHH pathway stimulation determines the phosphorylation and thus proteolytic cleavage of the Glis into either the active or inactive form. Gli1 and Gli2 are the two main activators of the pathway and have different gene targets. As such Gli2 loss is embryonically lethal [69] but Gli1 loss is not [70]. In contrast to Gli1 and Gli2, Gli3 is primarily considered a repressor [71]. Gene expression downstream of these transcription factors can thus be controlled by either activation of Gli1 and Gli2 or by the removal of repression by Gli3 [44]. Overall, Glis have a wide array of target genes including the genes mentioned in the previous section regarding stem cell maintenance and FOXM1, IGF2, PTHR1, EPHA7, MTSS1, OSF2, H19, and SPP1 [5].

The canonical signaling described above can be modified by a wide array of proteins that interact with the SHH pathway. One way is through four co-receptors, CAM-related/downregulated by oncogenes (CDO), brother of CDO (BOC), hedgehog interacting protein (HIP) and growth arrest-specific 1 (GAS1). These bind PTCH in the presence of heparin and Ca^{2+} and promote HH signaling. In addition, other molecules such as glypicans, megalin and cyclin B1 can bind to PTCH and HH, and alter signaling [44, 72].

The SHH pathway also interacts with many other signaling pathways, some of which involve only specific components of SHH pathway. For example, signaling through the SHH pathway can result in cellular functions independent of a Gli transcriptional response, such as axonal guidance, fibroblast chemotaxis, and cell metabolism [44]. SMO can activate mTOR and SRC family kinases for axonal guidance [73], fibroblast chemotaxis utilizes SMO g-coupled protein activation of RHOA and RAC1 [74] and PTCH can induce apoptosis through DRAL and caspase 9 in the absence of SHH [75]. Regarding the Glis, transcriptional activity is regulated by many genes outside the SHH pathway including Ren, Dyrk1, K-Ras, TGF-β, PKC-α, p53, and PI3K-AKT [64, 76-80].

1.6 SHH signaling in cancer

SHH has been associated with a wide variety of cancer including basel cell carcinoma, medulloblastoma, rhabdomyosarcoma, glioma, and breast, esophageal, gastric, pancreatic, prostate, small cell lung, biliary tract, bladder and oral cancers (compiled by [47]). Three models have been proposed to describe the mechanism by which tumors respond to SHH. The type I model describes those tumors in which a mutation in the pathway is driving constitutive pathway activation. This group contains patients that are heterozygotes for PTCH and as a result develop Gorlin syndrome and associated basal cell carcinoma and medulloblastoma. Also in this group are similar cancers that are instead triggered by PTCH, SMO and SuFu mutations [81]. Type II is an autocrine model in which a cells rely on their own production of, and response to, SHH and thus require the endogenous pathway activation for their growth. Type II tumors are very common and constitute the majority of

the other cancers mentioned above. [82]. Type IIIa is a paracrine model that resembles canonical signaling in which a tumor cell secretes SHH to stimulate the release of growth factors from stromal cells. These cancers do not directly respond to blockade of the SHH pathway but rather to the drop in growth factors from the stroma when SHH is no longer produced [83]. Examples have been found in colon, pancreatic and ovarian cancer [84] where it is important to block SHH reception by the stroma before the concomitant release of growth factors such as IGF or Wnt. Type IIIb is a reverse paracrine model in which stromal cells support tumor growth by secreting SHH. Type IIIb tumors appear to be isolated to lymphoma, leukemia, multiple myeloma and glioma in which SHH simulation is required for its anti-apoptotic effect [82].

In addition to tumor growth SHH can have other associated effects on cancer cells. Due to the prominent role of SHH signaling in stem cell maintenance, evidence suggests that deregulation of SHH in cancer stem cells (CSCs) may promote cancer growth and progression [85, 86]. This was found to be the case in glioma, multiple myeloma, chronic myelogenous leukemia and breast colon and pancreatic cancer [82, 87, 88]. It has been suggested that CSCs are more resistant to drug toxicity and remain viable after most cells in a tumor have been destroyed. SHH has been shown to increase ABC transporters in stem cells to confer drug resistance [89, 90]. Given the importance of SHH in stem cell maintenance it has become a potential target for cancer therapy.

Another mechanism of treatment escape is the role of SHH in epithelial-mesenchymal transition (EMT). Epithelial cells are normally differentiated with contact inhibition and

limited motility and cancers derived from these cells would be expected to be similar. As a tumor progresses, cells undergo a transition to a more mesenchymal phenotype characterized by an increased ability to migrate and invade through cells and the lamina propria, lack of contact inhibition and lower differentiation status. This transition is thought to be necessary for tumor metastasis. SHH has been implicated in enabling this transition through a reduction of the epithelial markers E-cadherin and ZO-1 and increase in genes indicating mesenchymal transition, SNAIL [91, 92], Zeb, and N-cad [93]. This transition is also mediated through Gli1 activity in association with the PI3K-AKT pathway [78].

1.7 Inhibition of SHH signaling

The role of SHH in such a vast array of tumors has led to the pursuit of inhibitors to attenuate pathway function. Early natural compounds derived from the lily *Veratrum californicum* were isolated after reports of the developmental abnormality (cyclopia) in sheep consuming these plants [94]. Since that time many synthetic antagonists have been identified by small molecule drug screening, the majority of which target SMO upstream in the pathway. Two of these inhibitors GDC-0449 and LDE 225 are approved by the FDA for cancer treatment with others in clinical trials [95, 96]. Other popular targets are the Gli proteins themselves but these compounds have not been well tolerated *in vivo* due to difficulties of formulation and delivery. Only one, Arsenic trioxide, has entered clinical trials [97]. A comprehensible table of current inhibitors is found below and a recent review has summarized the findings to date [98].

Table 1.1: Sonic hedgehog pathway inhibitors and targets.

Compound	Trade Name	Target	Source	Notes	Reference	Clinical Trial
Cyclopamine		SMO	Lily, *Veratrum californicum*	Binds transmembrane region. Has side effects such as weight loss and death	(Cooper, Porter et al. 1998)	
KAAD-cyclopamine		SMO	Lily, *Veratrum californicum*	Modified form of cyclopamine that is 10 to 20-fold more potent with less toxicity	(Siegelin, Siegelin et al. 2009)	
Jevine		SMO	Lily, *Veratrum californicum*	Teratogenic side effects	(Cooper, Porter et al. 1998)	
GDC-0449	Vismodegib, Erivedge	SMO	Synthetic	SMO mutations after treatment confer resistance.	(Robarge, Brunton et al. 2009)	Clinical trials. FDA approved
LDE225	Erismodegib, Sonidegib, Odomzo	SMO	Synthetic	Effective on tumor epithelial cells and stem cells.	(Pan, Wu et al. 2010)	Clinical trials. FDA approved
BMS-833923, XL139		SMO	Synthetic	Effective on native and mutated SMO.	(Gendreau, Hawkins et al. 2009)	Clinical trials
PF-04449913	Glasdegib	SMO	Synthetic	Tested for hematological therapies.	(Munchhof, Li et al. 2012)	Clinical trials
LY2940680	Taladegib	SMO	Synthetic	Binds extracellular tail of SMO. Effective against Vismotegib resistant tumors.	(Bender, Hipskind et al. 2011)	Clinical trials
IPI-926	Saridegib	SMO	Synthetic	No effect on epithelial tumor cells.	(Tremblay, Lescarbeau et al. 2009)	Clinical trials
PF-5274857		SMO	Synthetic	Can penetrate the blood-brain barrier.	(Rohner, Spilker et al. 2012)	
Tak-441		SMO	Synthetic	Effective against Vismodegib resistant tumors.	(Ohashi, Oguro et al. 2012)	
CUR61414		SMO	Synthetic	Could not penetrate human skin for BCC.	(Frank-Kamenetsky, Zhang et al. 2002)	
MRT-92		SMO	Synthetic	Effective against Vismodegib resistant tumors. Sub-nanomolar concentration.	(Hoch, Faure et al. 2015)	Clinical trial stopped
SANT-1,2,3,4		SMO	Synthetic	SANT-1 has 17-fold higher binding affinity to SMO than 2, 3, or 4.	(Chen, Taipale et al. 2002)	
SEN-450		SMO	Synthetic	Effective in glioblastoma.	(Ferruzzi, Mennillo et al. 2012)	
Cholecalciferol		SMO	Vitamin D3	Binds and inhibits SMO	[67]	
GANT-58		Gli1,2	Synthetic	Binds Gli1 and 2 preventing transcriptional activity.	(Lauth, Bergstrom et al. 2007)	

Compound	Trade Name	Target	Source	Notes	Reference	Clinical Trial
Arsenic Trioxide	Trisenox	Gli1,2	Synthetic	Effective against tumor and tumor-initiating cells.	(List, Beran et al. 2003)	Clinical trials
HPI-1		Gli1,2	Synthetic	Disrupts phosphorylation of Gli to activator form.		
HPI-2		Gli2	Synthetic	Blocks ciliary process involving Gli2.	(Hyman, Firestone et al. 2009)	
HPI-3		Gli2	Synthetic	Blocks Gli2 activator formation.		
HPI-4		ciliogenesis	Synthetic	Disrupts ciliogenesis and therefore Gli processing.		
NanoHHI		Gli1,2	Synthetic	Encapsulated HPI-1 to increase bioavailability	(Chenna, Hu et al. 2012)	
Zerumbone/ Zerumbone epoxide		Gli1,2	Shampoo ginger, *Zingiber zerumbet*			
Staurosporinone/ 6-hydroxystaurosporinone		Gli1,2	*Streptomyces staurosporeus*	Determined to reduce transcription activity by reporter assay.	(Hosoya, Arai et al. 2008)	
arcyriaflavin C/ 5,6-dihydroxyarcyriaflavin A		Gli1,2	Marine acidian, *Eudistoma sp*.			
Physalin F and B		Gli1,2	Native gooseberry, *Physalis minima*			
(-)-epigallocatechin-3-gallate (EGCG) / Quercetin		Gli1,2	Green Tea, *Camellia sinensis*	Prevents Gli translocation to the nucleus	[99]	
5E1		SHH	Antibody	Targets SHH ligand to prevent binmding.	(Coon, Laukert et al. 2010)	
Robotnikinin		SHH	Synthetic	Binds SHH ligand and prevents signalling.	(Stanton, Peng et al. 2009)	
RU-SKI 43		SHHat	Synthetic	Blocks palmitoylation of SHH protein by SHHat.	(Petrova, Rios-Esteves et al. 2013)	
Forskolin / Coleonol		Adenylyl cyclase	*Indian coleus, Coleus forskohlii / Plectranthus barbatus*	Stimulates adenylyl cyclase, increasing cAMP and PKA phosphylation of Gli to be degraded.	(Yamanaka, Oue et al. 2010)	
JK184		Adh7	Synthetic	Binds to alcohol dehydrogenase 7, reducing Gli mRNA	(Lee, Wu et al. 2007)	

Table is adapted from review [1] and expanded.

1.8 SHH in bladder cancer

SHH is required for proper development of the embryological bladder. Malformations of the urinary tract have been linked to SHH signaling in Smith-Lemli-Opitz syndrome, patients with holoprosencephaly and Grieg cephalopolysyndactyly [100-102]. SHH is present in the urothelium of the developing bladder from which Gli1 induces smooth muscle alpha and gamma actin formation in the developing mesenchyme of the bladder and where Gli2 aids in mesenchymal patterning [103-106]. Concordantly, mice with SHH mutations display hypoplasia of the bladder wall [107] and megabladder. Mice lacking bladder smooth muscle have alterations in SHH, PTCH, Gli1 and Gli3 temporal-spatial patterning during embryological development [57]. Although SHH expression is essential for bladder development, pathway signaling is vital for urothelial regeneration by basal stem cells throughout the life of an organism. SHH from the basal layer of the urothelium is required to stimulate Wnt production by stromal cells and trigger urothelial proliferation [65].

The importance of SHH in BCa development was first indicated when greater than 50% of urothelial cell carcinoma was found to have a loss of PTCH heterozygosity at the chormosomal location 9q22 [108, 109]. Thievessen et al. [110] later tested the BCa cell lines VMCub1, VMCub2, SW1710, SD, HT1376, 5637, and BFTC905 for SHH responsiveness and pathway activation and found that although normal urothelial cells respond to stimulation, BCa cell lines did not, concluding SHH is of limited importance in urothelial carcinoma (UC). An analysis of more current BCa cell lines RT4, 243J-P, 253J-

BV, UM-UC-6 and UM-UC-3 found that growth and invasiveness increased in the order given but that none of these lines respond to SHH inhibition [111]. Invasiveness was increased and decreased by manipulating Gli2 levels but this effect was thought to be due to non-canonical signaling. Further cell analysis of HTB2, HTB4, HTB9, CRL1472, CRL1749, and CRL2169 determined that only HTB2 showed increased SHH expression [5]. It is evident that there is high variability in pathway activation between cell lines.

Despite the variability in *in vitro* pathway activity, SHH activation has been found in patients with UC. Furthermore, pollutants such as arsenic have been linked to UC through SHH signaling [112]. Interestingly, single nucleotide polymorphisms in Gli and SHH have been linked to clinical outcomes in UC patients after TURBT and BCG treatment [113]. A stronger indication of SHH activation in UC was found by Pignot et al. [5] when they analyzed a panel of 71 UC patients. SHH was increased in 95% of NMIBC and 50% of MIBC and high expression of PTCH 2 was linked to poorer survival in the muscle invasive group. A similar study by He et al. [114] of 118 samples found that SHH, PTCH and Gli1 protein expression was prognostic as it was positively correlated with pathological stage of the tumor, venous invasion and lymph-node metastasis. The presence of these proteins was also linked to poorer disease-free and overall survival [114]. Recently, a smaller study on 22 individuals found that SHH was positively correlated with tumor grade and stage and that Gli2 was upregulated in more invasive tumors [115].

In support of clinical results, the BBN toxin induced model of invasive BCa has been used to demonstrate the necessity of SHH signaling for the origination of the invasive tumor

[116]. Basal urothelial stem cells have been tagged by SHH expression from the tumor but expression is lost before the CIS-like tumors become invasive. This result, combined with the observation that SHH inhibition hastened invasion, led the authors to suggest that SHH provides a protective effect against transition to an invasive phenotype, contrary to what is seen in other tumors [117]. A later study by Islam et al. [115] contradicts this conclusion by showing that in bladder cells, TGF-β acts through SHH resulting in an induction of EMT, increased cell migration, invasiveness and clonogenicity, and that this change can be reversed by SHH inhibition. In addition, Xenografts treated with TGF-β showed increased stem cell markers, presumably through SHH activation. A large body of evidence exists for the role of SHH in BCa progression in patients and in animal models but how this effect is represented in BCa cell lines remains to be established.

1.9 Hypotheses and objectives

As previously stated, the SHH signaling plays a fundamental role in many malignancies and is essential for embryogenesis and possibly tumorigenesis. Current treatments for BCa do not specifically target tumor cells and thus can result in significant side effects. BCa offers a unique opportunity to treat tumors directly by intravesical instillation without exposure to surrounding tissues or off-target organs as is the case in systemic therapy. Hence, there is a strong need for a more specific, targeted intravesical therapy for urothelial carcinoma.

Therefore, I hypothesize that SHH pathway activation, specifically activation of Gli1 and Gli2, is responsible for growth and progression of BCa, and as such can be inhibited by a targeted therapy. This inhibition can be demonstrated by a reduction in cell proliferation, pathway signaling and tumor growth. The following specific objectives were pursued.

Objective 1

In this objective I (Chapter 2) I assessed the state of SHH pathway activity in an in-house panel of clinical BCa samples. I then assessed if SHH activity was similar in BCa cell lines and whether this pathway was responsive to SHH. A panel of cell lines were measured for SHH, Gli1 and Gli2 protein levels and secreted SHH. The presence of the primary cilia organelle responsible for SHH signaling was assesed in two BCa cell lines, 253J-BV and UM-UC-3. The cellular response to exogenous SHH, a SMO agonist and Gli over-expression was determined.

Objective 2

In this objective (Chapter 3) I assessed the degree to which SHH pathway could be inhibited in BCa cell lines. A panel of currently available inhibitors was applied to BCa cells and viability was determined. Two common and effective inhibitors cyclopamine and SANT-1 were evaluated in 253J-BV and UM-UC-3 and SHH pathway expression was measured. In addition, SHH ligand inhibitors antibody 5E1 and Robotnikinin were tested. Anti-sense oligonucleotides custom designed to Gli1 and Gli2 were evaluated for efficacy

against the above mentioned inhibitors. The efficacy of combination therapy was also assessed.

Objective 3

In this objective (Chapter 4) I evaluated the efficacy of Gli2 ASO therapy on *in vivo* orthotopic xenograft tumors. Firstly, I developed an intravesical *in vivo* model of non-invasive BCa in an athymic nude mouse and validated it against current chemotherapy. Using this model I confirmed SHH pathway inhibition and a reduction in tumor growth by Gli ASO.

Chapter 2: Assessment of Gli1 and Gli2 activation in bladder cancer

2.1 Introduction

Sonic hedgehog pathway components have been linked to clinical outcomes or have been shown to be prognostic in BCa. Single nucleotide polymorphisms in Gli and SHH have been associated with prognosis [113] and PTCH2 expression has been linked to poorer survival in muscle invasive BCa [5]. SHH levels are increased in 95% of NMIBC and 50% of MIBC and the presence of SHH, PTCH and Gli1 has been linked to poorer disease-fee survival [114]. In addition, Gli2 is upregulated in more invasive tumors [115].

Contrary to the expression patterns of the SHH pathway in patient samples, BCa cell lines have shown wide variability. Generally, BCa cell lines have been unresponsive to SHH stimulation and inhibition (including VMCub1, VMCub2, SW1710, SD, HT1376, 5637, BFTC905, RT4, 243JP, 253BV, UMUC6, UMUC3, HTB4, HTB9, CRL1472, CRL1749, CRL2169)[5, 110]. The cell line HTB2 was found to be SHH responsive and some increases in cell invasiveness were seen as a result of increases in Gli2 but the effects are not nearly as pronounced as the trends seen in patient samples [5].

I assessed the state of SHH pathway activity in a selection of BCa cell lines and analyzed whether the SHH pathway was responsive to SHH. A panel of cell lines were measured for SHH, Gli1 and Gli2 protein levels and baselines for secreted SHH. I then assessed if two of these cell lines responded in viability and pathway expression to exogenous SHH.

To bypass the receptor PTCH I used an SMO agonist to stimulate the SHH pathway and also transfected cells with a Gli over-expressing construct.

Canonical SHH function relies on protein shuttling up the primary cilia, a non-motile flagellar organelle on the cell surface. Only a small fraction of the total cellular content of SHH pathway proteins is located in the primary cilium at a given time. As such it is still unknown if the cilia is required for SHH signaling [47]. It has been commonly thought that due to constitutive proliferation, cancer cells do not remain in the G_0 phase long enough to form a primary cilia. To address this issue I also assessed if this organelle is present in BCa cells.

2.2 Materials and methods

2.2.1 Cell lines

Human BCa cell lines RT4, UM-UC-3, UM-UC14, T24, TCC-Sup, and immortalized epithelial cell line SV-HUC were kindly provided by Dr. Peter Black (Vancouver Prostate Centre, Vancouver, BC, CA). The prostate cancer cell line PC3 (used as a positive control) was attained from American Type Culture Collection (Manassas, Virginia, USA). PC3 cells were cultured in Dubucco's Modified Eagle's Medium, RT4 in McCoy's 5A medium, SV-HUC in F12K medium, T24 in RPMI medium, and 253J-BV and UM-UC-3 in Minimal Essential Medium with 1% L-glutamine (GlutaMax), 1% non-essential amino acids, and 1% sodium pyruvate. The above reagents were obtained from Thermo Fisher Scientific,

Burlington, ON, CA. All media were supplemented with 10% fetal bovine serum (Hyclone, South Logan, UT, USA). Cells were cultured at 37°C in a 5% CO_2 incubator and mycoplasma contamination was tested at regular intervals for each cell-line. When cells were confluent they were passaged by incubation at 37°C for 5-15 minutes with 0.25% trypsin (Thermo Fisher Scientific), centrifugation at 300 RCF for 5 minutes and resuspension in media. Cells were stored long term in media with 10% dimethyl sulfoxide at a concentration of one million cells per mL and at a temperature of -80°C.

2.2.2 Assessment of secreted sonic hedgehog protein

Cell lines UM-UC-3, 253J-BV and SV-HUC were cultured; after 48 hours media was collected and fresh media was used as control. Cells were approximately 80% confluent at the time of collection. Human SHH was measured by ELISA (ELH-SHHN-1, RayBiotech, Norcross, GA, USA) following manufacturer's protocols and background levels of SHH in the media were subtracted from the results. Briefly, 100 µl of standard or sample was added to each well of a human SHH-N antibody coated 96-well plate and incubated for 2.5 hours at room temperature followed by 100 µl of prepared biotin antibody for 1 hour and then 100 µl prepared Streptavidin solution for 45 minutes. Between each reagent the plate was washed 4 times with wash buffer and aspirated dry. 100 µl of TMB One-Step Substrate Reagent was added for 30 minutes followed by 50 µl of Stop Solution. Absorbance was immediately measured at 450 nm.

2.2.3 Western blot

Western blot of pathway proteins was carried out on cell lysates obtained with RIPA lysis buffer, phosphatase inhibitor (one tablet per 10 ml RIPA, PhosSTOP, Sigma-Aldritch Canada Co., Oakville, ON, CA) and protease inhibitor (one tablet per 100 ml RIPA, SIGMAFAST, PhosSTOP, Sigma-Aldritch Canada Co.) following manufacturers protocols. Proteins were quantified by BCA assay (Pierce, Thermo Fisher Scientific, Burlington, ON, CA) which uses the detection of the Cu^{+1} ion resulting from the biuret reaction (two bicinchoninic acid molecules chelates a Cu^{+1} ion to produce a purple colored product with linear absorbance at 562 nm up 2000 μg/ml initial protein). Proteins were denatured by boiling for 5 minutes and separated by sodium dodecyl sulfate–polyacrylamide gel electrophoresis (SDS-PAGE) before being transferred to methanol-activated polyvinylidene difluoride membranes (Immobilon-P, Sigma-Aldritch Canada Co.) using transfer cassettes (Mini Trans-Blot Cell, Bio-Rad, Hercules, California, USA) overnight at a current of 30 mA at 4°C. Membranes were washed with tris-buffered saline plus 0.1% polysorbate 20 (TBST) and transferred to Odyssey Blocking Buffer (LI-COR, Lincoln, NE, USA) for 1 hour and incubated overnight at 4°C with primary antibody in blocking buffer.

Primary antibodies included: Anti-vinculin at 1:10000 (V4505, mouse monoclonal, Sigma-Aldritch Canada Co.), anti-Gli1 at 1:500 (#2553, rabbit polyclonal, Cell Signaling Technology, Danvers, MA, USA) , anti-Gli2 (R770) at 1:500 (#2585, rabbit polyclonal, Cell Signaling Technology), anti-SHH at 1:1000 (EP1190Y, ab53281, rabbit monoclonal,

Abcam plc, Cambridge, UK) and anti-cleaved PARP (Asp214) at 1:1000 (#9541, rabbit polyclonal, Cell Signaling Technology).

After primary antibody incubation membranes were washed three times for 10 minutes with TBST and incubated at room temperature in blocking buffer for 1 hour with a 1:10000 concentration of Alexa Fluor Plus 680 fluorescent conjugated secondary antibody (Thermo Fisher Scientific) or a 1:10000 concentration of HRP conjugated secondary antibody (Thermo Fisher Scientific). Scans were collected directly using a LI-COR Odyssey scanner in the case of Alexa Fluor secondary antibodies. For HRP secondary antibodies membranes were treated with SuperSignal West Femto Maximum Sensitivity Substrate (Thermo Fisher Scientific) as per recommended protocols and imaged on a Dyversity image analysis system (Syngene, Frederick, MD, USA).

2.2.4 Tissue microarray

BCa tissue microarrays (TMAs) were compiled from patients at the Urology Clinic at Vancouver General Hospital under Consent Version 9.3 as part of the GU Biobanking protocol of The University of British Columbia. TMAs consist of two cores of each specimen and comprise normal epithelium, NMIBC, MIBC, associated lymph node metastases and carcinoma *in situ* (Arrays: Bladder 2012 - #1-3). Staining was performed as previously published [118]. In brief, tissue sections were incubated in Tris EDTA buffer (CC1, Ventana Medical Systems Inc., Tucson, AZ, USA) at 95°C for 64 minutes to retrieve antigenicity, followed by incubation with a respective primary antibody at 37°C for 2 hours. Bound primary antibodies were incubated with Ventana universal secondary

antibody (Ventana Medical Systems Inc.) at 37°C for 32 minutes and visualized using Ventana DAB Map detection kit. The procedure was run on the Ventana Discovery Ultra Platform (Ventana Medical Systems Inc.). Primary antibodies included anti-SHH at 1:50 dilution (EP1190Y, ab53281, rabbit monoclonal, Abcam plc), ant-Gli1 at 1:25 dilution (H-300, sc-20687, rabbit polyclonal, Santa Cruz Biotechnology, Dallas, TX, USA) and anti-Gli2 at 1:50 dilution (ab26056, rabbit polyclonal, Abcam plc).

2.2.5 Immunofluorescent staining

UM-UC-3 and 254J-BV cells were grown to confluence in normal media at which point media was replace with the same medium minus fetal bovine serum. Following 48 hours of serum starvation cells were fixed in methanol with 3% acetone at -20°C for 10 minutes, washed with phosphate buffered saline (PBS), incubated with 0.2% Triton X in PBS for 10 minutes at room temperature, washed, and blocked for 10 minutes at room temperature in 5% goat IgG in PBS. Cells were then incubated with primary antibodies to α-tubulin (PA5-29444, rabbit polyclonal, Thermo Fisher Scientific) and acetylated α-tubulin (MABT868, clone 6-11B-1, mouse monoclonal, Sigma-Aldritch Canada Co.) at 1:600 dilution in PBS plus 1% bovine serum albumin (BSA) overnight at 4°C. Following incubation cells were washed with PBS plus 0.1% Triton X and incubated with fluorescein isothiocyanate (FITC) conjugated goat polyclonal anti-rabbit (NB7182, Novus Biologicals, Oakville, ON, CA) or Alexa Fluor 546 conjugated goat polyclonal anti-mouse (A-11003, Thermo Fisher Scientific) secondary antibodies at 1:200 for 1 hour in the dark at room temperature. Cells were mounted onto slides using Vectashield with DAPI (Vector

Laboratories, Burlingame, CA, USA) and imaged on a Zeiss LSM 780 confocal microscope (Zeiss, Oberkochen, Germany).

2.2.6 Viability and invasion assays

Cell viability was measured using a 3-(4,5-dimethylthiazol-2-yl)-5-(3-carboxymethoxyphenyl)-2-(4-sulfophenyl)-2H-tetrazolium (MTS) cell proliferation kit (Abcam plc) as per recommended protocols. Briefly, MTS compound in electrocoupling solution was added to cell media 24, 48 or 72 hours after a select drug treatment. The compound is metabolized from yellow MTS tetrazolium to a brown formazan product with absorbance at 490 nm. Absorbance was measured between 1 and 4 hours post MTS addition on an Epoch spectrophotometer (BioTek, Winooski, VT, USA) and is displayed as a relative quantity to control cells. Cell invasion assays were performed by seeding cells in a Matrigel coated Boyden chamber (Corning BioCoat chambers, Thermo Fisher Scientific) containing appropriate media without fetal bovine serum in the upper reservoir and media containing fetal bovine serum in the lower reservoir. Growth factors preent in the serum acted as an attractant for cell invasion into the lower chamber. Cells were left to invade for 24 hours in a humidified incubator at 37°C. The cells that progressed through the Matrigel and had adhered to the bottom of the chamber were fixed in cold methanol with 3% acetone at -20°C for 10 minutes and stained with the nuclear stain crystal violet. Cells were then counted under a microscope in six fields of view and compared to the initial number of seeded cells to determine a relative value of cell invasion.

2.2.7 Drug treatment

BCa cell lines were treated with 200 ng/ml of recombinant human SHH protein (cell culture tested) 24 hours prior to MTS and invasion assays and 24, 48 and 72 hours prior to western blot. A concentration curve for SMO Agonist (SAG dihydrochloride) was performed from 0.39 to 25 nM, 48 hours prior to MTS assay to assess changes in viability as a result of SMO activation without SHH ligand. In order to assess if changes to Gli2 overexpression could be reversed, a SMO protein antagonist cyclopamine (cyclopamine hydrate) was administered alongside its biologically inactive control compound tomatidine (tomatidine hydrochloride) at a concentration of 15 μM for both compounds. Dimethyl sulfoxide (DMSO) was a vehicle control. All compounds here mentioned were obtained from Sigma-Aldritch Canada Co. (Oakville, ON, CA).

2.2.8 Gli2 plasmid transfection

The coding sequence for human Gli2 protein (NCBI Reference Sequence NM_005270.4) was inserted into the pDEST26 plasmid following recommended protocols (Gateway Cloning System, Thermo Fisher Scientific). Briefly, the mRNA sequence was reverse transcribed with a Gli2 primer sequence (SuperScript IV First-Strand Synthesis System, Thermo Fisher Scientific), purified by PCR and gel electrophoresis and ligated into an entry plasmid capable of recombining with a variety of expression plasmids. Using a Gateway cloning reaction the gene was transferred from the entry plasmid to the pDEST26 expression plasmid containing a CMV promoter and neomycin resistance (pDESTGli2). The expression plasmid was transformed into *Escherichia coli* (One Shot TOP10

Chemically competent *Escherichia coli*, Thermo Fisher Scientific) cultured, screened for neomycin resistance, colonies selected and grown and plasmids isolated (QIAprep Spin Miniprep Kit, Qiagen, Hilden, Germany). When cell lines had reached 80% confluency they were transfected with pDESTGli2 in lipofectamine 2000 transfection reagent (Thermo Fisher Scientific) following recommended protocols and transfected a second time 24 hours after first transfection. Cells were measured for viability by MTS assay 48 hours after second transfection.

2.2.9 Statistical analysis

All data is represented by mean +/- standard error. Data normality was tested with a Shapiro-Wilk test and equal variance by Brown-Forsyth tests. In the case of data normality and equal variance, differences between groups were determined by a one way ANOVA followed by post hoc Holm-Sidak multiple comparison tests. All analysis was performed in SigmaPlot (Systat Software Inc., San Jose, CA, USA). Groups with a $p \leq 0.05$ were considered significantly different and indicated by different letter annotations. Groups with annotations that contain a letter similar to that of another group are not significantly different from that group.

2.3 Results

2.3.1 SHH pathway activity is highly variable between cell lines

An in-house tissue microarray of transitional cell carcinoma clinical samples was immunohistologically stained for SHH, Gli1 and Gli2 protein (Fig 2.1A). Expression of these proteins was limited to the urothelium in normal bladders where cell proliferation is occurring. Protein expression was detected throughout the sample in non-invasive and invasive tumors where staining was more intense in the invasive tumors. This staining was consistent with epithelial cells not being confined to the epithelium but distributed more diffusely throughout the tumor. In comparison to non-invasive tumors, lymph node metastases appear to have higher levels of all three proteins.

To evaluate if SHH, Gli1 or Gli2 expression was associated with aggressiveness in BCa cell lines, Gli1 and Gli2 protein expression was assessed in a panel of: 3 invasive BCa cell lines (UM-UC-3, T24 and 253J-BV), one non-invasive BCa cell line (RT4), an immortalized non-cancerous line (SV-HUC) and a prostate cancer cell line known to highly express Gli1 and Gli2 (PC3) as a control (Figure 2.1B). The invasive lines T24 and 253J-BV showed very strong expression in one of the two Gli proteins with lower expression over all in the other cell lines. RT4 and T24 did not express detectable Gli2 protein suggesting that the pathway may not be as active in these cells. For further experiments, UM-UC-3 and 253J-BV were chosen due to their expression of both Gli1 and Gli2 protein and invasive cell lines represent the most severe phenotype of BCa. UM-UC-3 was over twice as invasive as 253J-BV (45.2±3.1 cells vs 19.1±1.7 cells, $p<0.001$, N=3) and as such

I define UM-UC-3 as highly invasive cells and 253J-BV as intermediate (Figure 2.1C). Secreted SHH in cell media was measured to determine if these two lines were stimulated in an autocrine manner (Figure 2.1D). Interestingly, the cell line with the highest Gli2 expression, 253J-BV, produced very little SHH with 28.4±0.39-fold higher secretion by UM-UC-3 (560.1±9.7 pg/ml, $p<0.001$, N=3). The control line SV-HUC expressed both Gli1 and 2 protein and secreted high amounts of SHH protein (1042.8±19.6 pg/ml) possibly as a result of the SV40 transformation used to immortalize the cells as large T-antigen bind p53 and Rb proteins which may interact with the SHH pathway [119].

Canonically, SHH signaling functions through the primary cilia which is thought to be absent in cancer cells due to the proportionately large amount of time cancer cells spend in M phase as opposed to G1 through G2. In non-cancerous cells, primary cilia can be induced to form by slowing the cell cycle through serum starvation at cell confluence. This procedure was able to induce primary cilia in UM-UC-3 cells (Figure 2.2A) but not 253J-BV cells (Figure 2.2B). Acetylated α-tubulin is abundant in primary cilia structure and was used to stain the cilia red. In UM-UC-3, cilia were found in a very low frequency of cells and the image was chosen in figure 2 to highlight one of these cells. 253J-BV did not show any cells with primary cilia in replicate samples. Given the rarity of the primary cilia and difficulty inducing cilia presence it is likely that SHH is functioning in a non-canonical way in the absence of cilia in both UM-UC-3 and 253J-BV cells.

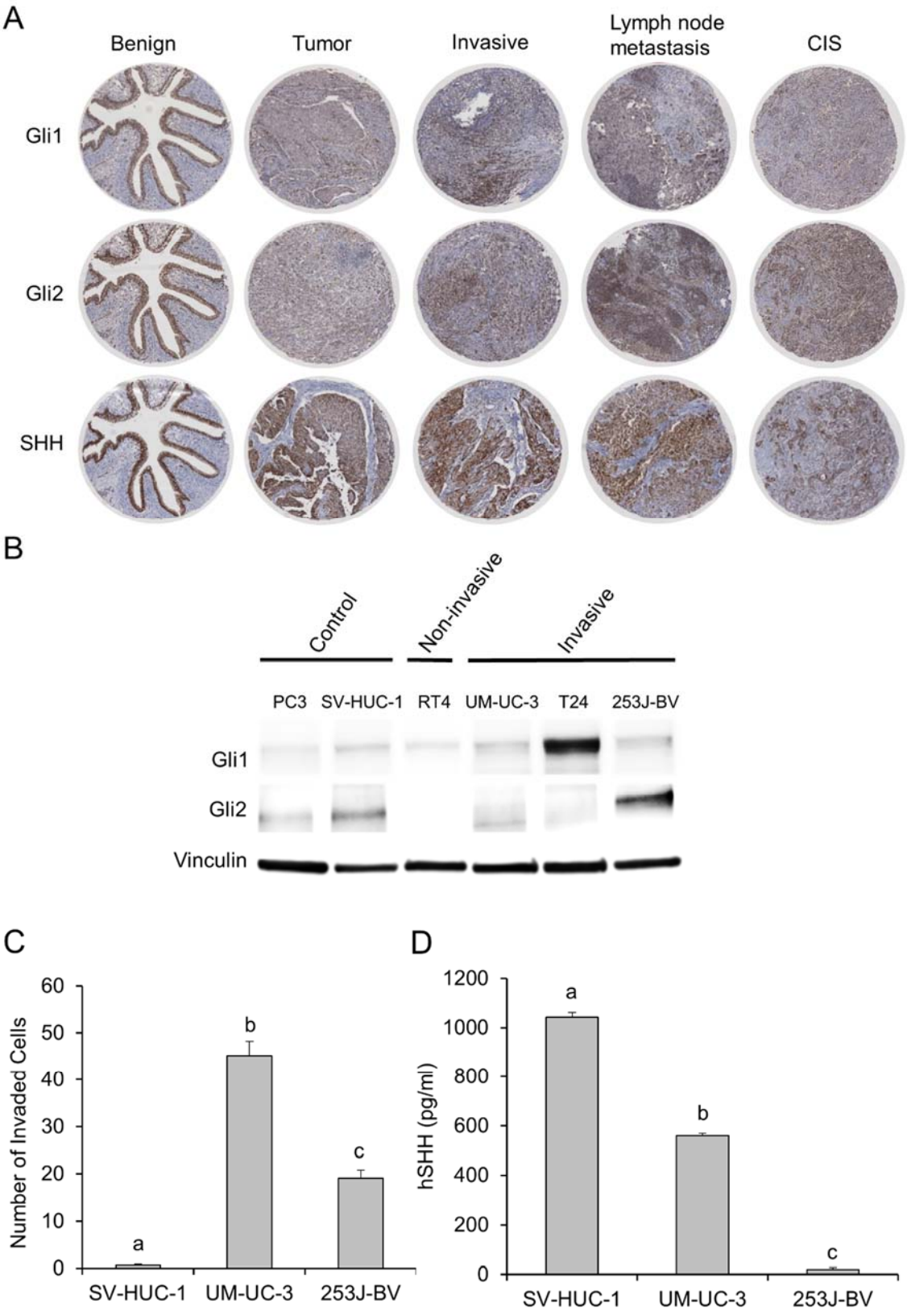
A
Benign
Tumor
Invasive
Lymph node metastasis
CIS
Gli1
Gli2
SHH
B
Control
Non-invasive
Invasive
PC3
SV-HUC-1
RT4
UM-UC-3
T24
253J-BV
Gli1
Gli2
Vinculin
C
Number of Invaded Cells
60
50
40
30
20
10
0
a
b
c
SV-HUC-1
UM-UC-3
253J-BV
D
hSHH (pg/ml)
1200
1000
800
600
400
200
0
a
b
c
SV-HUC-1
UM-UC-3
253J-BV

Figure 2.1. SHH is active in patient samples and UC cell lines. (A) SHH, Gli1 and Gli2 proteins levels as determined by immunohistological staining in a tissue microarray of patient samples. (B) Western blot or Gli1, Gli2 and Vinculin protein in various BCa cell lines. Prostate Cancer (PC3) cells were used as a positive control. (C) Invasive potential as measured by number of invaded cells for an immortalized control cell line SV-HUC-1 and two BCa cell lines, UM-UC-3 and 253J-BV. (D) Quantity of SHH protein secreted into growth media by BCa cells as measured by ELISA. Letters denote significant differences as determined by one way ANOVA and Holm-Sidak post hoc tests ($p \leq 0.05$, N=3).

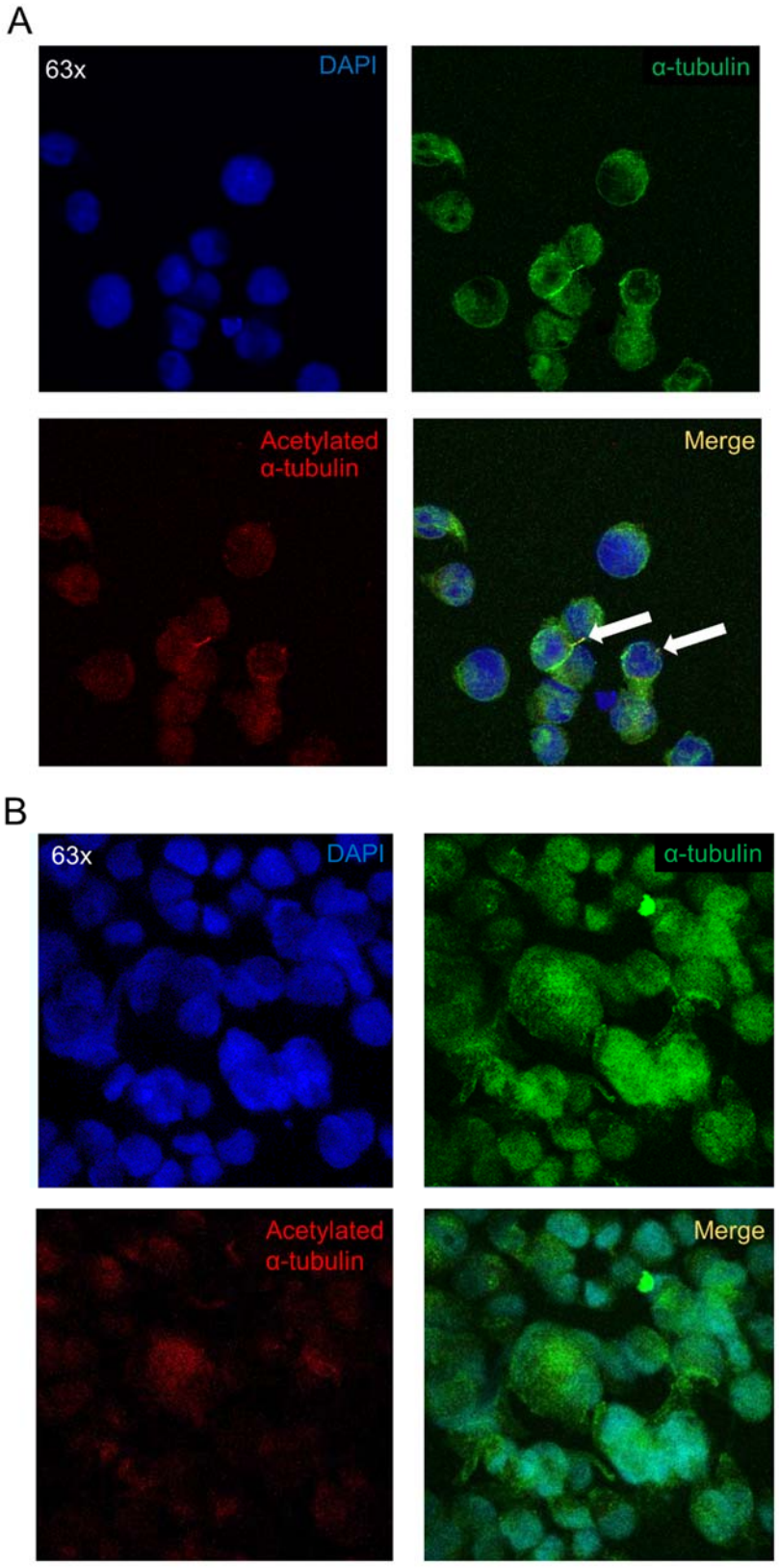
A
63x
DAPI
α-tubulin
Acetylated
α-tubulin
Merge
B
63x
DAPI
α-tubulin
Acetylated
α-tubulin
Merge

Figure 2.2. Primary cilia are only found in UM-UC-3 cells. UM-UC-3 cells (A) and 253J-BV cells (B) were serum starved for 12 hours, fixed with alcohol, stained with DAPI (blue nuclear stain), and probed with antibodies to the structural protein α-tubulin (green) and the primary cilia structural protein acetylated α-tubulin (red). The merged images are also included. The long tube-like projections stained yellow in UM-UC-3 cells (A) and marked with arrows are the primary cilia. This staining is absent in 235J-BV cells.

2.3.2 253J-BV but not UM-UC-3 respond to SHH ligand and smoothened agonist

In order to assess whether the SHH pathway in our chosen cell lines would respond to pathway stimulation, I treated cells with recombinant human SHH (rhSHH). After 24, 48 and 72 hours both the control cell line SV-HUC and UM-UC-3 were unaffected in viability as measured by MTS assay (Figure 2.3A) while 253J-BV had increased to 169.6 ± 3.2% by 48 hours ($p<0.001$, N=3) and 212.6 ± 11.5% by 72 hours ($p<0.001$, N=3). Baseline levels of invasiveness were very low in SV-HUC and approximately 20-fold higher in 253J-BV and 40-fold higher in UM-UC-3 (Figure 2.1C). After rhSHH addition, 253J-BV invasiveness doubled (169.2 ± 26.2% control, $p=0.046$, N=3) and UM-UC-3 and SV-HUC remained unchanged (Figure 2.3C). Contrary to the viability results protein expression of Gli1 and Gli2 was relatively unchanged in both cell lines although SHH protein was increased in 253J-BV 24 hours after rhSHH treatment (Figure 2.3C,D). Interestingly, a gradual increase in Gli1 expression was seen in both cell lines over a 72 hour period with and without rhSHH treatment. This trend was also mildly present in Gli2 protein expression. The cleaved product of PARP was measured as a marker of toxicity and cell death and this marker was not present due to rhSHH treatment. In order to bypass SHH binding to PTCH I treated both cell lines with a SMO agonist known to stimulate the SHH pathway (SAG, Figure 2.4). Over a range of concentrations (0.39 nM to 25 nM) an 8.3 ± 0.6% ($p=0.032$, N=3) increase in viability was seen in UM-UC-3 cells at 1.56 nM after which viability drastically drops likely due to drug toxicity. In agreement with the effects seen in rhSHH treatment, 253J-BV increased in viability to a greater extent than UM-UC-3, 21.9 ± 5.0% ($p<0.001$, N=3) at 3.125 nM, before toxicity reduced viability.

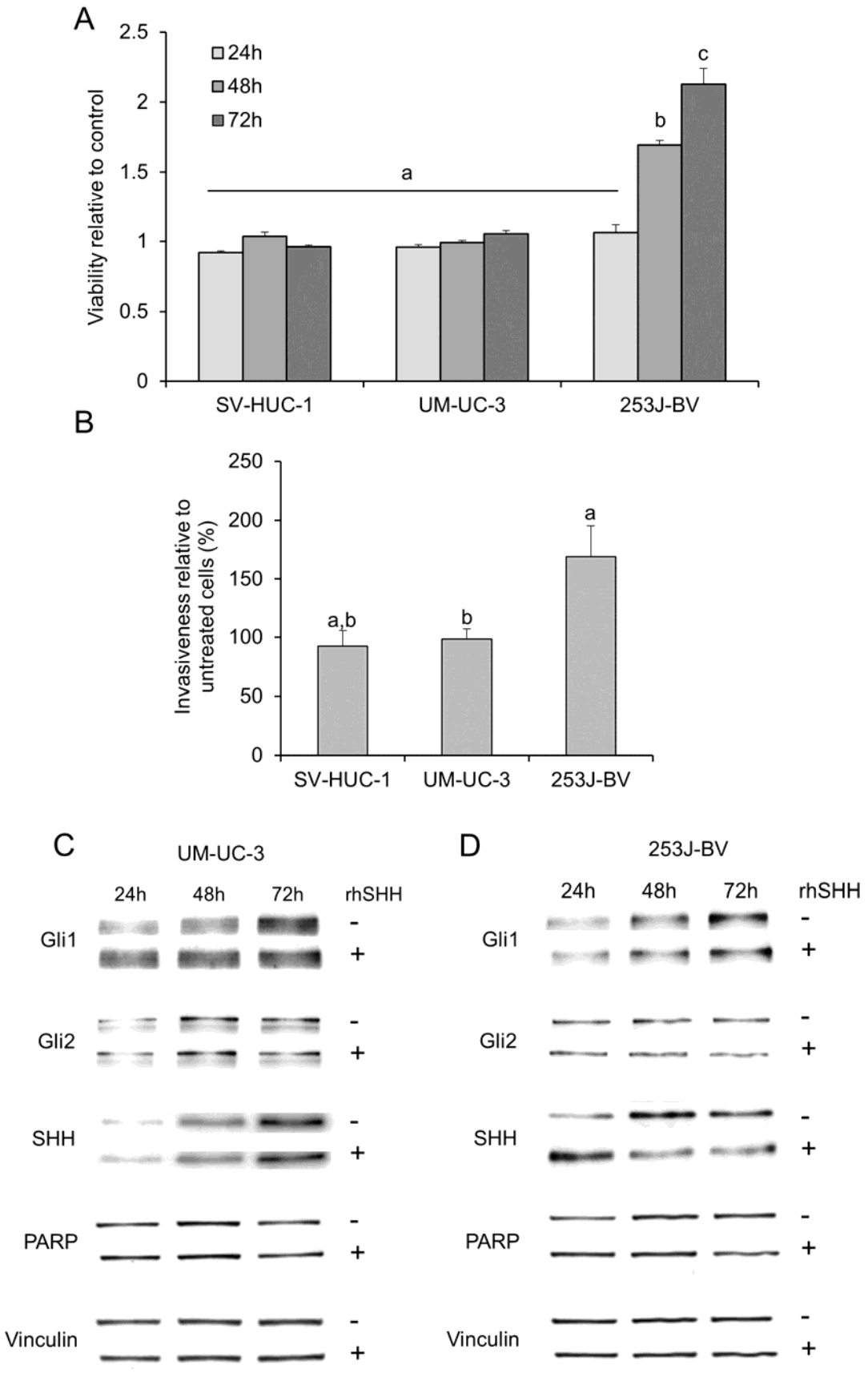
A
Viability relative to control
2.5
2
1.5
1
0.5
0
24h
48h
72h
a
b
c
SV-HUC-1
UM-UC-3
253J-BV
B
Invasiveness relative to untreated cells (%)
250
200
150
100
50
0
a,b
b
a
SV-HUC-1
UM-UC-3
253J-BV
C
UM-UC-3
24h
48h
72h
rhSHH
Gli1
Gli2
SHH
PARP
Vinculin
-
+
D
253J-BV
24h
48h
72h
rhSHH
Gli1
Gli2
SHH
PARP
Vinculin
-
+

Figure 2.3. Only 253J-BV responds to SHH ligand. (A) Viability of SV-HUC-1 control and UM-UC-3 and 253J-BV BCa cell lines when treated with 200 ng/ml recombinant human SHH (rhSHH) for 24 to 72 hours. (B) Invasiveness relative to matched untreated controls after rhSHH treatment. (C) Western blot for Gli1, Gli2, SHH, PARP and Vinculin control in UM-UC-3 cells over a 24 to 72 hour period following rhSHH treatment. (D) Western blot for Gli1, Gli2, SHH, PARP and Vinculin control in 253J-BV cells over a 24 to 72 hour period following rhSHH treatment. Letters denote significant differences as determined by one way ANOVA and Holm-Sidak post hoc tests ($p \leq 0.05$, N=3).

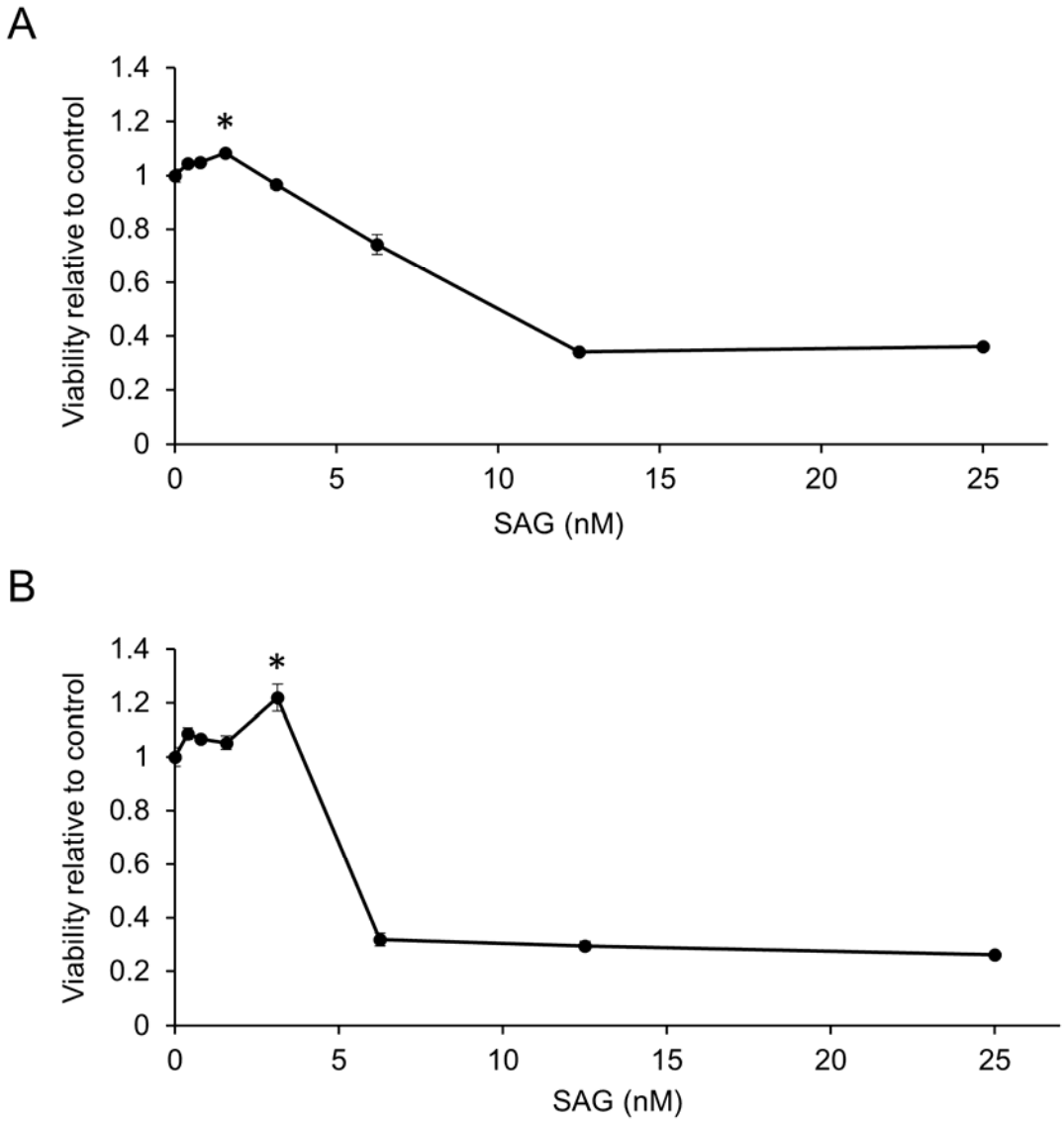

Figure 2.4. Smoothened activation has larger effect on 253J-BV cells. Stimulation of SMO protein with a SMO agonist (SAG) over a range of concentrations in UM-UC-3 cells (A) and 253J-BV cells (B). Asterisk denotes a significant increase in viability as determined by one way ANOVA and Holm-Sidak post hoc tests between concentrations ($p \leq 0.05$, N=3).

2.3.3 Direct over-expression of Gli2 did not affect cell viability

Transfection of UM-UC-3 and 253J-BV with a construct constitutively expressing Gli2 was successful as evidenced by increased Gli2 protein expression in both cell lines (Figure 2.5C,D) as compared to the sham plasmid. There was a concomitant increase in Gli1 protein expression in UM-UC-3 but not 253J-BV. In addition, cleaved PARP was not present suggesting a lack of toxicity from the plasmid transfection. The SMO inhibitor cyclopamine, was successful at knocking down Gli2 expression in both cell lines, although it was much more effective in 253J-BV. Despite this manipulation of Gli2 levels, cell viability measures were not increased in either cell line and were in fact decreased with transfection (Figure 2.5A,B). In 253J-BV there was a very small increase in viability due to Gli2 transfection (0.85 ± 0.04) over the sham control (0.82 ± 0.007), concomitant with higher Gli2 protein levels, but this increase was not significant ($p=0.515$, $N=3$). In 253J-BV but not UM-UC-3 the addition of cyclopamine had a small effect on viability when compared to tomatidine, which will be discussed in Chapter 3.

2.4 Discussion

Stimulation of the sonic hedgehog pathway has been linked to the development and progression of many forms of cancer including BCa [47]. In addition, expression of components in the SHH pathway have been linked to poorer prognosis and survival in BCa patients [5, 113-115]. Normally SHH expression is tightly regulated and as such enhanced

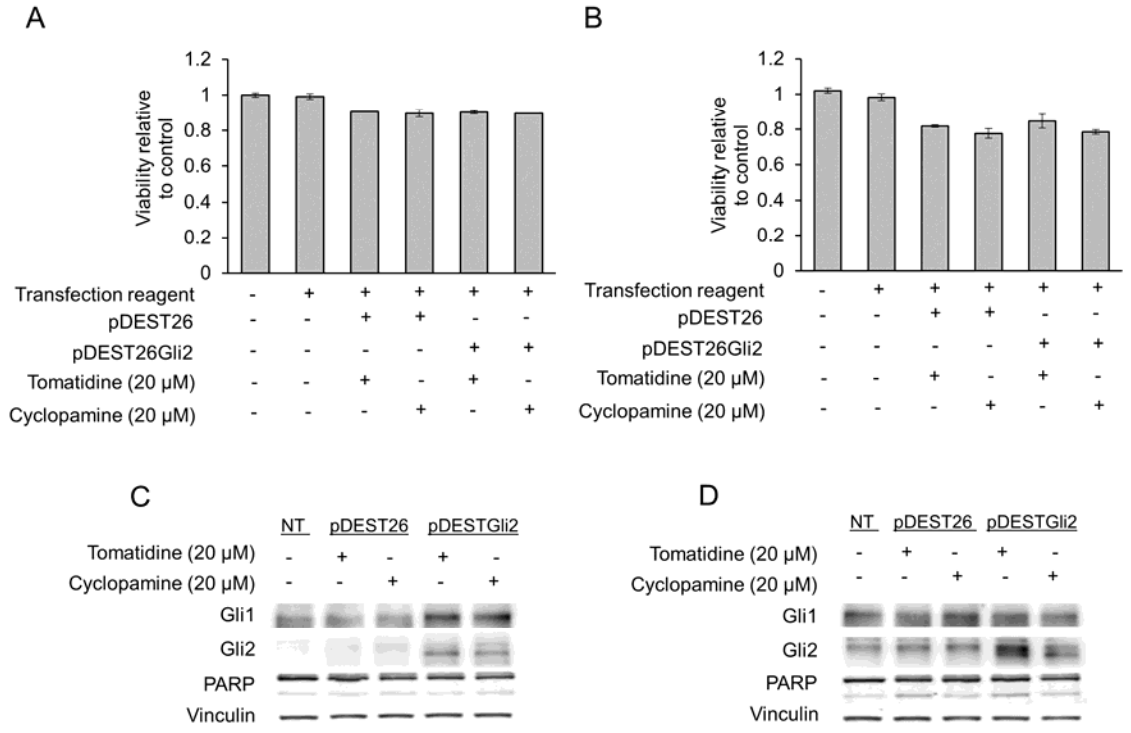

Figure 2.5. Overexpression of Gli2 did not increase cell viability. (A) Viability and (C) western blot of UM-UC-3 cells after transfection with a vector overexpressing Gli2 (pDESTGli2) and combination treatment with a SMO inhibitor, cyclopamine, and its inactive control, tomatadine. (B) Viability and (D) western blot of 253J-BV cells under similar conditions. Statistical tests by one way ANOVA found no significant differences in viability in either cell line (N=3).

pathway activity is an indicator of carcinogenesis and tumor progression. A panel of BCa cell lines was selected Gli1 and Gli2 protein levels were analyzed to assess pathway activation. In general, high levels of Gli1 and/or Gli2 were present in the cell lines with an invasive phenotype suggesting that the SHH pathway is activated in these lines. Two invasive lines chosen for their expression of both Gli1 and Gli2 were positive for SHH protein secretion but showed highly variable results. As a result, these data show that the SHH pathway is active in these cell lines.

Regarding primary cilia, SHH signaling was first identified to operate through primary cilia a decade ago and various ways in which the cilia formation can be disrupted can alter HH signaling [120]. Normally primary cilia are formed during cell quiescence and are reabsorbed when the cell prepares for mitosis, or are prevented from forming to aide in cell proliferation [121]. Until recently it was though that cancer cells did not form primary cilia due to their high proliferation rate but an analysis of six different cancers has shown that cilia are increased in number and structurally abnormal [122]. Indeed, disruption of proper signaling through the primary cilia has been found to be oncogenic [123]. One cell line, UM-UC-3, appears to display primary cilia in a very low frequency of cells while 253J-BV cells display no evidence of primary cilia. Despite this, the SHH pathway is active in both cells lines and measurable in a large number of cells as determined by the ease to which it is detected in cell culture. In this case, the SHH pathway is likely operating independent of the primary cilia.

Analysis of other urothelial carcinoma (UC) cell lines for SHH expression has shown mixed results. A study by Thievessen et al. [110] analyzed seven UC lines for Gli-dependent promoter activity (VMCub1, VMCub2, SW1710, SD, HT1376, 5637, BFTC905) and found that the promoter was down regulated in some lines and increased in others. Furthermore, the construct was not inducible in many lines likely due to the presence of a Gli suppressor or lack of a necessary cofactor [110]. SHH mRNA expression was present in most cells but absent in SD and very low in VMCub1 and 2, similar to the variability seen in our secreted SHH protein levels. Gene expression of Gli1, 2 and 3 and PTCH was highly variable between lines and increased expression in any of these genes was only found in BFTC905, 5637 and VMCub2 [110]. The authors concluded that the SHH pathway was of little importance in UC but the presence of pathway activity suggests that it could be very important in specific cell lines and as such the variability between lines is important to note.

A study by Mechlin et al. [111] analyzed five cell lines, including 253J-BV and UM-UC-3, for growth, invasiveness, and SHH pathway mRNA expression. They found that UM-UC-3 invasiveness was greater than that of 253J-BV which agrees with our results. In addition, invasiveness and viability increased in only 253J-BV cells with recombinant SHH addition. An increase in invasiveness was correlated with Gli2 expression by Mechlin et al. but no changes to Gli protein levels were found with an addition of rhSHH in our cell lines. Regarding pathway mRNA expression, results were highly variable but 253J-BV and UM-UC-3 did show Gli1 and 2 expression consistent with our findings. SHH mRNA expression was detected in UM-UC-3 and not 253J-BV which is also consistent with our

secreted SHH protein values. Due to low levels of some upstream SHH pathway components, the authors concluded that this pathway performs a small role in UC and that the Gli2 expression may be due to non-canonical signaling. Much like the previous study cited above it is important to note the variable nature of the pathway signaling and the fact that some cell lines may rely more heavily on SHH than others.

A further panel of BCa cell lines (HTB2, HTB4, HTB9, CRL1472, CRL1749, CRL2169) have been analyzed for SHH mRNA expression [5]. SHH was increased in HTB2 and was found at much lower levels in the other lines. The results obtained in this study further support the variability of the SHH pathway in UC. UM-UC-3 appears to have higher baseline pathway activity and as such cannot be further stimulated. 253J-BV on the other hand is very responsive to stimulation. UM-UC-3 has moderate levels of Gli1 and 2 protein but secretes relatively high levels of SHH. In addition, the cells are highly invasive and do not increase in cell invasion or viability with exogenous SHH. SMO agonists have no effect on viability nor does endogenous Gli2 overexpression. 253J-BV has higher Gli2 protein expression than UM-UC-3 and similar Gli1 expression. These cells do not secrete SHH protein to a great extent and are relatively non-invasive but exogenous SHH addition markedly increases cell viability and invasion. An increase in viability is seen with SMO agonists and a small effect on viability resulted from endogenous Gli2 overexpression. When considering the role of SHH on BCa and possible ways in which to inhibit this pathway one must consider this variability in cell lines and how this may be reflected in clinical samples.

Three models have been proposed to explain the manner in which the SHH pathway is utilized by the cancer cell. Type I is constitutive pathway activation by mutation, type II is autocrine stimulation by SHH and type III is paracrine stimulation by stromal cells adjacent to cancer cells [82]. Although the purpose of this study was not to determine the manner in which the pathway operates but rather to confirm pathway activation and assess pathway variability, my results form a basis for further study. UM-UC-3 displays characteristics that suggest it may be type I, autocrine stimulated. The transcription factors Gli1 and 2 are present, SHH ligand is being secreted, and UM-UM3 are highly viable and invasive. In addition, the pathway cannot be stimulated through exogenous or endogenous means. UM-UC-3 appears to be maximally stimulated by the secretion of its own SHH. Alternatively, it may be growing at a maximal rate that cannot be influenced by SHH stimulation, may have pathway activity that is partially independent of SMO, or may not have fully functional SMO protein. On the other hand, 253J-BV appears to be type III, paracrine stimulated directly by SHH. This cell line is relatively non-invasive but viability and invasion can be increased by both exogenous and endogenous pathway stimulation. In addition, 253J-BV secretes very little SHH protein and as such has a low baseline SHH activity that has room for further activation. Further studies on the specific expression of each pathway component will be needed to determine if this conclusion is correct.

My results show that the SHH pathway is present in many BCa cell lines and that two invasive lines, UM-UC-3 and 253J-BV have high expression of this pathway. To the best of my knowledge this is the first time such a large variation in how these two lines respond to SHH and pathway manipulation has been characterized. One must consider this

variation when assessing what treatments may be needed for BCa in general. The next chapter will discuss our methods at inhibiting this pathway to maximize effectiveness in these two highly different BCa lines.

2.5 Conclusion

Upregulation of the SHH pathway, specifically SHH, Gli1 and Gli2 protein was detected in invasive bladder tumors in a tissue microarray of patient UC samples. This discovery suggests that the SHH pathway may be involved in BCa progression as has been suggested previously in the literature and found in other cancers. I identified two invasive cell lines, UM-UC-3 and 253J-BV, exhibiting Gli1 and Gli2 protein expression to differing degrees. In addition, UM-UC-3 was found to be more invasive than 253J-BV. Differences between the cell lines in SHH pathway characteristics was further demonstrated by the lack of primary cilia in 253J-BV which may affect the ability of these cells to respond to SHH. Addition of recombinant human SHH contradicted this prediction as 253J-BV responded by an increase in viability and invasiveness while UM-UC-3 showed no response at all. Stimulation of the SHH pathway at the level of the protein SMO using SAG resulted in a small increase in viability in both lines but was more effective in 253J-BV. Stimulation further down the pathway at the level of the Gli2 transcription factor by mRNA overexpression once again had a small effect on viability but only in 253J-BV. These results suggest that there is large variability in invasive BCa cell line's response to SHH pathway stimulation, suggesting that UM-UC-3 may be at a near maximal level, potentially due to constitutive activation, and that 253J-BV responds to stimulation as would be

expected in canonical signaling. Next I will evaluate the efficacy of inhibiting the SHH pathway in these cell lines representing invasive BCa.

Chapter 3: Inhibition of Gli1 and Gli2 by antisense oligonucleotides to treat bladder cancer

3.1 Introduction

The role of sonic hedgehog in such a vast array of tumors has led to the pursuit of inhibitors to attenuate pathway function. Early natural compounds derived from the lily *Veratrum californicum* were isolated after reports of the developmental abnormality (cyclopia) in sheep consuming these plants [94]. Since that time many synthetic antagonists have been identified by small molecule drug screening, the majority of which target SMO upstream in the pathway (see Chapter 1, Table 1.1). Two of these inhibitors GDC-0449 and LDE 225 are approved by the FDA for cancer treatment with others in clinical trials [95, 96]. Other popular targets are the Gli proteins themselves but these compounds have not been well tolerated *in vivo* due to difficulties of formulation and delivery. Only one, arsenic trioxide, has entered clinical trials but has not been developed for clinical use [97].

Here I evaluated the effectiveness of a panel of SHH pathway inhibitors on the two invasive BCa cell lines analyzed in Chapter 2, UM-UC-3 and 253J-BV that were chosen for their positive Gli status and aggressive growth. These two lines do not respond similarly to pathway stimulation or in baseline pathway activation but both cell lines show expression of the Gli transcription factors. I endeavored to determine the effects of inhibition of the SHH pathway at various points along the signaling cascade. I compared drug inhibition, as determined by a decrease in viability and increase in apoptosis, to the most commonly

published benchmark for SHH inhibition, cyclopamine and to an array of available pathway inhibitors (Figure 3.1). In addition, I tested a new treatment modality, Gli antisense oligonucleotides, for the potential to bypass pathway variability.

3.2 Materials and methods

3.2.1 Cell culture

Human BCa cell lines UM-UC-3 and 253J-BV were kindly provided by Dr. Peter Black (Vancouver Prostate Centre, Vancouver, BC, CA). Cells were cultured as described in Chapter 2.

3.2.2 Western blot

Western blot of pathway proteins was carried out as described in Chapter 2. Primary antibodies included: Anti-vinculin at 1:10000 (V4505, mouse monoclonal, Sigma-Aldritch Canada Co., Oakville, ON, CA), anti-Gli1 at 1:500 (#2553, rabbit polyclonal, Cell Signaling Technology, Danvers, MA, USA) , anti-Gli2 (R770) at 1:500 (#2585, rabbit polyclonal, Cell Signaling Technology) and anti-cleaved PARP (Asp214) at 1:1000 (#9541, rabbit polyclonal, Cell Signaling Technology).

3.2.3 Drug treatment

Cells were exposed to small molecule inhibitors of the SHH pathway that were commercially available for research purposes in normal growth medium for 48 hours prior to assessing viability and determining cell cycle. Concentrations were chosen spanning the IC_{50} values reported for cells in the literature. Inhibitors included SANT-1, cyclopamine (and the inactive control tomatidine), Jervine, CUR61414, GANT 58, GANT 61, HPI-1, HPI-4 and JK184 and were purchased from Sigma-Aldritch Canada Co. DMSO and ethanol (EtOH) were vehicle controls. Ligand inhibitors Robotnikinin (VWR International, Radnor, PA, USA) and antibody 5E1 (Developmental Studies Hybridoma Bank, Iowa City, IA, USA) were applied to the cells in a similar way as described above.

Antisense oligonucleotides to Gli1 and Gli2 and the scrambled sequence control (SCR) were obtained from Ionis Pharmaceuticals Inc. (Carlsbad, CA, USA). All antisense oligonucleotides were modified at the 2' position of the sugar with a 2'-o-(methoxyethyl) group on the five bases at both the 5' and 3' termini. The central 10 bases contained deoxyribose and the entire oligonucleotide backbone contained phosphorothioate linkages. These chemical modifications prevent endonuclease activity from breaking down ASOs thereby increasing ASO half-life and cellular distribution [124]. The sequence of the Gli1 ASO is 5'-CCCCTTAGGAAATGCGATCT-3' (Ionis 124904) and Gli2 ASO 5'-GTGGCGGCACTCCAGCCAGG-3' (Ionis 183652). The SCR oligonucleotide was designed not to match any mRNA in the human or mouse transcriptomes and has the sequence 5'-CCTTCCCTGAAGGTTCCTCC-3' (Ionis 141923).

Transfections were performed by incubating ASO with Oligofectamine (ThermoFisher Scientific, Burlington, ON, CA) and OptiMEM (ThermoFisher Scientific) for a final concentration of 8 μL Oligofectamine per 1 mL OptiMEM. This concentration was optimized by a dose-response curve in which toxicity was measured by MTS assay and determined to be less than 5%. Cells were incubated for 4 hours with ASO after which media was replaced. This was repeated a second time after 24 hours. Viability was determined 48 hours following the second treatment. Cells were treated with a range of ASO concentrations and IC50's were determined. These concentrations were used in subsequent trials.

3.2.4 Viability and cell cycle analysis

Cell viability was measured as described in Chapter 2. Cell cycle analysis was performed by flow cytometry of propidium iodide–stained cells to determine their DNA profile and to quantify apoptotic rates by detection of cells with sub-G1 DNA content. After drug treatments, cells were trypsinized to produce a single-cell suspension and fixed with 70% ethanol. The next day, cells were washed with phosphate-citrate buffer to elute fragmented low–molecular weight DNA and incubated with 0.5 mg/ml RNase A (ThermoFisher Scientific, Burlington, ON, CA) at 37°C for 30 minutes. Subsequently, cells were stained on ice with 1 ml of 50 μg/ml propidium iodide (Sigma-Aldritch Canada Co.), a fluorescent dye that intercalates double-stranded DNA. Relative DNA content was then analyzed on a BD FACSCanto II flow cytometer (BD Biosciences, San Jose, CA, USA).

3.2.5 Statistical Analysis

All data is represented by mean +/- standard error. Data normality was tested with a Shapiro-Wilk test and equal variance by Brown-Forsyth tests. In the case of data normality and equal variance, differences between groups were determined by a one way ANOVA followed by post hoc Holm-Sidak multiple comparison tests. If data did not pass normality or equal variance an ANOVA on ranks was performed, followed by post hoc Tukey tests if group sizes were similar or post hoc Dunn's multiple comparison tests if group sizes differed. Figure 3.4 was analyzed with a two way ANOVA using ASO type and treatment concentration as factors with Holm-Sidak post hoc tests. All analysis was performed in SigmaPlot (Systat Software Inc., San Jose, CA, USA). Groups with a $p \leq 0.05$ were considered significantly different and indicated by different letter annotations. Groups with annotations that contain a letter similar to that of another group are not significantly different from that group.

3.3 Results

3.3.1 UM-UC-3 cells are resistant to pathway inhibition

UM-UC-3 cells are relatively unresponsive to pathway stimulation as seen previously (Chapter 2). As a result, I tested this cell line against a variety of sonic hedgehog pathway inhibitors to determine if these cells are also resistant to pathway inhibition and at what stage in the signaling cascade this might occur (Figure 3.1). Positive results from this

screening were then evaluated in the more sensitive 253J-BV cell line. Viability measured against a concentration curve of SANT-1, cyclopamine, jervine, CUR61414, GANT- 58 and 61, HPI-1 and 4, and JK184 spanning the published IC_{50}'s for other cell lines indicated that UM-UC-3 cells were marginally inhibited by SANT-1 (0.88 ± 0.02, p=0.039, N=3) and strongly inhibited by JK184 at concentrations of 15 μM and up (15 μM, 0.63 ± 0.02, p<0.001, N=3; Figure 3.2). Because JK184 targets alcohol dehydrogenase and indirectly acts on the SHH pathway, and due to its off-target effects on microtubule function in general, JK184 was not considered a suitable inhibitor. SANT-1 is a SMO inhibitor (SMO is a common target of SHH pathway inhibitors, see Table 1.1) and so SMO inhibition will be evaluated in these cells.

3.3.2 SHH ligand inhibition is not an effective treatment strategy

I began to evaluate inhibition by first starting at the level of the SHH ligand. Inhibition of SHH protein in the media was achieved through two drug treatments; an antibody to the receptor binding site of SHH to prevent PTCH activation, antibody 5E1, and a small molecule inhibitor of SHH, robotnikinin. Both UM-UC-3 and 253J-BV did not respond in viability to varying concentrations of antibody 5E1 and were only mildly affected (15% reduction in viability) by robotnikinin treatment at an exceedingly high concentration of 50 μM (UM-UC-3, 0.85 ± 0.01, p=0.042, N=3; 253J-BV, 0.86 ± 0.01, p<0.001, N=3; Figure 3.3A,B). There were no differences in the two cell line responses to these drugs. This may be due to the fact that UM-UC-3 cells do not require SHH for stimulation and that 253J-BV cells produce very little SHH in the media that can be inhibited (see Chapter 2).

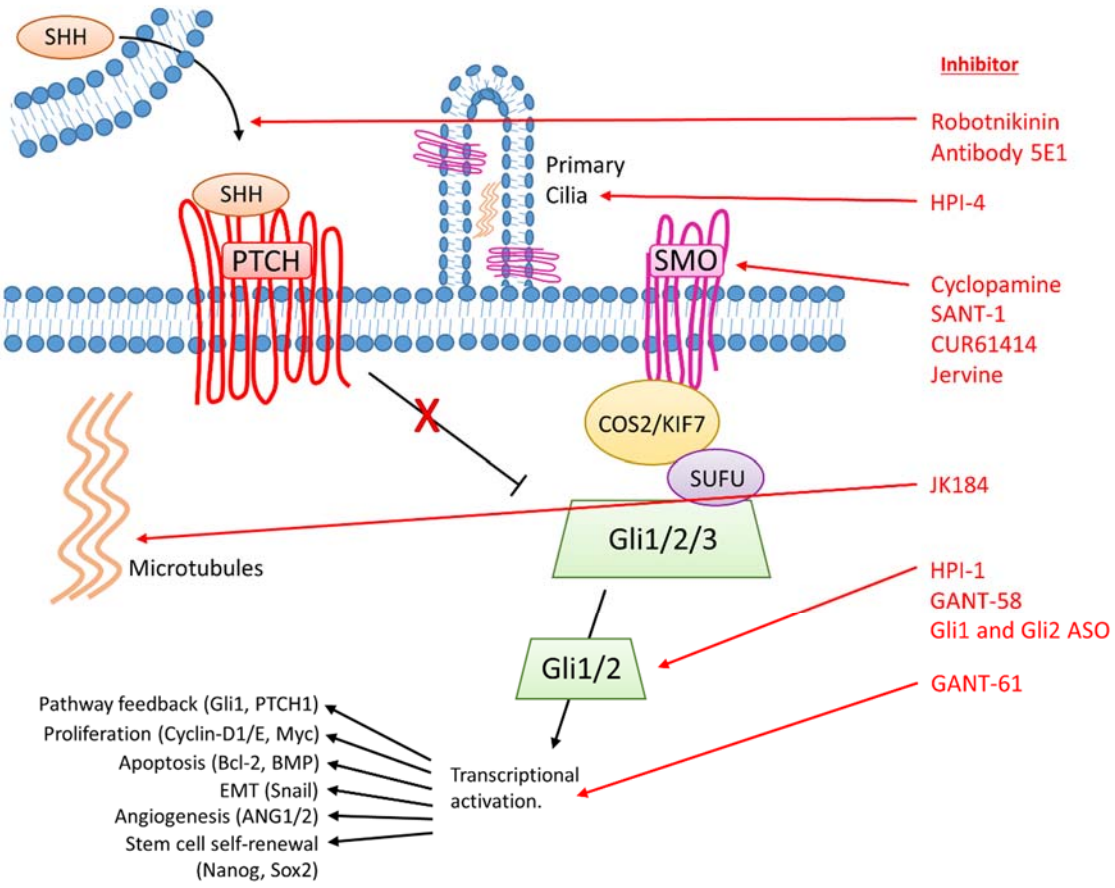

Figure 3.1. SHH pathway was targeted at a variety of locations. SHH pathway inhibitors tested in UM-UC-3 BCa cells and their location of action in the signaling cascade. SHH signaling in cancer is thought to occur both inside the primary cilia an on the cell surface.

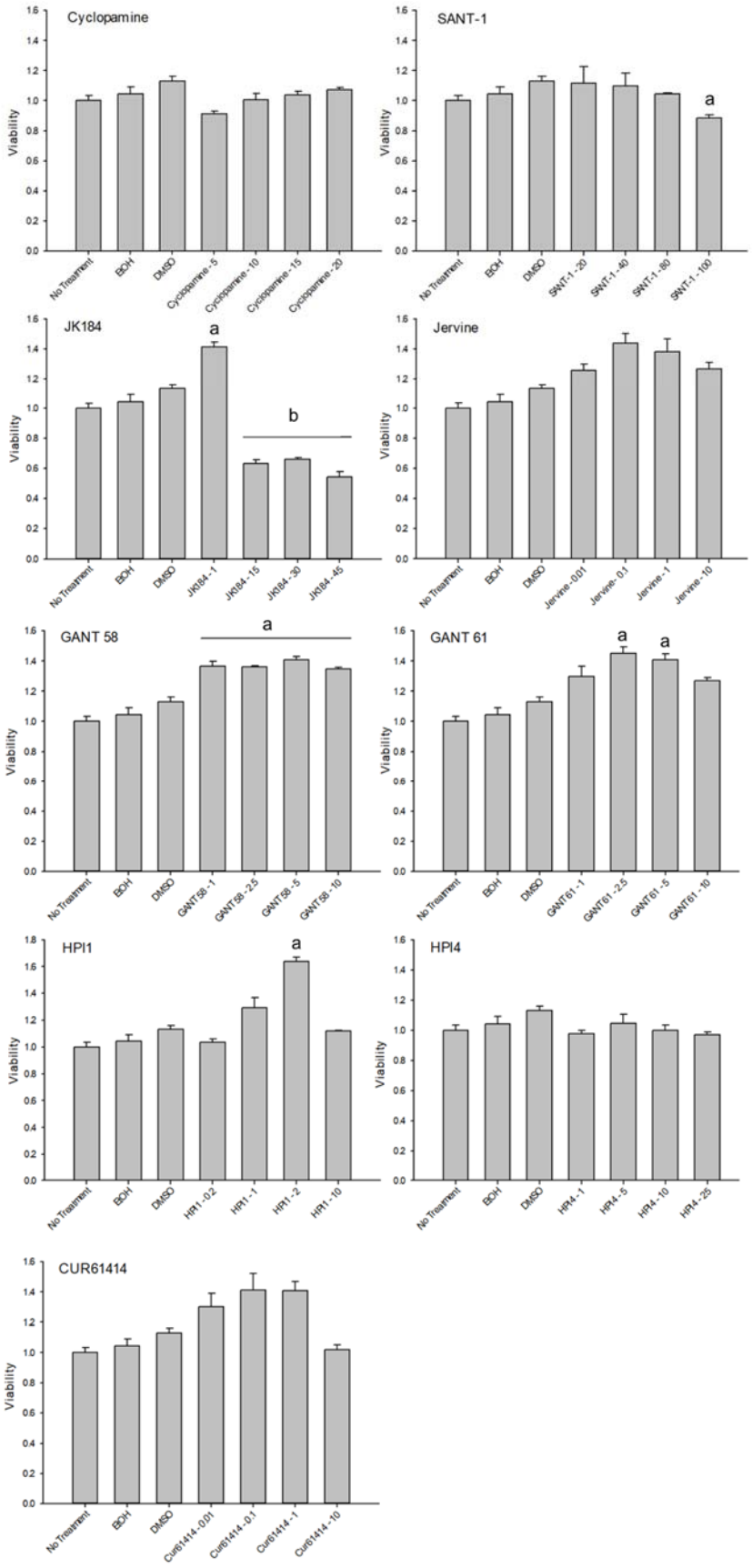
Cyclopamine
Viability
No Treatment
EtOH
DMSO
Cyclopamine - 5
Cyclopamine - 10
Cyclopamine - 15
Cyclopamine - 20
SANT-1
a
SNT-1 - 20
SNT-1 - 40
SNT-1 - 80
SNT-1 - 100
JK184
a
b
JK184 - 1
JK184 - 15
JK184 - 30
JK184 - 45
Jervine
Jervine - 0.01
Jervine - 0.1
Jervine - 1
Jervine - 10
GANT 58
a
GANT58 - 1
GANT58 - 2.5
GANT58 - 5
GANT58 - 10
GANT 61
a
a
GANT61 - 1
GANT61 - 2.5
GANT61 - 5
GANT61 - 10
HPI1
a
HPI1 - 0.2
HPI1 - 1
HPI1 - 2
HPI1 - 10
HPI4
HPI4 - 1
HPI4 - 5
HPI4 - 10
HPI4 - 25
CUR61414
Cur61414 - 0.01
Cur61414 - 0.1
Cur61414 - 1
Cur61414 - 10

Figure 3.2. SHH pathway inhibition by a panel of small molecule inhibitors. The BCa cell line, UM-UC-3 was treated with a wide variety of SHH pathway inhibitors to assess at which point in the pathway would be most responsive to treatment. UM-UC-3 was chosen due to its relative resistance to pathway modification as determined in Chapter 2. Treatments effective here were carried into 253J-BV cells. All concentrations are in μM, spanning IC_{50}'s available in published literature for other cell lines. DMSO and EtOH are vehicle controls. Letters denote significant differences as determined by one way ANOVA with Holm-Sidak post hoc tests ($p \leq 0.05$, N=3).

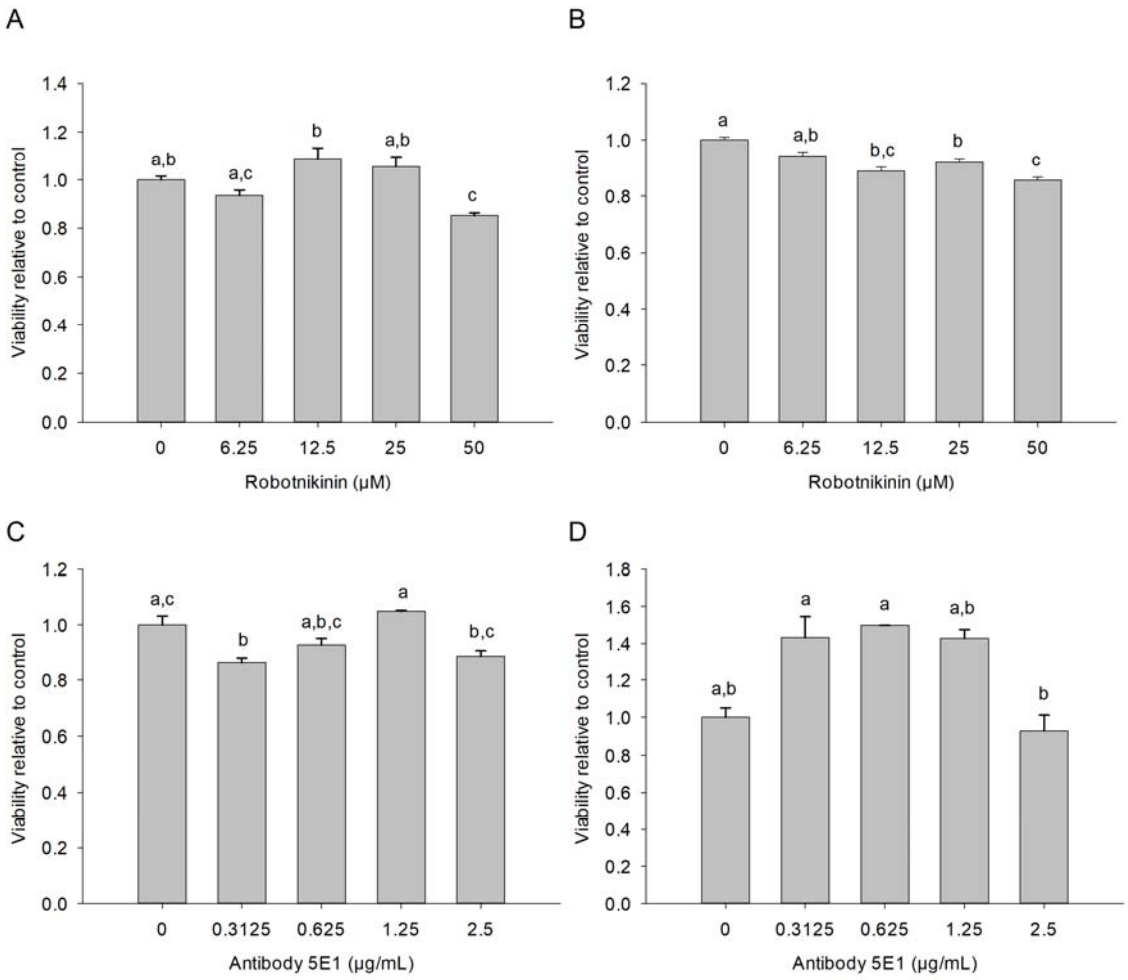

Figure 3.3. SHH ligand inhibition has a small effect on UC cells. UM-UC-3 cells (A,C) and 253J-BV cells (B,D) were treated with the SHH ligand inhibitors robotnikinin and antibody 5E1 and viability was measured relative to a vehicle control (concentration of 0). Different letters denote significant differences between groups as determined by one way ANOVA with Holm-Sidak post hoc tests ($p \leq 0.05$, N=3).

3.3.3 Smoothened inhibition is largely effective in 253J-BV but not UM-UC-3.

SMO protein is a common target of small molecule inhibitors and the drug screening I performed on UM-UC-3 showed that there was a small decrease in viability with the SMO inhibitor SANT-1. Despite the fact that UM-UC-3 did not respond to cyclopamine, this inhibitor was used as a source of comparison as it is the most commonly utilized inhibitor in previous studies. Viability was assessed with cyclopamine, tomatidine and SANT-1 inhibition in 253J-BV side-by-side with UM-UC-3 and corresponding protein levels of Gli1, Gli2 and an apoptosis marker, cleaved PARP, were measured (Figure 3.4). As expected cyclopamine had no effect on UM-UC-3 (Figure 3.4A) but was effective over the control compound tomatidine in 253J-BV at reducing viability (0.45 ± 0.05, $p<0.001$, N=3; Figure 3.4B). SANT-1 was effective in both cell lines although the effect was more pronounced in 253J-BV (253J-BV, 0.64 ± 0.03, $p<0.001$, N=3; UM-UC-3, 0.82 ± 0.03, $p=0.012$, N=3). At a concentration of 20 μM cyclopamine, Gli1 protein levels are reduced and cleaved PARP is present in UM-UC-3 even though no effect is yet seen in overall viability (Figure 3.4C). In addition, the decrease in viability due to SANT-1 is not mirrored by a decrease in Gli1 or Gli2 levels. There does not appear to be a strong link between Gli and viability due to these treatments in UM-UC-3. In contrast, Gli1 and Gli2 levels are decreased and cleaved PARP is present in 253J-BV when treated with cyclopamine and this change is mirrored by a decrease in viability (Figure 3.4B,D). Similarly, Gli1 and Gli2 protein levels are reduced due to SANT-1 treatment. Overall, 253J-BV responds as predicted due to SMO inhibition.

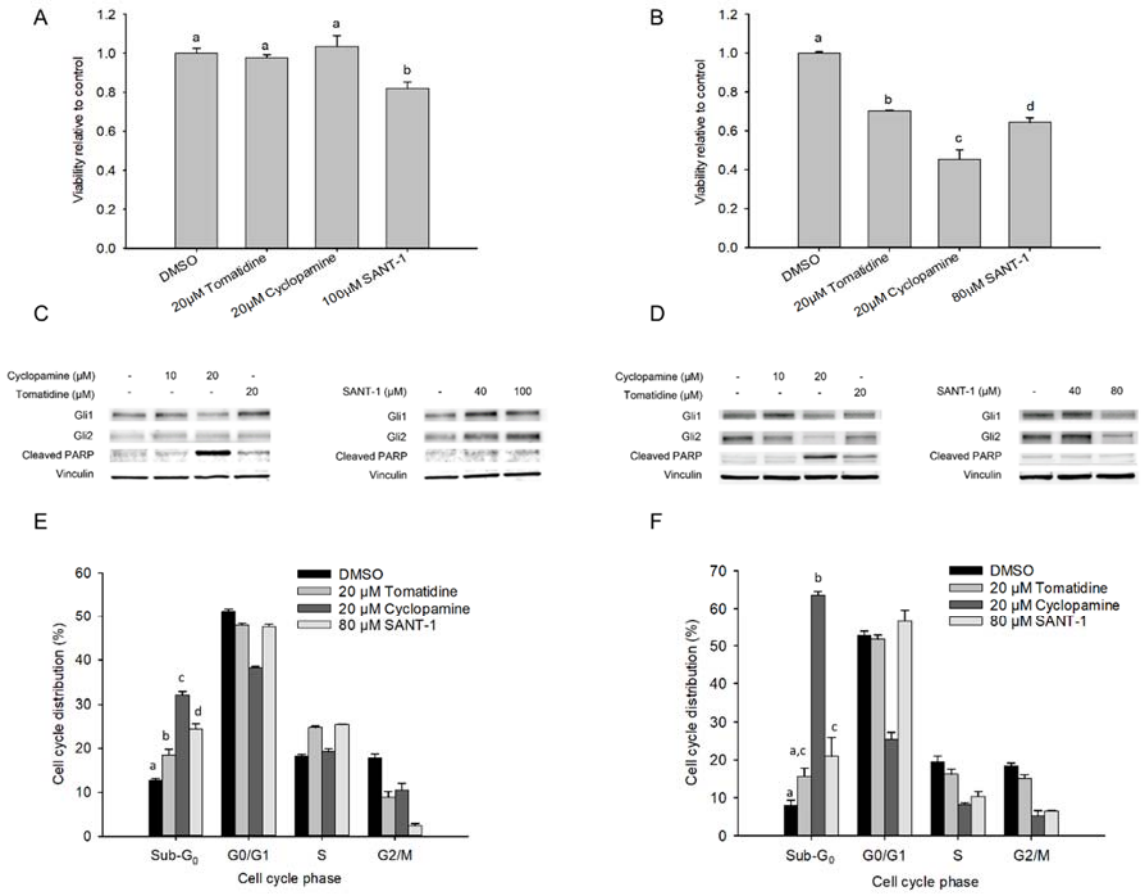

Figure 3.4. Smoothened inhibition was much more effective in 253J-BV cells. Viability of UM-UC-3 cells (A) and 253J-BV cells (B) treated with SMO inhibitors cyclopamine and SANT-1. Tomatidine is the inactive control for cyclopamine. Western blots of Gli1, Gli2, cleaved PARP and a vinculin control in UM-UC-3 (C) and 253J-BV cells (D) after SMO inhibitor treatment at increasing concentrations. Apoptosis, as measured by flow cytometry analysis of propidium iodide stained cells, and indicated by an increase in cells in the sub-G_0 phase for both UM-UC-3 (E) and 253J-BV (F) cells after SMO inhibitor treatment. DMSO is a vehicle control. Letters denote significant differences as determined by one way ANOVA with Holm-Sidak post hoc tests ($p \leq 0.05$, N=3).

Apoptosis was measured directly by flow cytometry in which the number of cells in each stage of the cell cycle was determined. Cells undergoing cell-cycle arrest and apoptosis appear in the sub-G_0 stage. Cyclopamine at 20 μM significantly increased the number of cells in sub-G_0 in both cell lines (UM-UC-3, 32.0 ± 0.87%, $p<0.001$, N=3; 253J-BV, 63.6 ± 1.00%, $p<0.001$, N=3; Figure 3.4E,F). This corresponds to the increased level of cleaved PARP after these treatments (Figure 3.4C,D). SANT-1 treatment also increased the number of apoptotic cells although, not to as great an extent as cyclopamine (UM-UC-3, 24.4 ± 1.14%, $p<0.001$, N=3; 253J-BV, 20.9 ± 5.00%, $p=0.031$, N=3).

Overall, the SMO inhibitor SANT-1 was effective in these two cell lines at reducing viability by a small degree and inducing apoptosis, although this was not detected through an increase in cleaved PARP. Cyclopamine was able to induce apoptosis in both cell lines but overall viability was unaffected in UM-UC-3. A decrease of approximately 10% in UM-UC-3 is not nearly large enough to warrant an investigation into its effect on tumor growth so I next tested the potential to block the Gli transcription factors.

3.3.4 Gli antisense oligonucleotide at low concentration effectively inhibits both cell lines

Given the variability seen in the response of UM-UC-3 and 253J-BV to pathway and ligand inhibition, I attempted to directly inhibit the transcription factors at the end of the pathway to bypass this variability. I treated both cell lines with antisense oligonucleotoides to Gli1 and Gli2 at concentrations up to 200 nM and measured viability, protein expression and apoptosis (Figures 3.5). In comparison to the scrambled control nucleotide (SCR) both Gli1 and Gli2 ASO were effective at reducing viability in UM-UC-3 cells at 50 nM and

above (Gli1 ASO, 0.82 ± 0.02, p=0.015, N=3; Gli2 ASO, 0.70 ± 0.06, p=0.015, N=3; Figure 3.5A). Gli2 ASO was more effective with an IC_{50} at 100 nM (0.51 ± 0.01, p<0.001, N=3). Protein expression confirmed Gli1 and Gli2 knockdown with the matching ASO with a 61.4% reduction in Gli protein (p<0.001, N=3) and a 58.1% reduction in Gli2 protein (p=0.024, N=3) at 100 nM concentration. Gli1 ASO did significantly reduce Gli2 protein levels (Figure 3.5C,E). Cleaved PARP was present in all measured ASO concentrations (50, 100 and 250 nM) but was the strongest with Gli2 ASO at all concentrations. 253J-BV viability was more sensitive to Gli2 ASO than UM-UC-3 (IC_{50} of 50 nM in 253J-BV, 0.49 ± 0.04, p<0.001, N=3) but surprisingly was unaffected by Gli1 ASO despite confirmation of Gli1 protein knockdown by western blot with a 42.0% reduction at 15nM (p=0.017, N=3; Figure 3.5B,D,F). Gli2 knockdown was also confirmed by western blot with a 25% reduction at 50 nM (p=0.049, N=3) and cleaved PARP was only detected with Gli2 ASO, matching the results seen in viability. In 253J-BV, Gli2 ASO treatment significantly increased Gli1 protein expression (108.6% increase at 15nM), potentially as compensatory response to a reduction in viability. Interestingly, the SCR ASO decreased Gli2 protein expression in UM-UC-3 cells and increased expression in 253J-BV cells, possibly due to cell responses to exogenous nucleotide sequences. Apoptosis was confirmed by flow cytometry where the percentage of cell in the sub-G_0 stage was dramatically increased by Gli1 ASO (100 nM, 45.6 ± 1.25%, p<0.001, N=3) and Gli2 ASO (100 nM, 63.3 ± 1.25%, p<0.001, N=3) in UM-UC-3 but only by Gli2 ASO in 253J-BV (50 nM, 53.6 ± 2.80%, p=0.004, N=3; Figure 3.5G,H). As Gli2 ASO was the most effective in UM-UC-3 and the only effective ASO in 253J-BV, I tested the potential for combination therapy with the highly published SMO inhibitor cyclopamine. I found no increased effect of adding

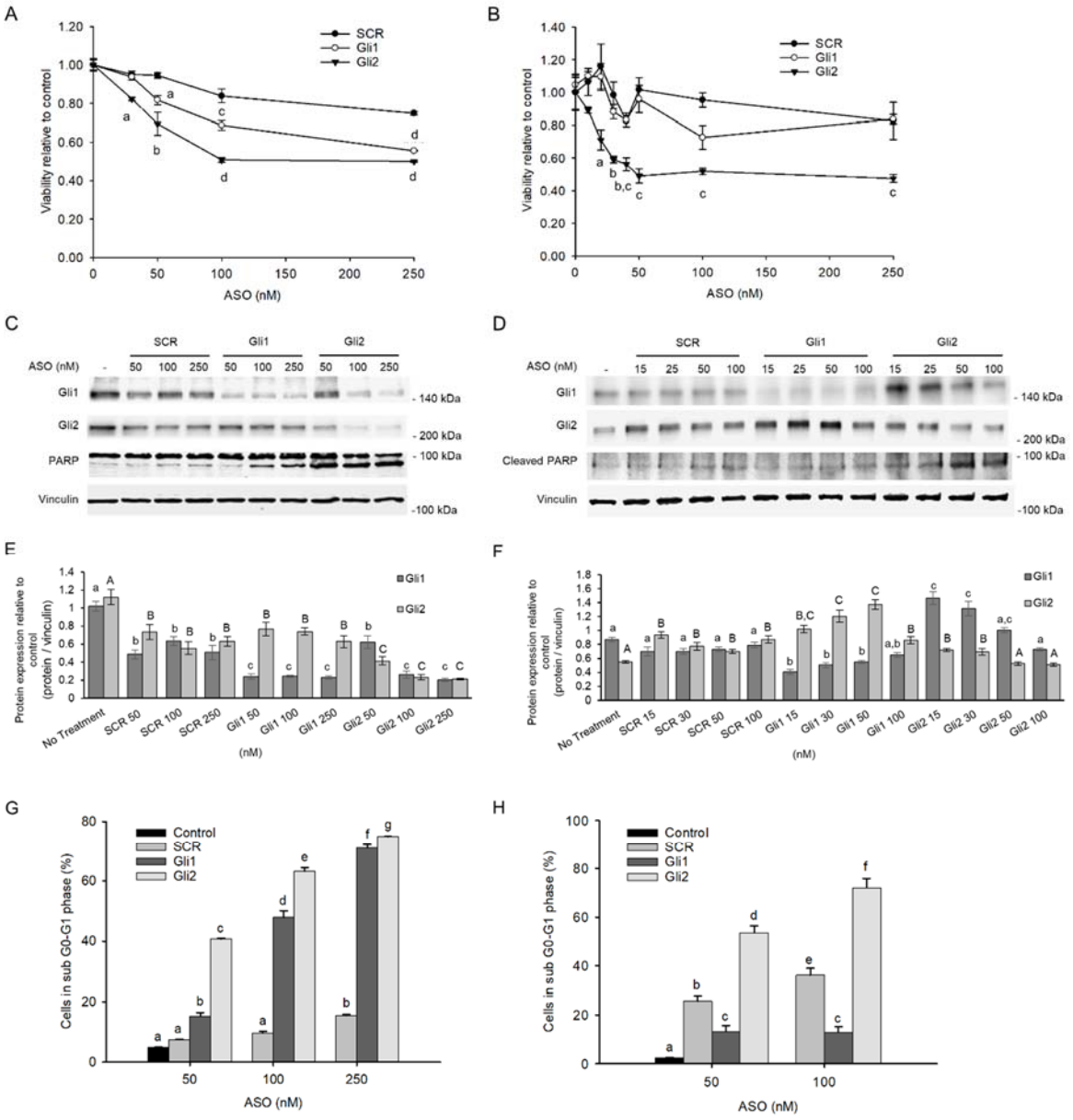
A
Viability relative to control
ASO (nM)
SCR
Gli1
Gli2
B
Viability relative to control
ASO (nM)
SCR
Gli1
Gli2
C
SCR
Gli1
Gli2
ASO (nM)
Gli1
Gli2
PARP
Vinculin
- 140 kDa
- 200 kDa
- 100 kDa
-100 kDa
D
SCR
Gli1
Gli2
ASO (nM)
Gli1
Gli2
Cleaved PARP
Vinculin
- 140 kDa
- 200 kDa
- 100 kDa
-100 kDa
E
Protein expression relative to control (protein / vinculin)
Gli1
Gli2
No Treatment
SCR 50
SCR 100
SCR 250
Gli1 50
Gli1 100
Gli1 250
Gli2 50
Gli2 100
Gli2 250
(nM)
F
Protein expression relative to control (protein / vinculin)
Gli1
Gli2
No Treatment
SCR 15
SCR 30
SCR 50
SCR 100
Gli1 15
Gli1 30
Gli1 50
Gli1 100
Gli2 15
Gli2 30
Gli2 50
Gli2 100
(nM)
G
Cells in sub G0-G1 phase (%)
Control
SCR
Gli1
Gli2
ASO (nM)
H
Cells in sub G0-G1 phase (%)
Control
SCR
Gli1
Gli2
ASO (nM)

Figure 3.5. Gli2 ASO reduces viability and increases apoptosis in both UCC cell lines. Viability of UM-UC-3 cells (A) and 253J-BV cells (B) treated with Gli1, Gli2 and a scrambled control (SCR) ASO at increasing concentrations. Western blots and protein levels of Gli1, Gli2, cleaved PARP and a vinculin control in UM-UC-3 (C,E) and 253J-BV cells (D,F) after ASO treatment Apoptosis, as measured by flow cytometry analysis of propidium iodide stained cells, and indicated by the percent cells in the sub-G_0 phase for both UM-UC-3 (G) and 253J-BV (H) cells after ASO treatment. In A,B,G and H, letters denote significant differences as determined by a two way ANOVA using ASO type and treatment concentration as factors.. In E and F lower case letters denote differences between groups in GL1 protein levels and upper case in Gli2 protein levels as determined by one way ANOVA. Holm-Sidak post hoc tests were used for multiple comparisons ($p \leq 0.05$, N=3).

cyclopamine to Gli2 ASO treatment as would be expected from existing pathway knockdown downstream of cyclopamine action (Figure 3.6). Gli2 ASO treatment significantly decreased viability in UM-UC-3 (0.76 ± 0.01, $p<0.001$, N=6) and 253J-BV (0.23 ± 0.01, $p<0.001$, N=6). Similar to previously shown results, cyclopamine only reduced viability in 253J-BV controls (0.56 ± 0.02, $p<0.001$, N=3). These results support that the SHH pathway is already largely inhibited by Gli2 ASO and there is no benefit to a combination treatment designed to further reduce pathway activity.

3.4 Discussion

Sonic hedgehog signaling plays an important role in the development of the urogenital system including the bladder in which it is involved in smooth muscle formation and mesenchymal patterning [103-106]. Throughout adult life SHH signaling continues to be important for maintenance and regeneration of the bladder urothelium [65]. Given the importance of this pathway in tissue growth and differentiation, it is not surprising that components of the pathway are upregulated in bladder tumors and in some cases can be prognostic of disease outcomes [5, 112-115].

Inhibition of SHH is a treatment modality that has been vigorously pursued for many types of cancer and has resulted in the development of a large variety of inhibitors ranging from natural compounds to small molecules and antibodies (see Table 1.1). Unfortunately, many of these treatments are validated in reporter assays or specific cell systems and only a few

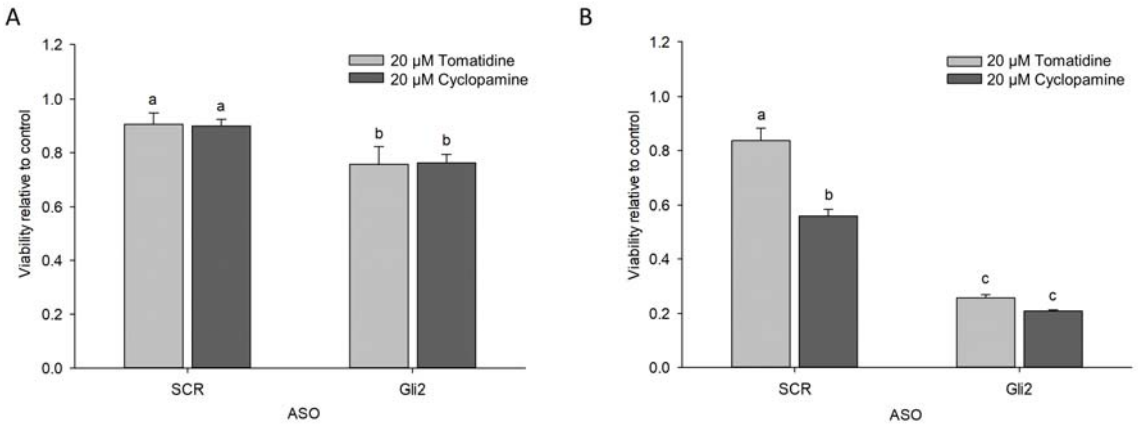

Figure 3.6. Gli2 ASO blocks upstream SHH pathway inhibition. Viability of UM-UC-3 (A) and 253J-BV (B) cells when treated with Gli2 ASO or control SCR ASO at a concentration of 50nM in combination with the SMO inhibitor cyclopamine and its inactive control compound tomatidine. Letters denote significant differences as determined by a one way ANOVA with Holm-Sidak post hoc tests ($p \leq 0.05$, N=3).

have proven successful *in vivo* and none have been developed clinically. In addition, the SHH pathway has been reported to be of varying importance in BCa cell lines and in some cases has been determined to be only a minor driver of BCa *in vitro* [5, 110, 111]. This raises the question as to whether existing inhibitors are applicable to BCa cells and if so, whether they will be efficacious *in vivo*.

To address this question, I chose two BCa cell lines, UM-UC-3 and 253J-BV, that are relatively unresponsive and responsive to SHH pathway stimulation respectively. An ideal treatment should be able to reduce the growth of a wide variety of urothelial carcinoma phenotypes and genotypes and as such should be able to inhibit cells that are less SHH responsive and in which SHH is potentially constitutively active. Viability was analyzed as a response to Gli inhibition due to the fact that Gli activity has been linked to cell viability in a large variety of cancers and decreased viability, as measured by mitochondrial activity, represents an increase in senescence, apoptosis or a decrease in proliferation [125-133]. Inhibition of UM-UC-3 viability was unsuccessful with almost all tested drugs, including cyclopamine. This agrees with the results of Mechlin et al. [111] that found that UM-UC-3 was only mildly affected by SHH inhibition using cyclopamine and tomatidine although their effect was more pronounced than ours. In contrast, 253J-BV was sensitive to cyclopamine and tomatidine in a similar way as the mentioned study [111]. This variability between cell lines is essential to consider when attempting to inhibit this pathway. SANT-1 treatment was able to reduce viability in both lines but to a much lesser extent in UM-UC-3, such that it is not suitable for significant tumor reduction. In addition,

SANT-1 did not show Gli1 or Gli2 protein reduction in UM-UC-3 although it strongly reduced these levels in 253J-BV. UM-UC-3 may respond differently to SMO inhibitors.

A concern with drugs such as cyclopamine is the potential for off target effects in the cell, especially at concentrations as high as 20 uM needed to be effective in UM-UC-3. Toxicity due to drug concentration may be responsible for the small reduction in viability here and is a problem that must be addressed in all inhibitors and targeted therapies. In addition to reducing viability, cyclopamine showed an increase in cleaved PARP, indicative of cell death. Cleaved PARP was not present in SANT-1 suggesting a PARP-independent pathway responsible for cell death or perhaps a delayed cleavage of PARP by caspases after SANT-1 treatment. Gli2 ASO did increase cleaved PARP consistent with a reduction in viability and increase in cell death by flow cytometry. Regardless of the specific pathway, a factor that limits the effectiveness of cyclopamine or SANT-1 *in vivo* where all cells will be exposed to these drugs is an increase in cell death due to indiscriminant toxic effects on healthy cells. An inhibitor at a lower concentration in the nanomolar range would be less toxic and more suitable. These are the concentrations in which the Gli ASOs are active.

Gli2 ASO at 50 to 100 nM was effective at reducing BCa cell growth. This ASO also increased apoptosis in both cell lines and resulted in Gli2 protein knockdown. An advantage to ASO treatment is that it can target a specific mRNA sequence and have minimal off-target effects if the sequence is confirmed unique [134]. This potentially solves some of the drawbacks of small molecule drug treatments where it is difficult to

target a unique site in a particular protein. If both a small molecule inhibitor and ASO are confirmed to be specific, an ASO may provide the advantage of preventing protein translation rather than impeding protein function, avoiding complications of mutational resistance to inhibitor binding. Antisense oligonucleotides are effective when treated systemically but given the nature of the bladder, intravesical instillation allows for direct contact between the ASO and the tumor and prevents ASOs from affecting non-target cells. The bladder is a unique location in which ASO therapy is potentially more viable.

An additional advantage to utilizing a Gli2 ASO is that this form of therapy directly targets the transcription factor at the end of the SHH pathway. In this way, variability or mutations in proteins up-stream will be ineffective at preventing Gli2 ASO action. I have shown the extent to which UM-UC-3 and 253J-BV cells differ in SHH pathway response (Chapters 2 and 3) and I expect that this variability exists in other cell lines and in patient tumors. UM-UC-3 may have a constitutively active SHH pathway that is largely unresponsive to SHH signaling and SMO inhibition. Conversely, 253J-BV appears to be more canonically regulated and is responsive to SHH stimulation and SMO inhibition.

Indeed there is large genetic variability in urothelial carcinoma where tumors stratify into 3 or 4 major subtypes [16-23]. Although both UM-UC-3 and 253J-BV are basal subtype, how this sub-type influence SHH pathway function is unknown [135]. I conclude that the variability between tumors must be considered when assessing an efficacy of SHH pathway inhibitors. Treatment with Gli2 ASO was capable of reducing viability in UM-UC-3 cells and 253J-BV cells despite pathway variability.

The SHH pathway has shown to be influence by other ligands, receptors or pathways within the cell and is not entirely driven by SHH ligand binding to PTCH. For instance, SHH can bind CAM-related/downregulated by oncogenes (CDO), brother of CDO (BOC), hedgehog interacting protein (HIP) and growth arrest-specific 1 (GAS1) to promote HH signaling [44]. In addition to SHH, PTCH can also be bound and activated by glypicans and megalin [44]. Most importantly, Gli1 activation and function can be triggered by other common cancer pathways without activation of SHH, PTCH or SMO. These include Ren, Dyrk1, K-Ras, TGF-β, PKC-α, p53, and PI3K-AKT [64, 76-80]. This interaction with other cell signals poses a serious complication for upstream pathway inhibitors such as the majority that target SMO. ASO treatment, will be effective in these cases and is independent of what mechanism activates the Gli transcription factors. As a result, this treatment can be effective in a wider variety of UC sub-types and may delay drug resistance as there are fewer options to bypass SMO inhibition.

3.5 Conclusion

I have shown the extent to which UM-UC-3 and 253J-BV cells differ in SHH pathway inhibition. Although both cell lines are largely unaffected by ligand inhibition UM-UC-3 is minimally responsive to SMO inhibitors while SMO inhibition was effective in 253J-BV. UM-UC-3 appears to have a constitutively active SHH pathway and 253J-BV appears to be more canonically regulated. I expect that this variability exists in other cell lines and in patient tumors. As such, I targeted the transcription factors regulated by the SHH

pathway, Gli1 and Gli2, with antisense oligonucleotides and found that Gli2 ASO was effective at reducing viability and increasing apoptosis in both cell lines. The bladder provides a unique opportunity for antisense oligonucleotide treatment as it can be applied locally as an intravesical instillation directly into the bladder. To evaluate if this treatment is clinically viable I next validated it in an animal model system I developed for human BCa.

Chapter 4: Development of a murine intravesical orthotropic human bladder cancer (mio-hBC) model

4.1 Introduction

In 2016, it is estimated that there will be 8,700 new cases of BCa occurring in Canada and 2,300 Canadians will die from the disease [136]. NMIBC accounts for approximately 70% of all BCa cases. The standard treatment for patients with non-invasive disease is transurethral resection with adjuvant intravesical treatments in select patients with high risk features. Even with optimal treatments, 60-70% of these tumors will recur, with 25% showing progression to a higher stage or grade highlighting a need to develop novel therapies [137].

In vitro assays using cultured primary or BCa cell lines provide valuable data to study mechanism of development, mutagenesis, invasion, migration and evaluation of antineoplastic drugs. However, there are a number of limitations such as environmental differences, loss of natural heterogeneity, loss of vascularization and perfusion, artificial levels of growth factors and cytokines within the cell culture media. Most importantly, *in vitro* cell culture is limited to 1 to 2 different types of cells in monolayer restricting the study of the interactions between cell types [138].

To overcome this, animal models are needed that more closely mimic human tumors to facilitate the study of carcinogenesis mechanisms while avoiding the limitations of the *in vitro* studies. Thus, a suitable bladder tumor model that resembles human disease both

histologically and in behavior is essential for evaluating new therapeutic agents and modalities. The ideal animal bladder tumor model should include the following characteristics:

1) Tumor should grow intravesically (orthotopically to allow for interaction with normal urothelium, lamina propria and muscle layers).
2) Tumor should be of urothelial carcinoma origin to mimic the natural history of BCa progression.
3) Tumor should be technically easy to develop within a reasonable time period and highly reproducible and reliable.

Many different orthotopic BCa animal models have been developed, from chemical carcinogenesis models [139-141] to genetically modified animal models [142]. However, the models have all shown to be either very toxic or extremely expensive, and no model has shown good reliability [143, 144].

Orthotopic xenografts have shown to be a better approach that allow cell-cell interactions of the local environment and more closely mimic non-invasive BCa (NMIBC) in which primary tumor grows in the urothelium and progresses to invasion into the muscle layers of the bladder [145, 146]. Unfortunately, a current intravesical orthotopic xenograft grown in mice (nude/athymic) and utilizing human urothelial carcinoma cells does not exist. A previous and highly cited intravesical model used KU7 cells which have been determined to have characteristics of HeLa cells and are not of bladder origin [2, 147]. To address this

I have developed a murine intravesical orthotropic human BCa (mio-hBC) model with high reproducibility using intravesical bladder instillation of cancer cells. In addition I have validated this model by assessing the potential of Gli2 ASO treatment determine *in vitro* (Chapter 3) at reducing tumor growth.

4.2 Materials and methods

4.2.1 Animals

One hundred and thirty-seven female athymic nu/nu mice were used to carry out this project (Envigo, South Kent, Washington, USA). All animal procedures were performed according to the guidelines of the Canadian Council on Animal Care (CCAC). The protocol was approved by the Animal Care Committee of the University of British Columbia (Protocol No. A15-0073). Aseptic surgical techniques were used for all procedures. Poly-L-lysine pretreatment was applied to the bladder by instilling 50 µL of 0.1% poly-L-lysine (Sigma-Aldritch Canada Co., Oakville, Ontario, Canada) using a 25G intravenous catheter and letting it dwell for 15 minutes before removing the catheter [2]. Tumor instillation was performed as previously described [2]: Briefly, 6-week old female nude mice were anesthetized (isoflurane, 3% induction, 1.8% maintenance, 1l/minute oxygen), placed on a heating pad and the bladder was emptied (Figure 4.1). Under continuous anesthesia an intravenous catheter was inserted through the urethra. BCa cells in suspension were inoculated (luciferase transfected UM-UC-3-luc at a density of $3x10^6$ cells in 50 µl) into the bladder. A Vascu-Statt plastic clamp (midi, angled) was placed around the urethral

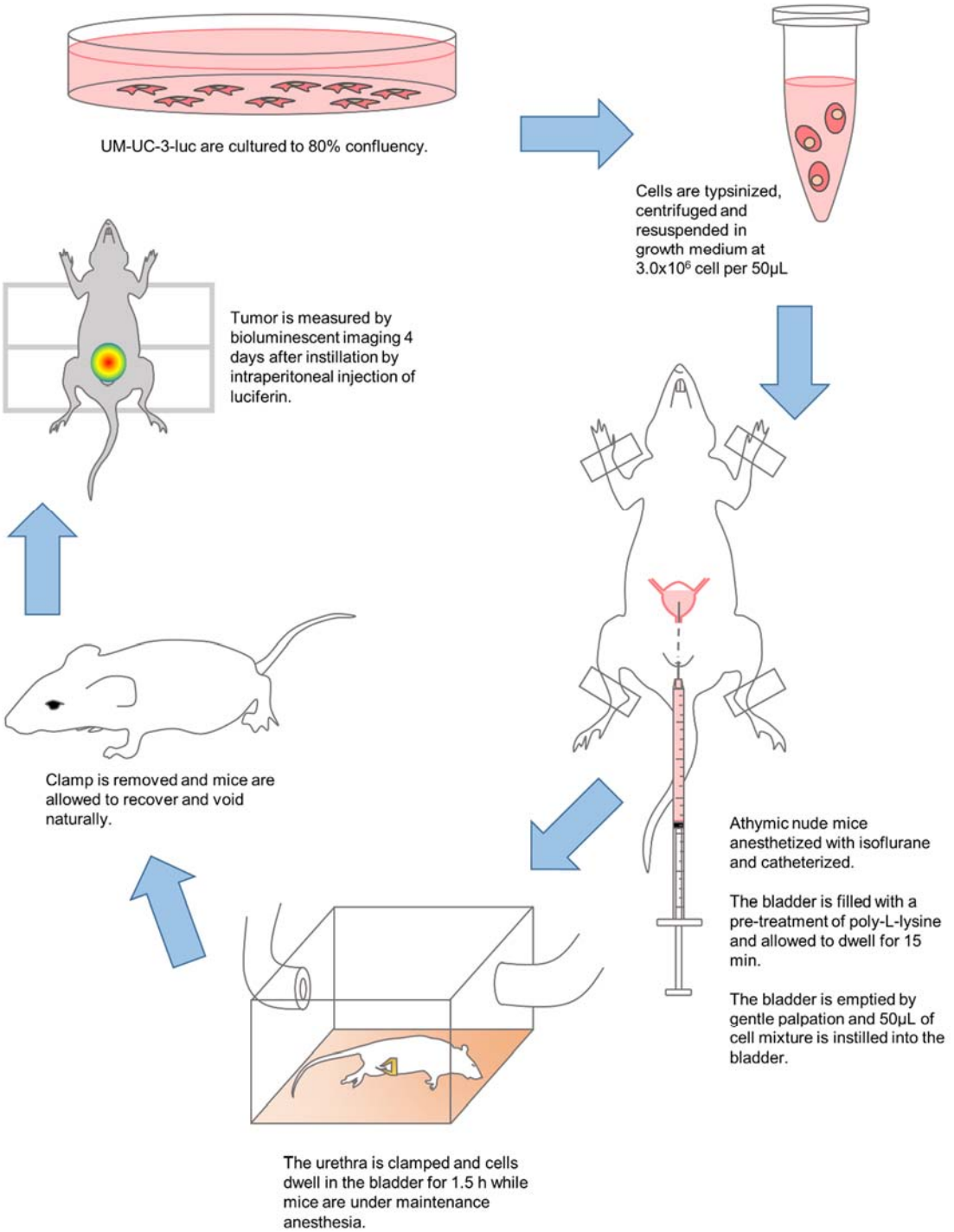
UM-UC-3-luc are cultured to 80% confluency.
Cells are typsinized, centrifuged and resuspended in growth medium at 3.0x10⁶ cell per 50µL
Athymic nude mice anesthetized with isoflurane and catheterized.
The bladder is filled with a pre-treatment of poly-L-lysine and allowed to dwell for 15 min.
The bladder is emptied by gentle palpation and 50µL of cell mixture is instilled into the bladder.
The urethra is clamped and cells dwell in the bladder for 1.5 h while mice are under maintenance anesthesia.
Clamp is removed and mice are allowed to recover and void naturally.
Tumor is measured by bioluminescent imaging 4 days after instillation by intraperitoneal injection of luciferin.

Figure 4.1. Schematic of the murine intravesical orthotopic human bladder cancer (mio-hBC) model. Poly-L-lysine pretreatment is applied to the bladder of anesthetized 6 week athymic nude mice by instilling 50 µL of 0.1% poly-L-lysine using a 25G intravenous catheter and letting it dwell for 15 minutes before removing the catheter. UM-UC-3-luc cells at a density of $3x10^6$ cells in 50 µl are instilled into the bladder. A plastic clamp was placed around the urethral meatus to avoid leakage of the inoculated cells. The inoculated solution was kept in the bladder for 1.5 hours through which time the mice were kept under anesthesia after which the clamp was removed and the bladder emptied spontaneously. At each imaging time point anesthetized mice were intraperitoneally injected with 15 mg/kg sterile D-luciferin in PBS. Fifteen minutes following injection mice were placed in a supine position in an IVIS Spectrum and imaged.

meatus to avoid leakage of the inoculated cells. The inoculated solution was kept in the bladder for 1.5 hours through which the mice were kept under anesthesia. During this time, the mice were surveilled for changes in respiratory patterns, skin color and temperature. After 1.5 hours the clamp and the catheter were removed and the bladder emptied spontaneously. At this moment the mice were removed from anesthesia and places into a heated recovery chamber until they were mobile and urinating normally.

4.2.2 Cell culture

Human BCa cell lines UM-UC-3 (ATCC CRL-1749), UM-UC-14 (ECACC 08090509), T24 (ATCC HTB-4), TCC-Sup (ATCC HTB-5), and SV-HUC-1 (ATCC CRL-9520) were kindly provided by Dr. Peter Black (Vancouver Prostate Centre, Vancouver, BC, Canada) and J82 (ATCC HTB-1) and 5637 (ATCC HTB-9) were kindly provided by Dr. Yoshiyuki Matsui (Kyoto University, Kyoto, Japan). All cells were cultured as described in Chapter 2. Before being used for *in vivo* testing, cells were trypsinized (0.25% trypsin, Thermo Fisher Scientific, Burlington, Ontario, Canada), and centrifuging at 200 x g for 5 minutes. Cell pellets were re-suspended in media, counted (TC20, Biorad, Hercules, California, USA), centrifuged and re-suspended in media at a concentration of $3x10^6$ cells per 50 µL. Cells were immediately placed on ice until instillation.

4.2.3 Luciferase transfection of bladder cancer cell lines

The firefly luciferase gene was transfected into each parental cell line to generate luciferase equivalents (e.g. UM-UC-3-luc) using lentiviral construct as per manufacturer's instruction

(Dual-Luciferase Reporter Assay System, Promega, Madison, Wisconsin, USA) and as previously described [2]. Briefly, a mixture of 10 µg of FUGWB transducing vector, 10 µg pR*.91 packaging vector and 5 µg vesicular stomatitis virus glycoprotein (VSV-G) encoding plasmid was added to 37 µl of $CaCl_2$ (2 M, pH 7.2). 2X HEPES buffer was then added to the DNA-calcium complex and incubated for 30 minutes. After 30 minutes incubation, the complex solution was added to HEK 293T cells. The media of infected HEK 293T cells was changed after 24 hours and after an additional 24 hours the media containing recombinant lentiviral vector was collected, filtered with a 0.45 µm filter and added to BCa cell lines for transduction. The luciferase plasmids contained blasticidin resistance gene to enable positive selection with 10 mg/ml blasticidin (Thermo Fisher Scientific). Quantitative PCR was performed to ensure transcription of luciferase (data not shown) and luciferase activity was tested by adding D-Luciferin (150 ug/ml, GoldBio, St. Louis, Missouri, USA) before measuring bioluminescence on an IVIS Spectrum (Perkin Elmer, Waltham, Massachusetts, USA).

4.2.4 Animal drug treatment

In order to demonstrate the use of our described model 10 untreated mice were chosen at day 40 and assigned to either a mitomycin C (5 mice) or phosphate-buffered saline (PBS) treatment (5 mice) group. Sample sizes were determined using power analysis and the expected values were chosen from the typical growth of the previous model that utilized KU7 cells as we endeavored to replace that model. An alpha of 0.05, beta of 0.8 and expected difference in tumor sizes of $3x10^6$ photons/sec with a standard deviation of $1x10^6$ photons/sec required a minimum N of 4 mice. These mice were instilled with saline (82.5

μL) or mitomycin C (3.3 mg/kg in 82.5 μL solution, Sigma-Aldritch Canada Co., Oakville, Ontario, Canada) for 1.5h following the protocol described for tumor inoculation on days 41 and 47. Tumor size was measured until day 54 (2 weeks post treatment).

4.2.5 Tumor imaging

IVIS Bioluminescence: At each imaging time point mice were anesthetized with isoflurane, weighed, and intraperitoneally injected with 15 mg/kg sterile D-luciferin in PBS. Fifteen minutes following injection mice were placed in a supine position in an IVIS Spectrum bioluminescent imager and photographed at 10 minutes post injection using Living Image 4.0 software. Data was collected as photons/second and displayed as a regionalized heat map with increasing intensity from blue to red. Red represents the upper limit of the color spectrum but does not indicate saturation of the imager. The color range settings are arbitrary to each individual image so that low luminescing tumors can be visualized alongside high luminescing tumors. In figure 4.4 color setting were standardized across all images of the representative mouse to be comparable between imaging days.

4.2.6 Tissue harvesting

At 40 days after UM-UC-3-luc tumor cell instillation, mice were euthanized by 5% isoflurane anesthetization followed by cervical dislocation. Full bladders were excised and harvested. They were preserved by immersion in 10% formalin for 24 hours and then transferred to 70% ethanol until embedded in paraffin.

4.2.7 Immunohistochemistry

Following formalin fixation, tissues were embedded in paraffin. Sections (4 μm) were then prepared and mounted on slides for staining. De-paraffinization was performed by incubating slides at 60°C for 1 hour followed by repeated xylene and ethanol submersion. Antigen retrieval was performed by immersing slides in a container of 0.1 M citrate buffer (pH 6.0) and steaming for 30 minutes after which they were rinsed with water and incubated with 3% hydrogen peroxide for 3 minutes and rinsed again. Blocking buffer (2.5% bovine serum albumin in PBS) was applied to the sections and allowed to incubate for 1 hour at room temperature.

Ki67 (MA5-14520, monoclonal rabbit, Thermo Fisher Scientific, Burlington, ON, CA) and Gli2 (ab26056, polyclonal rabbit, Abcam plc, Cambridge, UK) staining were performed by incubating slides over night at 4°C with the primary antibodies at 1:50 concentration in Dako Antibody Diluent (Agilent Technologies, Santa Clara, CA, USA). Slides were rinsed in PBS and incubated for 1 hour at room temperature in a secondary HRP conjugated antibody at 1:1000 concentration before being rinsed again. Terminal deoxynucleotidyl transferase nick end labelling (TUNEL) was performed by incubating slides for one hour at 37°C with terminal deoxynucleotidyl transferase enzyme in a buffered solution containing bromodeoxyuridine (BrdU) incorporated nucleotides, rinsing with PBS, and incubating with an anti-BrdU antibody conjugated to biotin before rinsing again. A secondary HRP conjugated antibody was applied as mentioned above. All slides above were stained with a DAB+ kit (Agilent Technologies) for 30 minutes, rinsed and stained

with hematoxylin. For hematoxylin and eosin (H&E) staining slides were immersed for one minute in Mayer's hematoxylin solution (Sigma-Aldritch Canada Co., Oakville, ON, CA), rinsed for 15 minutes with water, exposed to reagent alcohol for 30 seconds, immersed in eosin Y solution (Sigma-Aldritch Canada Co.) for one minute and rinsed again. All slides were dehydrated by repeated submersion in ethanol and then xylene and coverslips were affixed using Cytoseal XYL (Thermo Fisher Scientific). Images were captured on a Zeiss Axioplan upright microscope and processed using Zen software suite (Zeiss, Oberkochen, Germany). Images were reviewed and interpreted by a pathologist (L. Fazli).

4.2.8 In vivo assessment of Gli ASOs

Antisense oligonucleotides to Gli2 and the scrambled sequence control (SCR) were obtained from Ionis Pharmaceuticals Inc. (Carlsbad, CA, USA). All antisense oligonucleotides were modified at the 2' position of the sugar with a 2'-o-(methoxyethyl) group on the five bases at both the 5' and 3' termini. The central 10 bases contained deoxyribose and the entire oligonucleotide backbone contained phosphorothioate linkages. The sequence of the Gli2 ASO is 5'-GTGGCGGCACTCCAGCCAGG-3' (Ionis 183652). The SCR oligonucleotide was designed not to match any mRNA in the human or mouse transcriptomes and has the sequence 5'-CCTTCCCTGAAGGTTCCTCC-3' (Ionis 141923).

In order to assess the efficacy of Gli ASO treatment *in vivo* 18 athymic female nude mice were instilled with tumors. Four days following instillation the mice were anesthetized, and injected intraperitoneally with 15 mg/kg luciferin 10 minutes prior to bioluminescent tumor imaging. At this time nine mice were assigned to a Gli2 ASO treatment arm and nine to a SCR ASO treatment arm so that each contained the same mean tumor sizes as determined by bioluminescence. On days 5, 7, 9, 11, 13 and 15 each mouse was intravesically instilled with 15 mg/kg ASO in the same manner as tumor instillation but without tumor cells. Four mice from each group were euthanized by isoflurane anesthetization followed by cervical dislocation following the last ASO treatment and bladders were excised and flash frozen in liquid nitrogen for quantitative PCR analysis. Bioluminescent imaging was used to monitor tumor growth in the remaining mice over a 40 day period after which mice were euthanized and full bladders were harvested to be used for immunohistochemical analysis.

4.2.9 Quantitative PCR

Bladders from the *in vivo* experiment were measured for Gli2 mRNA expression relative to a GAPDH control. Gli2 (Hs01119974_m1) and GAPDH (Hs02786624_g1) TaqMan primer sets were obtained from ThermoFisher Scientific. Frozen bladders were ground in a Precellys 24 bead homogenizer (Bertin Instruments, Rockville, MD, USA) in lysis buffer before being extracted with an RNeasy Mini Kit (Qiagen, Hilden, Germany) following recommended protocols. RNA was quantified on a NanoDrop 2000 (Thermo Fisher Scientific), reverse transcribed using random hexamers (Transcriptor First Strand cDNA

Synthesis Kit, Roche, Laval, QC, CA) and qPCR performed on the resulting cDNA using TaqMan Universal PCR Master Mix (Thermo Fisher Scientific) on a Viia 7 Real-Time PCR System (Applied Biosystems, Thermo Fisher Scientific). ΔΔCT values in comparison to the GAPDH control were calculated [148].

4.2.10 Statistical analysis

All data is represented by mean +/- standard error. Data normality was tested with a Shapiro-Wilk test and equal variance by Brown-Forsyth tests. In the case of data normality and equal variance, differences between groups were determined by a one way ANOVA followed by post hoc Holm-Sidak multiple comparison tests. ASO treated tumors are expressed as a value relative to initial size. Parallel slope analysis on ln transformed data in SigmaPlot was used to determine differences in growth rate. $p \leq 0.05$ was considered statistically significant. All analysis was performed in SigmaPlot (Systat Software Inc., San Jose, CA, USA). Groups with a $p \leq 0.05$ were considered significantly different and indicated by different letter annotations. Groups with annotations that contain a letter similar to that of another group are not significantly different from that group.

4.2.11 Experimental design

I performed five experiments. In experiment 1 I assessed tumor engraftment and growth by instilling 10 mice with UM-UC-3-luc cells and measuring tumor growth over a 40-day period. Mice were imaged periodically (3-4 day intervals) by bioluminescent imaging and

also by small animal ultrasound [149]. After 40 days, mice were euthanized by 5% isoflurane anesthetization followed by cervical dislocation, and bladders were excised for immunohistochemical analysis. In experiment 2 I tested for an engraftment benefit from an instillation pretreatment of poly-L-lysine or trypsin. Tumor instillation was similar to that described previously but with the addition of a 50 uL instillation of either poly-L-lysine or 0.25% trypsin (Thermo Fisher Scientific) for a 15 minutes prior to the introduction of tumor cells. The bladder was gently palpated to express the pre-treatment after the 15 minute period. Tumor growth was then followed by bioluminescent imaging as in experiment 1. Experiment 3 duplicated experiment 2 except that the tumor response to chemotherapy with mitomycin C was tested as described for drug treatment. After optimizing the model with UM-UC-3-luc cells, experiment 4 tested whether this technique could be adapted to a variety of urothelial carcinoma cell lines. The instillation procedure that included poly-L-lysine pre-treatment was used to instill luciferase transfected UM-UC-14-luc (N=6), T24-luc (N=7), TCC-Sup-luc (N=10), J82-luc (N=7), 5637-luc (N=7). This sample size was determined using the power analysis previously mentioned (minimum 4 mice) and was expanded due to the fact that preliminary results and published literature suggested that many cell lines do not engraft well. We increased the mouse number to more accurately determine engraftment success. Tumor growth was monitored as in the other animal experiments. Experiment 5 validated the final UM-UC-3 model by treating tumors developed using this model with the experimental therapeutic Gli2 antisense oligonucleotide.

4.3 Results

4.3.1 Luciferase transfected bladder cell lines showed linear luminesce with cell number

Photon emission values measured *in vitro* are different from those measured *in vivo* due to interference by the abdominal wall in mice. Therefore, I first optimized the number of cells required for efficient bioluminescent intensities before intravesical instillation. I found that luciferase expressing bladder cell lines luminesce linearly with cell number in UM-UC-3 (Figure 4.2) and in the other cell lines tested. For UM-UC-3, baseline luminescence was $6.1x10^6$ photons/s with an increase of 313 photons/cell. Coefficients of determination varied from 0.95 to 0.99 depending on the cell line (data not shown) indicating that luminescence is a good proxy for cell number. Given the photon emission values *in vitro* and the expected interference of the mouse bladder and abdominal wall, I chose a cell number 10-fold greater (approximately $3x10^6$) to ensure equivalent photon transmission in initial *in vivo* trials. A previous validation has shown similar results [149, 150].

4.3.2 UM-UC-3-luc tumors grow quickly with poly-L-lysine pretreatment

One cell line tested, UM-UC-3-luc showed significant increase in luminescence, hereto referred as tumor growth, in select animals (>100-fold) in which engraftment was successful (experiment 1, data not shown). I attempted to increase the rate of successful engraftment by applying a pre-treatment to the bladder in experiment 2. Previous animal models for intravesical engraftment have used trypsin to open the junctions between and

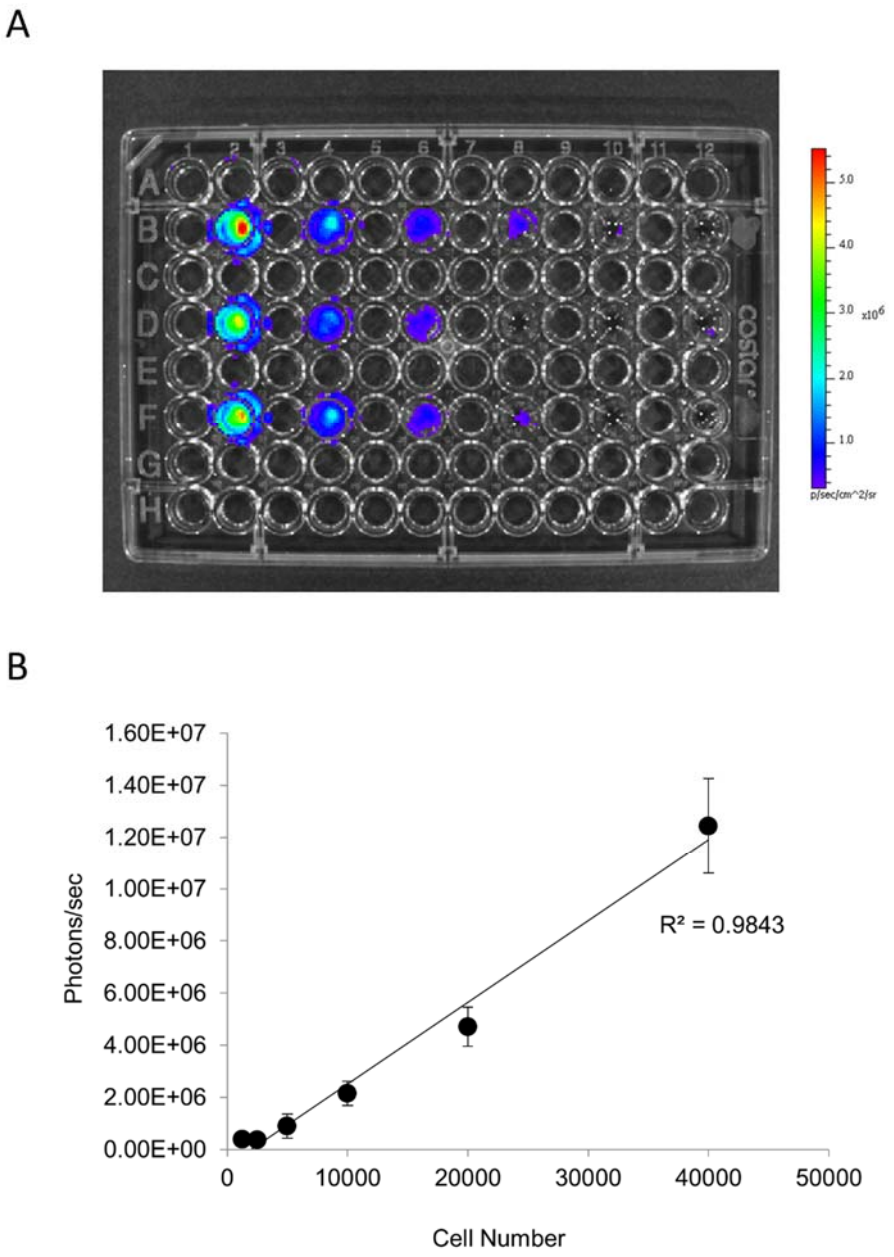

Figure 4.2. Cell Luminescence is linear with cell number. (A) Luminescence of UM-UC-3 cells as imaged on a bioluminescent imager. Columns 2,4,6,8,10,12 contain three replicates each of 40000, 20000, 10000, 5000, 2500, 1250 cells respectively. (B) Luminescence is linear with a coefficient of determination of 0.98, baseline of $6.1x10^6$ photons/s and increase of 313 photons/cell.

remove umbrella layer cells in the bladder lumen. This presumably allows for a better attachment site. Bladder pre-treatment with trypsin overwhelmingly resulted in tumor growth at a maximum of 10-fold over a one month period and reduced the extent to which some tumors grew in initial trials (Figure 4.3A). In addition, 40% of mice exhibited gross hematuria and as a result many mice reached humane endpoint before the experimental endpoint, including immediately after inoculation. Athymic nude mice were found to not be a suitable organism for trypsin pre-treatment in this experiment and as such the growth rate of the successful tumors do not entirely represent the efficiency of this pre-treatment which is much lower than the growth curve suggests. In this model I used a poly-L-lysine pretreatment that was first used for a syngeneic model in 2008 [151]. Poly-L-lysine coats the lumen with a positive charge and aides in tumor cell adhesion [151]. I did not see any adverse health effects in the treated mice as indicated by the lack of hematuria and urinary obstruction, change in mouse behavior or decrease in body weight. Tumor growth was enhanced by 541.6 ± 0.75-fold over trypsin pre-treatment with tumors reaching $3.27x10^9$ ± $1.98x10^9$ photons/sec (N=5) by 30 days (trypsin, $1.97x10^6$ ± $8.54x10^5$ photons/s, p=0.19, N=4) and poly-L-lysine pre-treated tumors had a higher growth rate (as per slope analysis; poly-L-lysine, 0.083±0.058; trypsin, 0.018±0.020, p=0.036, N=5,4). Engraftment variability with poly-L-lysine was reduced (Figure 4.3B) when compared to un-treated mice (see Figure 4.8B for an example of high variability engraftment). Engraftment efficiency was 84.4 ± 4.6% (Table 4.1) when both experiments using the pre-treatment, experiments 2 and 3, were considered together. Despite the fact that poly-L-lysine pre-treatment did not result in significantly larger tumors, the lack of hematuria, high engraftment efficiency, and low variability indicates that poly-L-lysine is at least an

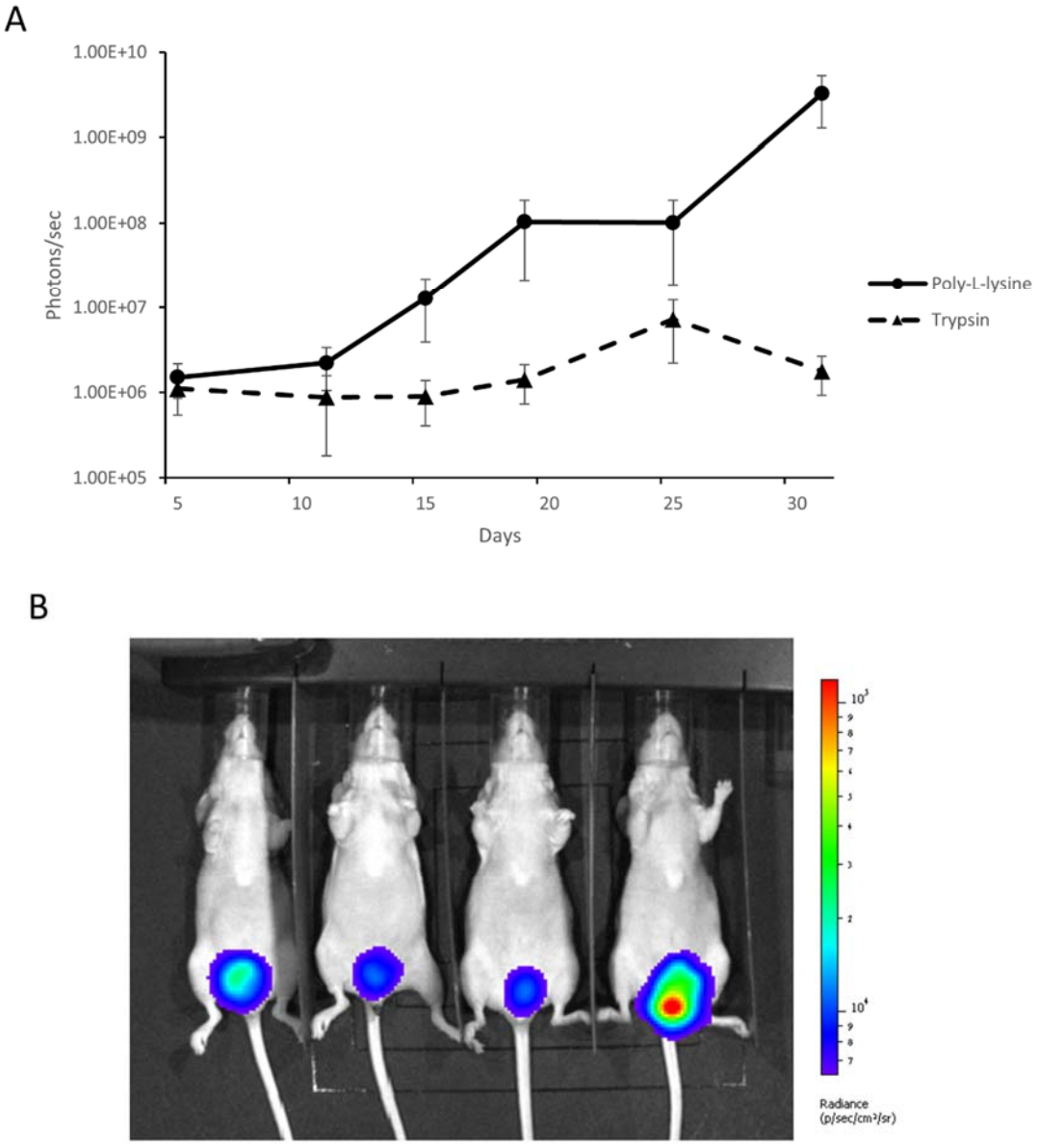

Figure 4.3. Poly-L-lysine pre-treatment resulted in larger and more consistent tumor growth. **(**A) Tumor growth after poly-L-lysine over a period of 30 days. (B) Tumor variability in growth and engraftment after poly-L-lysine pretreatment is much less than in previous trials and can been seen here as similar bioluminescent areas without large differences in intensity (see Figure 4.8 for an example of high variability).

equivalent pre-treatment to trypsin, and when considering the increased growth rate with poly-L-lysine, a better option.

Table 4.1. Tumor engraftment using poly-L-lysine pre-treatment.

Experiment	Mice Instilled (Day 0)	Bladder Tumors present (Day 4)	Engraft-ment Rate	Urethral tumors	Kidney tumors	Failed to engraft	Upper tract obstruction	Mean luminescence (± SE, photons/sec)
2	30	27	90.0%	2	1	0	0	$5.95x10^5 \pm 9.34x10^4$
3	47	38	80.9%	1	2	6	0	$3.81x10^5 \pm 4.17x10^4$
Total	77	65	84.4%	3	3	6	0	$4.74x10^5 \pm 6.42x10^4$

4.3.3 Tumor gross appearance by ultrasound corroborates bioluminescent activity

To compare the actual tumor size and measure luminescence, I used ultrasound technology to visualize tumor growth. Comparative views of a selected tumor's growth via bioluminescent imaging and small animal ultrasound can be seen in Figure 4.4. A region of interest was marked on the mouse at initial imaging and bioluminescence can be reliably compared over time using standardized software instrument settings (Figure 4.4B). A single tumor can be measured as it grows and the bioluminescence level compared to the number of cells that was determined *in vitro*. In addition, bioluminescence can be corroborated by ultrasound imaging of tumors *in vivo* as shown for a select mouse in Figure 4.4C. Our results substantiate that luminescent intensity is comparable to tumor size as has been previously determined [150].

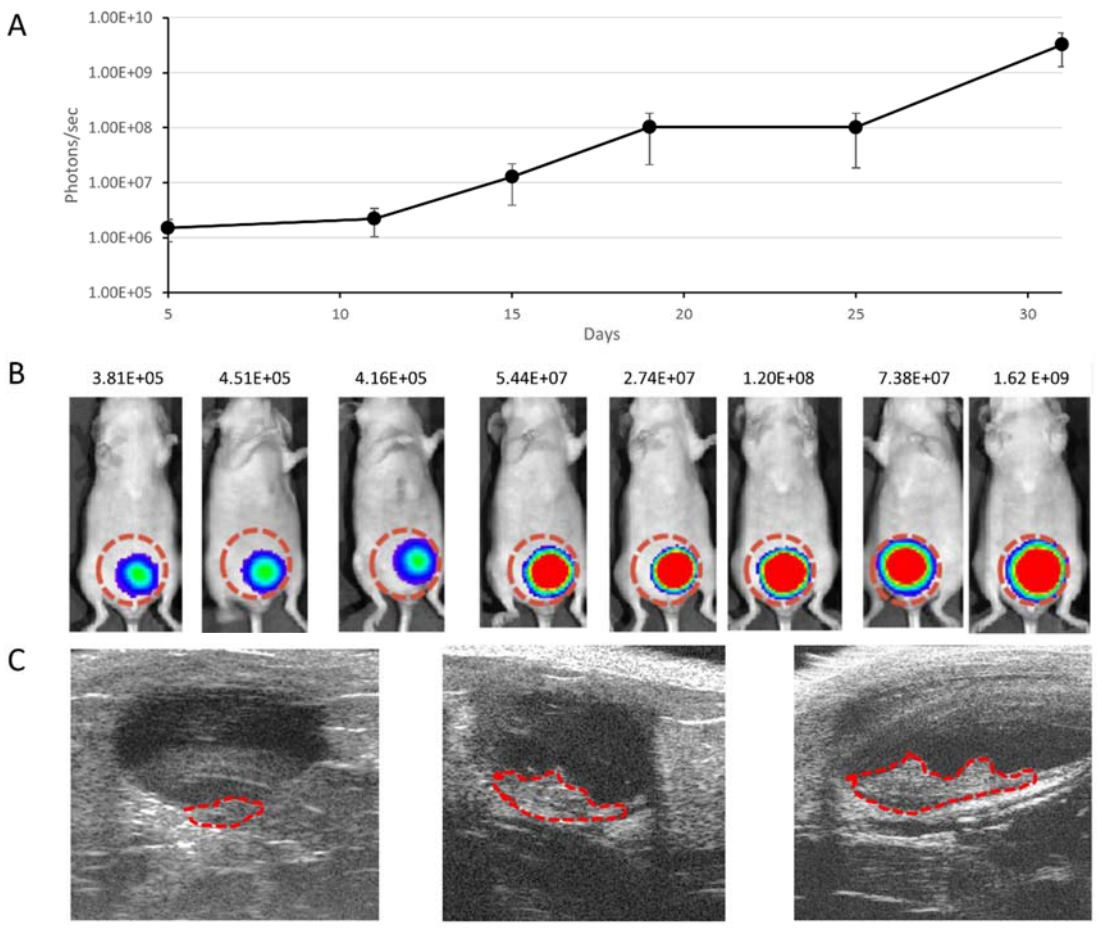

Figure 4.4. Growth in UM-UC-3-luc tumors visualized by bioluminescent imaging and small animal ultrasound. (A) Bioluminescence of UM-UC-3-luc tumors as they grow. (B) Images of a select mouse showing bioluminescence over the course of the experiment. Luminescent values are given above the images. The orange circle delineated the region of interest for measuring tumor luminescence. (C) Select ultrasound images of the bladder with tumors outlined in red at days 10, 20 and 30.

4.3.4 This bladder tumor model recapitulates patient tumors

Primary tumors in the urothelium are vascularized and have cell-cell interaction with the local environment. To establish that our BCa tumors in this model have similar microenvironment, sections of tumor were histologically evaluated. Histology of UM-UC-3-luc tumors showed dense cell growth with large nuclei and prominent nucleoli (Figure 4.5). Some vascularization had occurred but the tumor was vastly necrotic in the center likely due to insufficient blood supply and oxygenation. As can be seen in the top right panel, some tumors will grow to fill the bladder until urethral obstruction occurs and a humane endpoint is reached. These sections show one select tumor that did so by 40 days, our experimental end point. This time point can be altered to reflect an appropriate tumor size and free bladder volume given the permeability of a target drug and the volumes needed for treatment.

In order to determine that the UM-UC-3-luc tumors recapitulate a patient tumor I treated established tumors with a chemotherapeutic, mitomycin C, as would occur in a clinical setting (experiment 3, Figure 4.6). This treatment was applied at 40 days after tumors were well established. Tumor growth was accordingly arrested, and then reduced, by treatment while continued growth was observed in the control arm (mitomycin C, $9.86 \times 10^8 \pm 6.82 \times 10^8$ photons/sec; PBS, $1.22 \times 10^{10} \pm 4.74 \times 10^9$ photons/sec, $p=0.033$, $N=5$). Growth rates in both groups were equal until mitomycin treatment (slope analysis; mitomycin C, 0.052 ± 0.021; PBS, 0.057 ± 0.024; $p=0.89$, $N=5$) after which the treated group showed a

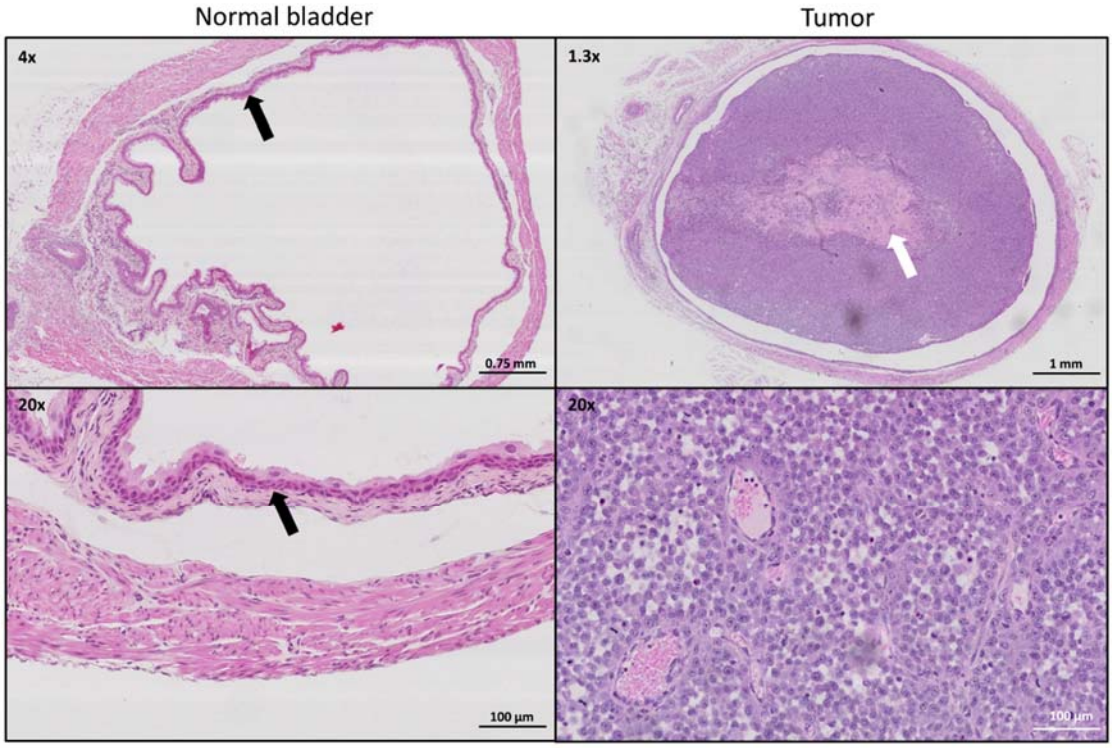

Figure 4.5. Hematoxylin and eosin (H&E) staining of normal mouse bladder and bladder containing UM-UC-3-luc tumors. Image of the entire normal bladder and below enlarged image of the urothelium show normal stratified cells layers marked by a black arrow. The bladder containing a tumor is much larger with a stretched urothelium and little free bladder volume. The tumor displays dense cell growth with large nuclei and prominent nucleoli. Some vascularization had occurred but the tumor is vastly necrotic in the center likely due to insufficient blood supply and oxygenation (marked by a white arrow).

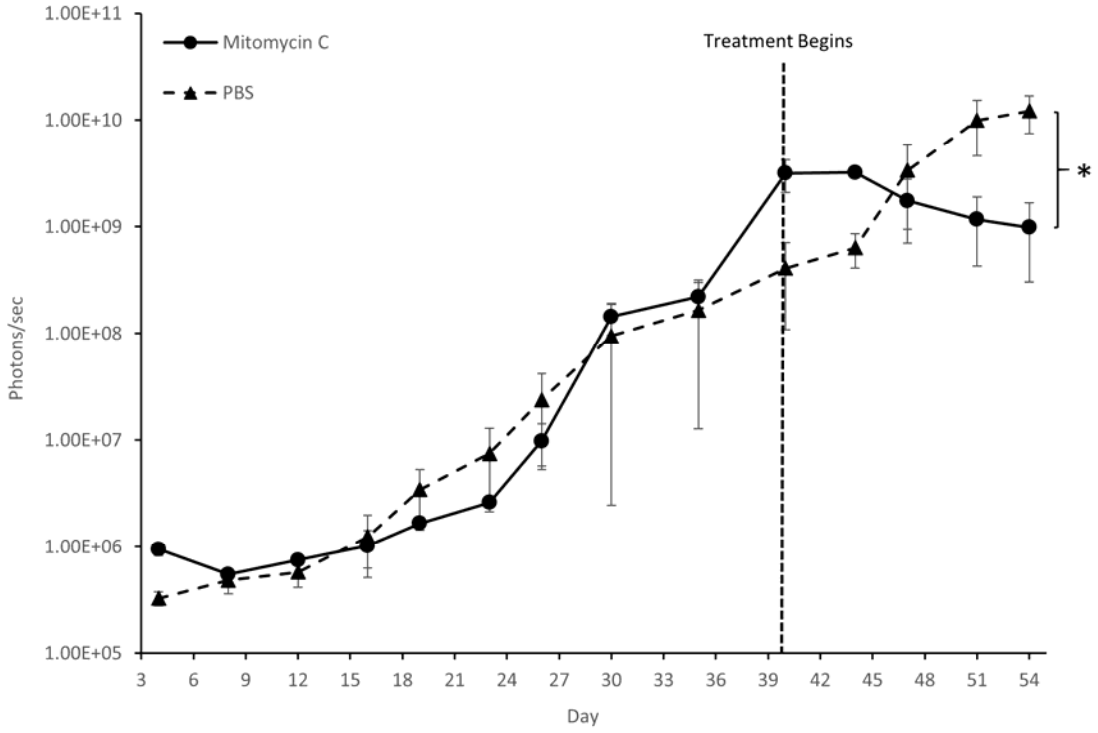

Figure 4.6. UM-UC-3-luc tumors respond to intravesical mitomycin C. Growth of UM-UC-3-luc tumors over 40 days at which point tumors were treated with 3.3 mg/kg mitomycin C. Tumor growth is arrested and then reduced compared to saline control. Vertical dotted line represents start time of treatment. Asterisk denotes significant difference between slopes of the curves by parallel slope analysis ($p \leq 0.05$, N=5).

reduction in growth and the PBS control group continued to grow (slope analysis; mitomycin C, -0.043 ± 0.055; PBS 0.082 ± 0.041; p=0.029, N=5). Immunohistological staining of the treated tumors with H&E, Ki67 as a marker for proliferation and TUNEL as a marker for apoptosis, showed that the surface of the tumor had been affected by mitomycin C treatment while the interior continued to proliferate (Figure 4.7). Diffuse proliferation (more than 10% of tumor cells) and apoptosis was also seen throughout the tumor. Untreated tumors (PBS control) show a staining pattern similar to what was observed in Figure 4.5. I can conclude that this model is responsive to conventional therapy and will be a suitable model for experimental therapeutics.

I have found no evidence of tumor invasion in our sections at experiment end. I cannot rule out the possibility that these tumors will progress to MIBC if given sufficient time. UM-UC-3 is an invasive BCa cell line and has the potential to invade the bladder wall. Truly non-invasive BCa cell lines or less invasive lines such as RT4 do not engraft in intravesical models. It is important to note that our tumors initially grow phenotypically as NIMBC but that this model is not a pure non-invasive tumor model. Despite this distinction, this model is much more applicable to NIMBC studies than the alternative intramural injection of the bladder wall.

4.3.5 Most bladder cancer cell lines had insufficient tumor growth when intravesically instilled in mice

Many BCa cell lines displayed insufficient growth when intravesically instilled at $3x10^6$ cells/mouse (experiment 4, Fig 4.8A). Two cohorts of bioluminescence were initially seen

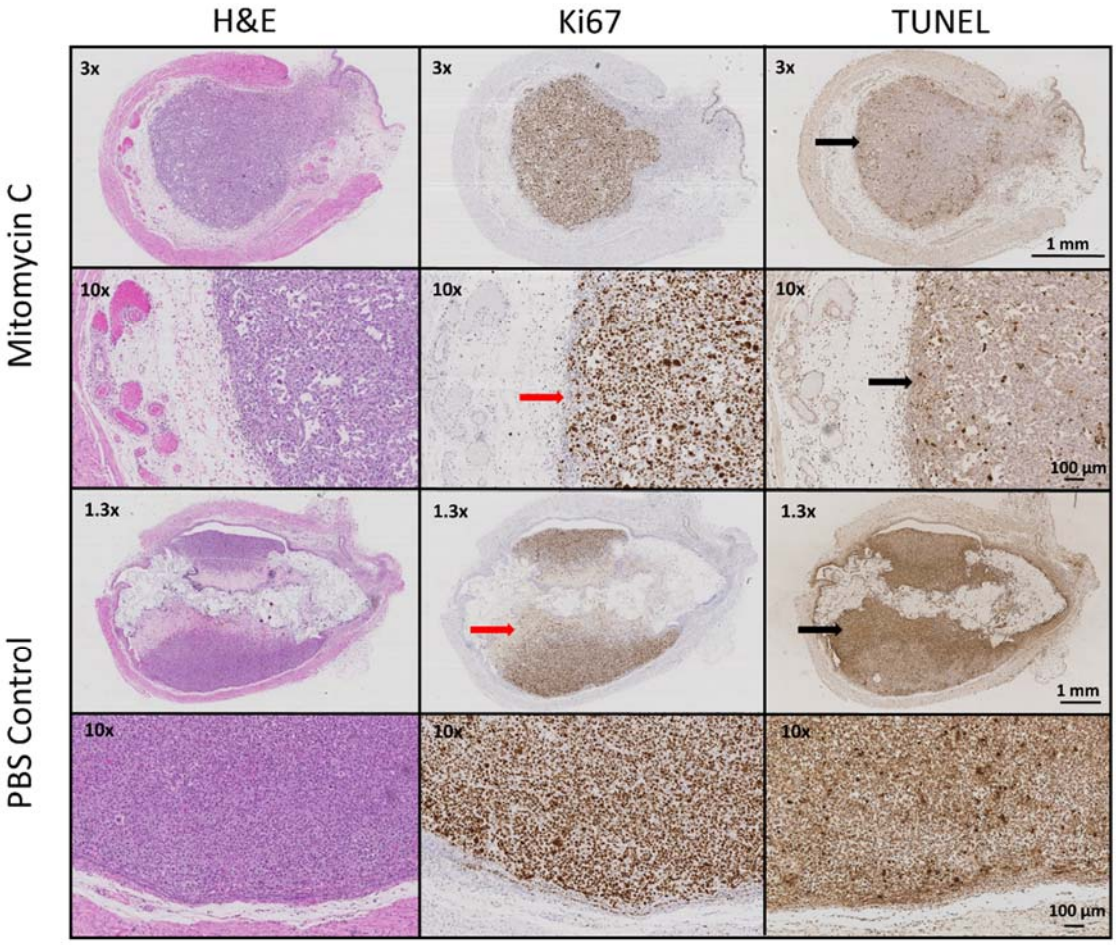

Figure 4.7. Histology of mitomycin C treated tumors. Hematoxylin and eosin (H&E) staining of a smaller mitomycin C tumor shows that it has not yet developed a necrotic core as seen in the much larger saline treated tumor. Ki67 shows cell proliferation in the centre of the mitomycin C treated tumor but not the edge exposed to the drug or in the necrotic core of the control tumor (red arrows). TUNEL shows apoptosis in the outer edge of the mitomycin C treated tumor when it was in contact with the drug and in the necrotic centre of control tumors (black arrows).

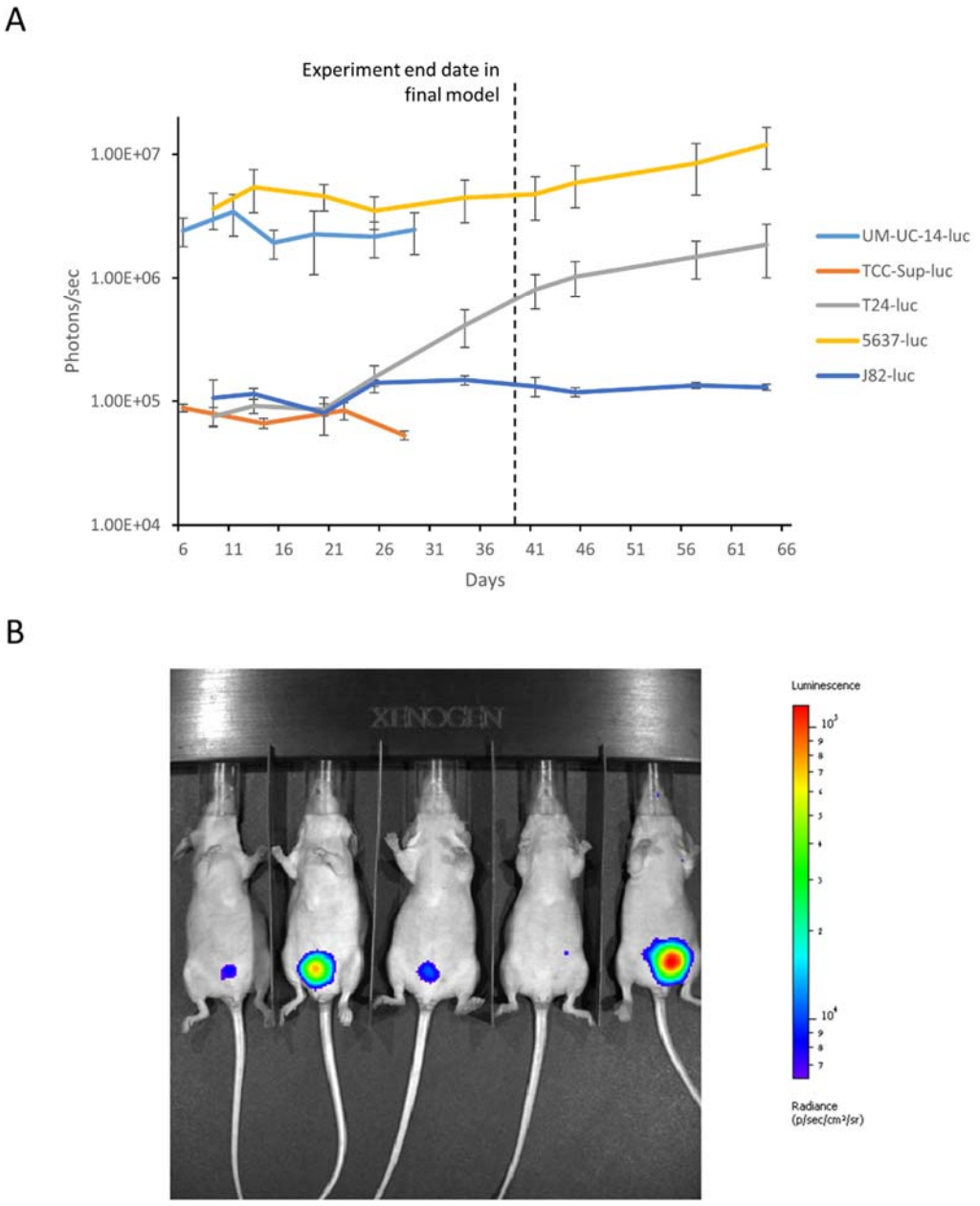

Figure 4.8. Many bladder cancer cell lines were unsuitable for an intravesical model. (A) Tumor growth of 5 BCa cell lines over 66 days. UM-UC-14-luc and TCC-Sup-luc trials were ended early after mice failed to show any changes in bioluminescence. (B) Bioluminescent image at end of trial of five mice instilled with UM-UC-14 tumors highlighting the variability in growth and engraftment within the cell line tumors. Red indicates increased luminescence in photons/sec. This image was consistent with the other cell lines shown in (A).

at $1x10^5$ and $3x10^5$ photons/sec. UM-UC-14-luc and TCC-Sup-luc did not grow over a 30-day period at which point these trials were ceased. J82-luc and 5637-luc showed very modest growth but did grow to a suitable extent by 40 days. Conversely, T24-luc grew 24.7 ± 0.49-fold (p=0.070, N=5) over a two-month period but due to the initially low bioluminescence ($7.52x10^4 \pm 1.35x10^4$ photons/sec), final tumor size did not surpass even the initial sizes of UM-UC-14-luc ($2.54x10^6 \pm 6.30x10^5$ photons/sec) or 5637-luc ($3.65x10^6 \pm 1.19x10^6$ photons/sec) tumors. In addition to the variability seen in tumor growth between cell lines, the lines mentioned above showed high variability in initial engraftment rate in which some tumors failed to engraft as defined by a background level of luminescence (UM-UC-14-luc, 6 of 6; TCC-Sup-luc, 0 of 10, T24-luc, 4 of 7; J82-luc, 6 of 7; 5637, 6 of 7) . An example of engraftment variability can be seen in Figure 4.8B during initial trials with UM-UC-14-luc cells in which bioluminescence varied ($6.0x10^2$ to $1.0x10^3$ photons/sec) and some tumors failed to engraft (defined as background luminescence). As is evident, these cell lines were not suitable for an intravesical model. UM-UC-3-luc appears to be the most efficient cell line for an intravesical orthotopic model.

4.3.6 Gli2 ASO reduced tumor growth in vivo

Mice were instilled with luciferase-expressing UM-UC-3-luc cells as described for previous experiments. These tumors were well established at day 4 and treated with an instillation of 15mg/kg Gli2 ASO or SCR ASO every other day for a total of six treatments. The Gli2 ASO treated tumors failed to grow over a period of 40 days as determined by bioluminescent imaging (p=0.139, N=4) and SCR ASO treated tumors grew to 589.0 ±

351.1-fold (p=0.066, N=5) their initial size (Figure 4.9A). Although final tumors sizes were not significantly different due to small sample size or unequal variance (SCR, 589.0 ± 351.1, N=5; Gli2 0.23 ± 0.06, N=4; p=0.091), parallel line analysis showed that growth rates were significantly higher in the SCR treated tumors (SCR slope, 10.5 relative size/day, N=5; Gli2 slope, -0.006 relative size/day, N=4; p=0.018). Quantitative PCR of bladders from this experiment showed a 7.85 ± 0.80-fold reduction (p=0.066, N=4) in Gli2 mRNA expression in Gli2 ASO treated tumors following the last treatment when compared to controls (Figure 4.9B).

Immunohistochemistry of Gli2 ASO treated bladders showed a smaller tumor in comparison to the control treatment when stained with H&E (Figure 4.9C). The control tumors had a highly necrotic core due to tumor size and lack of sufficient oxygen supply. Surrounding the necrotic area were highly proliferative cells as determined by Ki67 staining. The number of proliferative cells in the Gli2 ASO treated tumors were less. In addition, the Gli2 ASO treated tissue contained diffuse necrotic cells, darkly stained by TUNEL, throughout the tumor. TUNEL staining was lighter in the majority of the control tumor except in the region of necrosis that is concentrated in the tumor core. Gli2 staining showed ubiquitous Gli2 throughout the control tumor and the normal presence of Gli2 in the bladder urothelium. In contrast, Gli2 staining was absent in most of the Gli2 ASO treated tumor while still being detectable in the urothelium due to the fact that the antibody binds mouse Gli2 but the ASO does not target mouse Gli2 sequence.

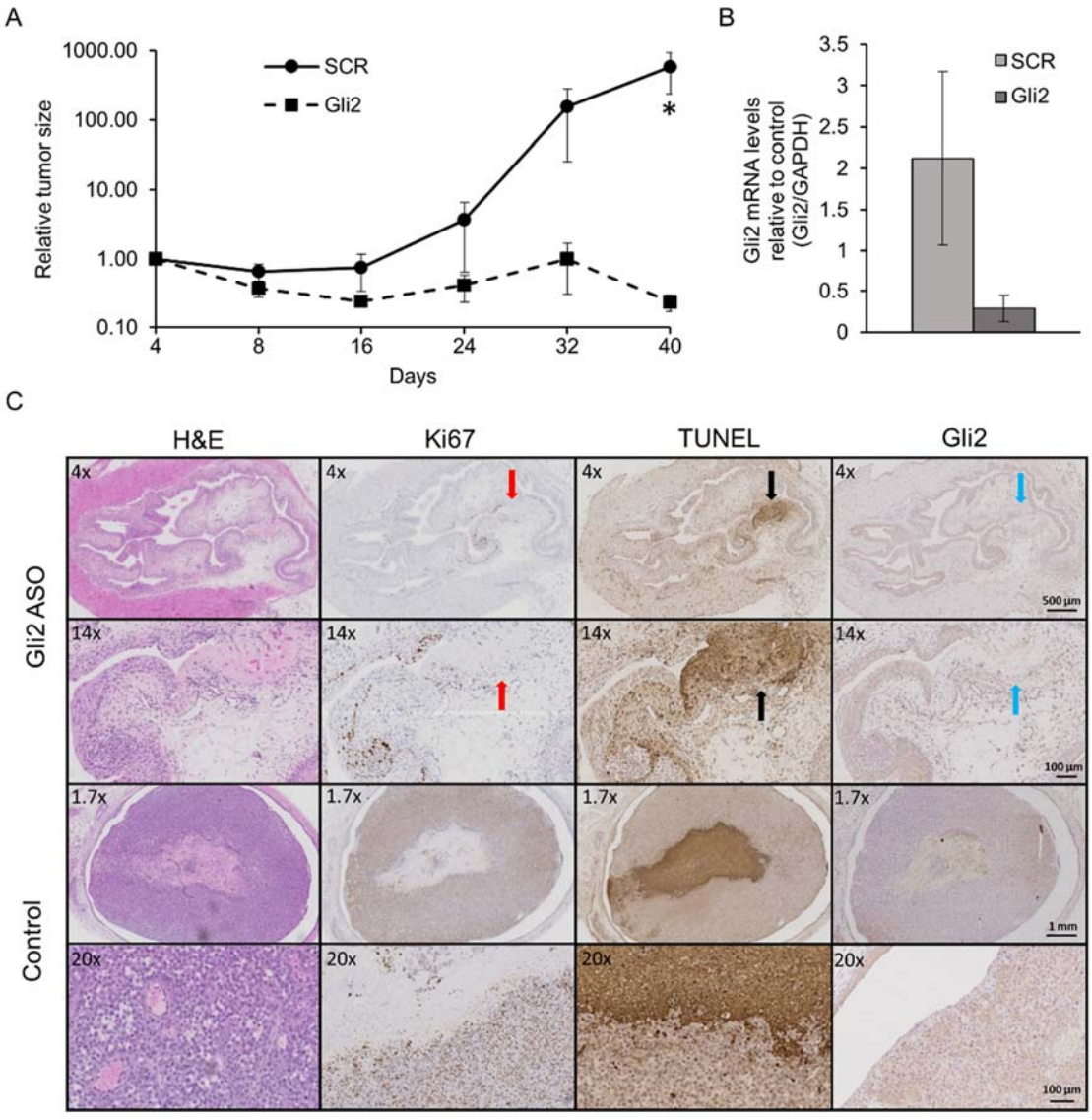

Figure 4.9. Gli2 ASO reduces tumor growth *in vivo*. (A) Growth rates of UM-UC-3-luc tumors when treated six times (over days 5 to 15) intravesically with 15mg/kg Gli2 ASO or a scrambled control oligonucleotide (SCR). (B) Gli2 mRNA expression by qPCR of treated and untreated tumors immediately after last treatment. (C) Immunohistochemical staining of tumors from Gli2 and control (SCR) treated tumors show a decrease in the proliferation marker Ki67 in treated tumors (red arrows) and an increase in the apoptosis marker, TUNEL, staining (black arrows). Gli2 staining is also absent in the treated tumor area (blue arrows). Control tumors show strong Ki67 and Gli2 staining throughout the tumor and strong TUNEL in the necrotic core. Asterisk denotes significant difference between slopes of the curves by parallel slope analysis ($p \leq 0.05$, N=5).

4.4 Discussion

A wide variety of BCa animal models have been previously utilized to evaluate experimental treatments and these have highlighted common pitfalls in model development. Firstly, it is technically more challenging to establish an orthotopic model in the bladder than to establish tumors subcutaneously. The proper placement within the bladder is also a challenge as the natural history of UC involves transition from a luminal non-invasive tumor to an aggressive muscle invasive tumor. The appropriate stage must be chosen in advance. Secondly, tumor take rate can vary greatly depending on tumor cell inoculation location, and the choice of chemical or physical pre-treatment methods to increase engraftment rate. Thirdly, tumor establishment can be time consuming and unreliable. Initial tumors may grow quickly and spread beyond the intended site or too slowly to be practical for drug screening or treatment trials. Lastly, tumors may initially engraft in off target sites, potentially impeding physiological function and being unsuitable for the intended trial.

Mouse models for *in vivo* studies of BCa have been in use for decades and fall mainly into three categories: syngeneic models, xenograft models and transgenic models. Syngeneic models include those in which BCa develops *in situ*, orthotopic models of mouse cell lines implanted into the mouse bladder and implantation outside the cell-originating site, most commonly subcutaneously. A major disadvantage of all syngeneic models is that they require the use of mouse-derived tumors. Results obtained from these models can only be

applied to human carcinoma if it is first determined that the mouse microenvironment and tumor cells are physiologically and biochemically similar to what is seen in patients. For these reasons the use of a human-derived BCa cell line (UM-UC-3 in our model) is often preferred. An important characteristic of syngeneic models is the intact immune system of the host mouse. Mouse BCa cells can effectively evade the adapted immune response of the host mouse and will often engraft and grow. This is ideal for studies requiring an immune component.

In situ syngeneic bladder tumors can be initiated with chemical carcinogens such as the nitrosamines N-Nitrosodimethylamine (NMDA) and N-butyl-N-(4-hydroxybutyl) nitrosamine (BBN) introduced in drinking water [152, 153] or through exposure of the bladder lumen to the parasite haemotobium [152]. Similar tumors arise in some patients with exposure to these agents making this model suitable for those carcinomas but many patients develop transitional cell carcinoma without toxic exposure and its associated mutagenic effects. In such cases, these models may not be applicable. Furthermore, a significant amount of time is needed to develop tumors in these models (commonly on the order of months) which may be unsuitable for large trials. It can therefore be advantageous to have a treatable tumor within a week of orthotopic instillation.

Early syngeneic orthotopic models have been extensively reviewed by Chan et al. (1999) and have been modified since. These models include the use of MB49 cells in the C57BL6/J mouse either through catheterization [154] or injection into the bladder wall with or without laparotomy [150, 155]. Alternatively, intravesically introduced MBT-2

cells have been used in the C3H/He mouse [156, 157]. The strength of an orthotopic model is that the developing tumor will experience a micro-environment similar to the natural tumor state and can interact with the appropriate tumor associated cells. Unfortunately, these models still operate under the restriction of all syngeneic models, the assumption that the mouse cells recapitulate the human counterparts. In addition, tumor take rates can be variable in these models, requiring more mice than the tumors required. A variety of techniques to enhance take rate have been employed and will be discussed below.

Non-orthotopic syngeneic models are commonly used due to the ease of establishing the tumor, the high take rate (often 100%) and the speed at which they grow. Sub-cutaneous injection of MBT-2 tumor cells in the flank and/or shoulder of C3H/He mice is one such example [158]. If treatments are to be applied intravenously or by intra-tumoral injection, then this model will suffice despite the lack of a proper microenvironment. An assumption must be made that the stromal compartment of the skin epithelium sufficiently recapitulates that of the bladder if results from these models are applied to BCa. Orthotopic trials are necessary to remove these potentially confounding factors. Despite this caveat, exploratory trials of new therapeutics can be reliably tested in this model before moving into an orthotopic trial, ideally using an intravesicular modality of administration for superficial tumors.

Unlike syngeneic models, xenograft models allow for *in vivo* studies using human BCa cell lines that have been validated *in vitro* to be similar to a human tumor. The adapted immune response of the host mice used in syngeneic models leads to rejection of human xenografts

and results in a very low take rate. Thus, mice with a compromised adapted immune response such as athymic nu/nu mice or compromised adapted and native immune responses such as severe combined immunodeficiency (SCID) mice are best used. As a result, xenograft models are unsuitable for cancer immunity studies. Orthotopic and non-orthotopic xenograft models are both used with disadvantages and benefits similar to orthotopic and non-orthotopic syngeneic models.

Orthotopic xenograft BCa models include EJ28 cells intravesically instilled into athymic nude mouse bladders [159] and T24 in Balb/C-nu-nu mice [160]. Due to the greater time needed for, and the higher complexity of, orthotopic instillation, sub-cutaneous xenografts in the flank and/or shoulder are often chosen. RT4 cells with and without a matrigel carrier [161, 162], BIU-87 [163], self-luminescent J82 in a matrigel carrier [164], T24 [165, 166] and 5637 [166, 167] have been established in athymic nude mice. Once again, non-orthotopic xenografts suffer the same limitations as those in the non-orthotopic syngeneic models.

The third group of mouse bladder models includes the varieties of transgenic mice with spontaneous bladder carcinoma development. Each genetic alteration can be used to model mutations seen in existing BCa patients without the complexity of tumor implantation. The draw backs are the high cost of transgenic mice and the specificity of the genetic alteration. Bladder tumors differ greatly in their genetic profiles and a single strain of transgenic mouse will target a very specific molecular pathway [23]. Two strains examined are the UPII-SV40T [168] and the Rb-EZH2 transgenic mouse [169]. Although these mice are

extremely useful for genetic studies on the function and effects of a single oncogene the tumors do not represent the comprehensive changes seen in a bladder tumor from a human patient or cell line resulting from cellular adaptation throughout the life of the tumor.

Our model addresses many of the shortcomings of existing models. I have established an orthotopic xenograft model utilizing fast growing UM-UC-3 cells in athymic nude mice. As such, tumors are human cell line derived unlike syngeneic models and experience the natural tumor microenvironment of the bladder absent in non-orthotopic models. Additionally, tumors develop within a week unlike BBN-induced or spontaneous in-situ models and the use of athymic nude mice is cost effective relative to transgenics. Our engraftment rate is 84.4% overall and as high as 90%. A criticism of intravesical models is that the tumor may establish itself in off-target sites such as the ureter and kidney due to reflux or in the urethra due to pressure from bladder filling during inoculation. Our engraftment rates only include mice with tumors in the bladder that did not cause urinary tract obstruction. Off target engraftment in this model was 7.8%. This model is tightly confined to the target site as I did not observe tumors invading through the bladder wall or establishment of tumors outside the bladder.

In order to obtain our engraftment rate, I evaluated previously utilized pre-treatment options. Various methods have been tested to increase cancer cell attachment by disrupting the glycosaminoglycan layer of the bladder or by separating or removing umbrella cells. I evaluated a pretreatment of trypsin as used in a previous orthotopic xenograft [170] at a concentration of 0.25% for 15 minutes. Forty percent of mice showed gross hematuria and

all xenografts grew slowly. I did not test physical bladder wall injury [160], or electrocautery [154, 159] as bladder damage has been found to cause undetected perforations and potential spread of the tumors to the intraperitoneal space [157]. Chemical damage using silver nitrate [171] and acid [172] was avoided due to expected hematuria in the nude mice as was found with trypsin treatment. In my model the cationic polypeptide, poly-L-lysine, for 15 minutes was the best alternative [151]. Tumor growth was rapid reaching a size 500-fold larger than the initial instillation over 40 days. Furthermore, poly-L-lysine increases the electrostatic interaction between cells rather than damaging them and I have found no complications as yet from this pretreatment [151].

An important factor in establishing this model was the need for a non-invasive orthotopic xenograft BCa model. An intramural orthotopic xenograft model that has been previously developed in our centre [149] and has been later adapted to a syngeneic model [155] is excellent for modelling muscle invasive BCa but is not ideal for initially non-invasive tumors or intravesical therapy. The mentioned model involves tumor cell injection into the intramural space next to the muscle in the bladder wall. Both this model and our current model utilize bioluminescent imaging with ultrasound confirmation as had been previously validated [150]. Unfortunately, these tumors do not follow the natural history of originating in the epithelium and growing into the lumen prior to muscle invasion and as such cannot be used to model NMIBC. In addition, this model has an intact epithelium and any therapeutics that are delivered intravesically will first have to be evaluated for their ability to diffuse through the tightly sealed bladder wall. Our model allows for direct

exposure to intravesical therapy similar to what occurs during BCG or chemotherapy following TURBT in the clinical setting.

Our model supplements the existing intramural model by providing a system to evaluate tumors prior to invasion, termed the non-invasive stage. Our cell line of choice, UM-UC-3-luc, displays invasive characteristics such as a high level of migration and invasion, much more so than less invasive-like cell lines such as RT4. I have found that non-invasive cell lines fail to engraft after intravesical instillation so the use of an invasive cell line is a required compromise (see Chapter 2 for UM-UC-3 invasion). Despite this, I have not observed any invasion in our model system at 40 days although progression to an invasive phenotype is a possibility. Treatment of tumors in our model within the first 40 days represents treatment of a tumor with a non-invasive phenotype to the closest extent that I can currently achieve.

The bladder provides a unique opportunity for antisense oligonucleotide treatment and I have used this treatment to validate the potential of this model for evaluating intravesical experimental therapeutics. I found Gli2 ASO at 50 to 100 nM to be effective at reducing BCa cell growth as modeled by UM-UC-3 cells *in vivo*. This ASO also increased apoptosis in both cell lines and resulted in Gli2 protein knockdown. More importantly, local application of Gli2 ASO was effective at reducing tumor growth *in vivo* without visible effects to mouse health. Gli2 knockdown was confirmed in mRNA expression and protein presence in the tumor. An advantage to ASO treatment is that it can target a specific mRNA sequence and have little to no off-target effects if the sequence is confirmed unique

[27]. This potentially solves some of the drawbacks of small molecule drug treatments such as the GANTS or HPIs where it is difficult to target a unique site in a particular protein.

Intravesical instillation of ASOs into the bladder provides direct contact between the ASO and the tumor which allows increased exposure compared to systemic treatment and prevents ASOs acting at off-target sites. The bladder is a unique location in which ASO therapy is potentially highly viable. An additional advantage to utilizing a Gli2 ASO is that this form of therapy directly targets the transcription factor at the end of the SHH pathway. In this way, variability or mutations in proteins up-stream will be ineffective at preventing GLI2 ASO action. Given the prevalence of SHH pathway over-expression in cancers and in BCa specifically, Gli inhibition with ASOs is a promising new treatment modality in urothelial carcinoma.

4.5 Conclusion

I have developed the mio-hBC model for the evaluation for experimental therapeutics on non-invasive human BCa. This model utilized UM-UC-3 luciferase transfected cells intravesically instilled into the bladder of athymic nude mice following an intravesical pretreatment of poly-L-lysine to aid adherence. The model is reliable and reproducible with treatable tumors from 4 to 40 days following instillation. Xenograft tumors recapitulate patient tumors and exhibit a similar response to chemotherapy. Of the other UC cell lines tested UM-UC-3-luc was the only suitable candidate for this model. Despite

this result, the mio-hBC model may be adaptable to other UC cell lines or potentially patient tumor samples for individualized medicine. I validated the model by testing the efficacy of the Gli2 ASO at reducing tumor growth. GLI2 ASO reduced tumor growth, ki67 protein, Gli2 protein and mRNA, and increased TUNEL staining relative to control. Overall GLI2 ASO is a potential treatment to reduce BCa growth and progression and has the advantage of being able to bypass the demonstrated variability in SHH pathway response between cell lines due to other forms of inhibition. Given the ease of intravesical application and the direct action of ASOs on the tumor, GLI2 ASO may be a promising new treatment avenue for BCa

Chapter 5: General discussion and conclusions

5.1 Rationale

BCa impact is high in Canada with the 8th highest mortality rate and higher worldwide where it has the 6th highest mortality rate [4, 136]. Approximately 70% of cases are NMIBC and are treated locally by transurethral tumor resection. The remainder are invasive or metastatic and require more radical treatment such as cystectomy and systemic chemotherapy respectively. Of the non-invasive tumors, 20-30% will recur and advance to invasive disease. In addition, the monetary impact of this disease is quite high at 96 to 180 thousand dollars per patient [6]. New therapies that can prevent the recurrence and progression of this disease will significantly benefit not only patients but also reduce the financial burden associated with BCa.

Development of new therapies in BCa treatment has been slow. The early discovery of the immune-stimulation treatment, BCG, in 1976 set it as the standard of care that is still in practice today [37]. In addition, use of chemotherapies such as gemcitabine, cysplatin, and mitomycin C in combination with transurethral resection of the bladder or cystectomy has allowed patients to survive this disease but not without significant side effects [30, 33, 35]. For example, systemic exposure to BCG can result in septic shock, and chemotherapies that are not selective to tumor cells have many off target effects. Additionally, radical cystectomy, although an efficacious treatment, is not curative in all patients and is associated with significant morbidity. In response to these issues, many research groups,

ourselves included, endeavor to develop targeted therapies to effectively inhibit tumor growth but spare healthy tissue and minimize the need for radical surgery. These therapies have been compiled in the table in Chapter 1.

Our therapy targets the SHH pathway, which was first linked to BCa development in 1993 when 50% of urothelial carcinomas (UC) were determined to have a loss of PTCH receptor heterozygosity [108]. Gli1 is linked to clinical outcomes, pathologic stage, disease free survival and overall survival of patients with BCa [113, 114]. The growing body of evidence suggests that the SHH pathway is important in disease progression and may be a good therapeutic target.

5.2 SHH pathway variability

A panel of cell lines was assessed for protein expression of the SHH pathway transcription factors Gli1 and Gli2 and chose two invasive lines that displayed expression of both factors. Two invasive cell lines that represent a moderate (253J-BV) and severe (UM-UC-3) stage of UC was expected to be biologically similar but this was not the case. Overall, UM-UC-3 appears to be non-responsive to SHH pathway stimulation or inhibition and may be autocrine stimulated or constituently active to a near maximal level. 253J-BV appears to be very responsive to SHH stimulation and inhibition and may be operating in a more canonical paracrine manner. Further studies will be needed to confirm if these modes of pathway activation are correct and will be discussed in a later section. My results are not consistent with previous reports that BCa cell lines rely minimally on the SHH pathway

and that inhibition has only minor effects in BCa [5, 110, 111]. This may be due to the fact that lower concentrations of inhibitors were used or that these studies did not evaluate as wide a range of potential pathway inhibitors. I found only one direct pathway inhibitor, SANT-1, that was effective in UM-UC-3 cells although I did not have access to all published inhibitors or the SMO inhibitors such as GDC-0449 or LDE255, which are ongoing in oncologic clinical trials. Although these cell lines respond differently to current inhibitors, GLI2 ASO was effective at reducing cell growth in both.

The variability in SHH pathway activation presents a significant challenge in developing a treatment that would be pan-effective in BCa. Genetic variability in clinical samples of BCa is well known and classifications have been developed and modified in order to group these tumors into semi-predictable categories [19-23]. Where the cell lines used in this study fit into these various categories and how that knowledge can be used to further understand the SHH pathway remains to be seen. Careful scanning of these genetic data sets has shown no obvious trends in SHH signaling or Gli levels between categories (data not shown). As can be seen by the number of publications in this emerging field, thoughts regarding proper classifications greatly differ and a group meeting last year was convened to begin to understand these discrepancies. Combining data sets including protein levels, mRNA expression and genetic variation would be a first step to address variability in a pathway such as SHH where ultimately pathway function is the desired outcome.

Data regarding the mutational status of oncogenes in select BCa cell lines is available [173]. 253J-BV are low differentiation, p53 wildtype, PTEN wildtype and mesenchymal

with an epithelial morphology. UM-UC-3 are low differentiation, p53 mutant, RB normal, PTEN deleted, CDKN2A homozygous deleted and mesenchymal with a spindle morphology. More severe mutations and gene loss in UM-UC-3 may explain the increased invasiveness in this cell line relative to 253J-BV. This transition is also supported by the spindle morphology seen in these cells. Another morphological difference was the detectable presence of primary cilia in UM-UC-3 only. SHH pathway is thought to function through the primary cilia where smoothened trafficking and Gli activation occur. Despite the lack of primary cilia in 253J-BV, the SHH pathway is stimulated and inhibited as would be expected in canonical signally. UM-UC-3, on the other hand, had activated pathway signaling but was relatively unresponsive to stimulation and inhibition despite having primary cilia. This discrepancy raise the question of the exact function of primary cilia in cancer cells and whether SHH signaling is indeed required to operate through this organelle.

The SHH pathway is impacted by other pathways in cancer cells. Proteins that can affect Gli1 activity include Ren, Dyrk1, K-Ras, TGF-β, PKC-α, p53, and PI3K-AKT [64, 76-80]. It is possible that active oncogenes or the pathways influencing Gli1 are partially responsible for Gli activity in the two BCa cell lines chosen, although blocking the Glis with ASOs would attenuate the effects of these pathways as well. It is currently unknown how UM-UC-3 and 253J-BV fit into all of the genomic classifications for clinical BCa and whether knowledge of the general characteristics of these classes would be helpful in inhibiting the SHH pathway.

5.3 Inhibition

In order to elucidate the most effective form of pathway inhibition I targeted the SHH pathway at three major nodes. The first was at the level of the ligand with two treatments, robonikinin and antibody 5E1, that bind directly to the SHH protein and prevent binding with the PTCH receptor. This treatment modality is most effective when cells are receiving SHH from stromal cells to promote receiving cell growth. In an *in vitro* monoculture SHH must be made by the cancer cells themselves in an autocrine stimulatory manner. I found that UM-UC-3 produce high levels of SHH protein but that 253J-BV do not. Interestingly, both cell lines responded to a very small degree to SHH blockade, likely due to the fact that UM-UC-3 does not respond to exogenous SHH and 253J-BV does not produce any to stimulate its pathway.

The second node targeted was the endosomally bound protein SMO. It is currently unknown how the SHH receptor PTCH prevents SMO translocation to the cell surface but several methods have been suggested [44, 66, 67]. Regardless, SMO is required to bind the complex responsible for the activation of Gli1 and Gli2 and the deactivation of Gli3 [44, 68]. There are 16 inhibitors that have been published that target SMO and prevent Gli activation, two of which are the only FDA approved inhibitors of the SHH pathway, GDC-0449 (Vismodegib) and LDE225 (Erismodegib). This target site was identified as one of the earliest potential sites when the naturally derived compound, cyclopamine, caused birth defects due to SHH interruption in lambs. Surprisingly, of the 4 SMO inhibitors tested using the cell line UM-UC-3, only the inhibitor SANT-1, had any effect that was small.

This was not the case for 253J-BV where both cyclopamine and SANT-1 were effective (others were not tested as they had already failed in UM-UC-3). It was evident that another approach is needed to successfully treat UM-UC-3 and other cancers like it.

The final node that was targeted was the transcription factors at the end of the SHH pathway, Gli1 and Gli2. I endeavored to bypass the variability between cell lines that I found at every stage in my experiments by utilizing an antisense oligonucleotide to Gli1 and 2. Although both ASOs were effective in UM-UC-3, only Gli2 ASO was effective in 253J-BV. This contrasted the results from the other inhibitors in which 253J-BV was always the more responsive cell line. It appears that this line relies on Gli2 to a greater extent for growth and viability. Gli2 is considered to be almost exclusively regulated by the SHH pathway, while Gli1 can interact with other signaling cascades. The decrease in viability, Gli protein levels and increase in apoptosis *in vitro* was confirmed *in vivo* utilizing an animal model that was developed to mimic NMIBC. Gli2 ASO reduced UM-UC-3-luc tumor growth and Gli2 mRNA expression in treated tumors. In addition, IHC of treated tumors showed decreased proliferation and increased apoptosis with Gli2 protein knockdown. Given the ease at which ASOs can be instilled locally into the bladder, this therapy may be a promising new treatment for BCa.

5.4 Animal model

The mio-hBC model addresses limitations of other animal model utilized for BCa trials. Firstly, it is a xenograft model that uses human BCa cells rather than the large variety of syngenic model using mouse cell lines. Secondly, as an orthotopic model the tumor grows

in the appropriate microenvironment (albiet in a mouse), requiring less assumptions about appropriate cell-cell signaling. Thirdly, the procedure is short and the tumors grow quickly relative to *in situ* spontaneous models. Fourthly, this model is more economical than transgenic models. In addition, an intramural, muscle invasive BCa model has been developed in this centre to replicate tumors that have invaded through the bladder wall [149, 174]. Our NMIBC model is an essential pairing to the invasive model in order to be able to evaluate tumor growth and function from the initial non-invasive stage through to invasion, the natural history of BCa progression. The mio-hBC model has the potential to be adapted to other BCa cell lines. UM-UC-3 is an "invasive" line growing as a "non-invasive" tumor and is not a completely NMIBC model as it may progress to invasion into the muscular layers of the bladder. I did not find a non-invasive BCa cell line that would grow in the bladder but many other lines remain to be tested. Other invasive cell lines with different genetic backgrounds or mutations of interest may be suitable for this model.

In order to evaluate the *in vivo* efficacy of Gli ASO treatment an animal model for NMIBC was needed that used true human BCa cells. The model in general comprises two optimizations: a pretreatment and a suitable cell line. The pretreatment is required to open gaps in the tightly sealed umbrella layer of the bladder lumen to allow an anchor point for tumor cells and prevent the cells from being flushed out by urine. The pre-treatment of a 0.25% trypsin rinse of the bladder used in the previous model [2] resulted in hematuria in approximately 40% of the treated mice. This outcome was a humane endpoint for the affected mice and the remaining mice showed little to no tumor growth over the course of the experiment (40 days). Other techniques to increase attachment such as bladder wall

injury were avoided for the same reason and due to he risk of possible perforation [154, 157, 159, 160, 171, 172]. Poly-L-lysine applied for 15 minutes provided a significant increase in tumor growth and attachment efficiency and did not result in any observable negative side effects.

The second optimization was the selection of a suitable BCa cell line; a cell line that can be instilled in a low enough cell number that it can adequately be instilled in the small volume of a mouse bladder and that will attach and grow quickly enough as to be a suitable size for tissue analysis after treatment. I tested a selection of luciferase transfected lines including UM-UC-14, TCC-Sup, T24, 5637 and J82 and found that these lines had either high engraftment variability or did not grow over the duration of the experiment. 253J-BV was not tested due to complications during the lentivirus transformation procedure used to inset the luciferase construct. In addition, 253J-BV is responsive to SHH manipulation and would not reflect the most difficult to treat tumors. UM-UC-3 not only engrafted with a high efficiency but grew to approximately 500-fold initial size in 40 days. This cell line fit the criteria for a robust animal model and characterization of this cell line in Chapters 2 and 3 has shown that the SHH pathway in this cell line is active and difficult to inhibit. As such, UM-UC-3 was suitable for the validation of the model through the evaluation of Gli2 ASO treatment as an experimental therapeutic.

5.5 Limitations and future directions

5.5.1 SHH function in bladder cancer

The purpose of this study was to evaluate the response of the SHH pathway to modulation in BCa cell lines but fully understanding the mechanisms of SHH signaling would be essential to further elucidate the role of SHH in BCa growth and progression. In UM-UC-3 and 253J-BV cells gene copy number, protein levels and mRNA expression of PTCH1, PTCH2, SMO and SUFU would begin to elucidate the greater propensity for pathway activation in 253J-BV. More importantly, knowing the mutational status of these proteins, particularly SMO, could determine if one of these proteins is responsible for constitutive pathway activity or the phenotypic characteristics in UM-UC-3. As such, SMO and PTCH gene sequences should be analyzed. A mutation that prevents SMO dimerization may allow for SMO activity or likewise the inactivation of PTCH's ability to lower phosphatidylinositol-4-phosphate concentrations or allow for vitamin D efflux may prevent PTCH inactivation of SMO. In addition, protein binding assays, such as co-precipitation or the Octet Red System (Pall ForteBio, Fremont, CA, USA) can be used to determine if SHH ligand binding to PTCH is indeed occurring and required.

To assess the importance of upstream regulation, gene knockouts of SMO or PTCH using CRISPR/Cas9 technology can be used to determine if these regulators are entirely responsible for Gli activity or if other actors such as Rb or PKA may driving transcription at the level of the SUFU complex or GSK-3β. In general, little is known of the cellular mechanisms between PTCH binding to SHH and Gli translocation to the nucleus. Over

the course of this thesis this area has greatly increased in attention and comprehensive reviews of the current state of knowledge surrounding SHH pathway function can be found for normal development [175] and in individual urological cancers [176]. A comparison of SHH signaling between these two cell lines (of the same disease) may provide a unique opportunity for understanding pathway variability in general.

Gli proteins are a set of transcription factors that require protein processing and activation or deactivation. As such, total protein or mRNA levels may not provide as clear a picture of pathway activity as direct measurements of protein activity. However, large increases or decreases in protein levels are likely to result in a larger proportion of activated and deactivated forms as well. Indeed, I found phenotypic outcomes such as viability and apoptosis were linked to total Gli protein levels.

In this thesis I addressed Gli1 and Gli2 but not the transcriptional repressor Gli3. This is largely because I was interested in inhibition or deactivation of the SHH pathway and as a repressor, Gli3 would already be performing this function in the absence of SHH signaling. Therefore, to decrease signaling I decided to target the transcriptional activators Gli1 and Gli2. In addition, at the outset of this thesis there were no reliable commercially available antibodies to Gli3. Multiple different commercially available sources of Gli3 antibody were later obtained but none provided reliable or valid results in either western blot analysis or immunohistochemistry. A privately developed antibody had some success but I was unable to procure it (personal communication). There was also a large body of previous research surrounding Gli1 and Gli2 on which I could expand on in BCa. Since then,

research on Gli3 has continued and Gli3 has been found to be essential in regulating SHH pathway function. Removal of repression is an important aspect of gene expression [44]. Assessing the function of Gli3 is an important future direction for this project.

The readout for Gli activity in this project was cell viability and apoptosis. The link between Glis and these phenotypic effects is evidenced by the decrease in viability due to Gli inhibition, increase in apoptosis and the large body of literature supporting Glis and cell growth. It is possible that the targeted therapies in this study may directly interfere with other pathways that affect cell viability but it is likely that these pathways are downstream of the Gli transcription factors as has been introduced in Chapter 1. Further studies will be needed to determine exactly what these pathways may be in these BCa cell lines. There is some discussion surrounding the assay to determine viability, MTS, as to whether it is measuring proliferation. This assay is marketed and commonly used in the literature as a proliferation assay [177] and my results can be interpreted as proliferation according to this standard. The mechanism of the assay involves measuring the metabolized MTS product to determine cell number but this result can be influenced by total mitochondrial content, or enhanced mitochondrial activity of cells that have not proliferated. As such, I have reported all my results as viability. Confusion can arise when interpreting the meaning of a decrease in viability as cells cannot become less viable. In this case the cells have reduced metabolic activity or cell number has decreased. A future experiment could use an assay that detects cell number such as CyQUANT (Thermo Fisher Scientific, Burlington, ON, CA) or BrdU.

I recently assessed the Gli inhibitors GANT-61 and HPI-1 in UM-UC-3 and 253J-BV cells over the course of 7 days and analyzed the results using the more recent CyQUANT assay for proliferation (Figure 5.1). In addition, I evaluated Gli1 and PTCH mRNA levels as potential reporter genes for pathway activity as they are directly regulated by the Gli transcription factors (Figure 5.1). CyQUANT showed a dose dependent decrease in cell number with drug concentration, a trend that was less apparent in viabilty. This result suggests that although cell number is decreasing there may be an enhancement in mitochondrial activity in treated cells that prevents a noticeable decrease in viability. These growth results do confirm the efficacy of Gli inhibition in BCa cell lines but UM-UC-3 was only growth inhibited to approximately 80% at a very high drug concentration of 25 µl. Gli2 was more effective with an IC_{50} of 100 nM. In addition, both GANT-61 and HPI-1 have low solubility in biological fluids and require DMSO or EtOH vehicles which can limit their delivery *in vivo*. Regarding the reporter genes, Gli and PTCH mRNA was reduced by inhibitor treatment in UM-UC-3 but not in 253J-BV indicating that they may not be suitable reporters for every BCa that exhibits SHH activity, even if growth is reduced by Gli inhibition. Once again, there is large variability in pathway response between cell lines.

CyQUANT analysis seems a reliable way to assess SHH effects on growth in future studies. Viability analysis by MTS assay does still appear to be a conservative indicator of SHH inhibition, detecting relatively strong effects of pathway inhibition. Viability would detect, but not discriminate between, decreases in mitochondrial activity due to senescence, apoptosis and decreased proliferation. Indeed, there is a large body of evidence linking

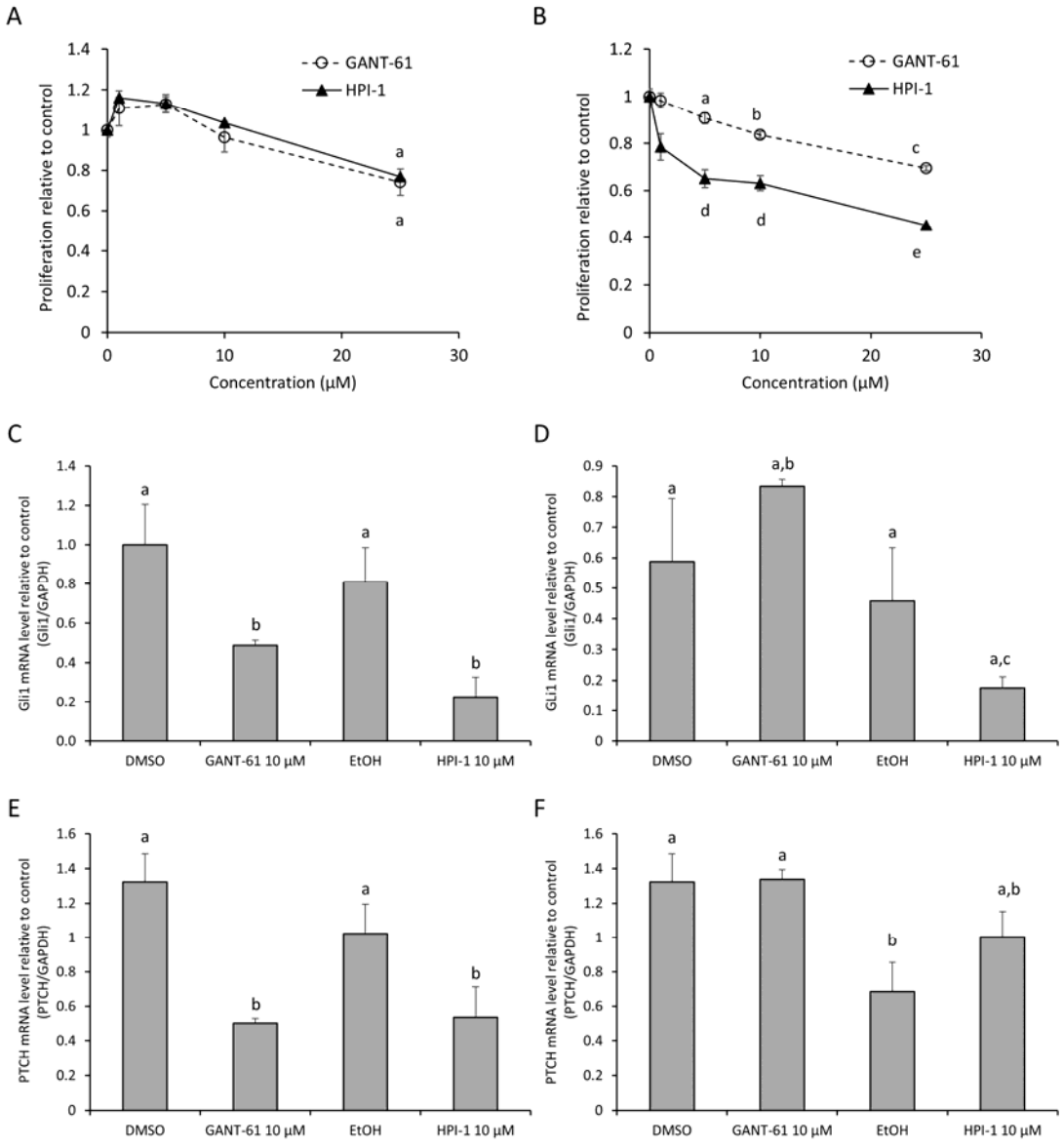

Figure 5.1. BCa cell lines respond in growth to GANT-61 and HPI-1. UM-UC-3 cells (A) and 253J-BV cells (B) show a dose dependent decrease with both GANT-61 and HPI-1 inhibitors when compared to a vehicle control (0 concentration) and when analyzed by CyQUANT. Gli1 mRNA expression and PTCH mRNA expression show a decrease when UM-UC-3 is treated with both inhibitors (C,E) but 253J-BV only shows a mRNA decrease in Gli1 when treated with HPI-1 (D,F). Different letters denote significant differences between groups as determined by one way ANOVA with Holm-Sidak post hoc tests ($p \leq 0.05$, N=3)

anti-Gli therapies to viability in cancer. GANT-61 has been used to reduce viability in acute myeloid leukemia, melanoma, neuroendocrine carcinoma of the lung and in pediatric tumors [125, 128, 132, 133]. Gli inhibitors including SANT-1 and cyclopamine decrease viability in prostate cancer, gastrointestinal stromal tumors and cervical cancer [127, 129, 178]. Conversely, SHH stimulation increases viability in colorectal and breast cancer and Gli2 protects viability in hepatoma cells [126, 130, 131]. In addition to viability, another phenotypic readout could be migration and invasion. SHH is tightly linked to epithelial-mesenchymal transition (EMT) that is marked by an increase in migration and invasion [78, 91-93]. Both migration and invasion can be included with proliferation/viability as a hallmark of disease progression.

5.5.2 SHH inhibition

A limitation in this study regarding SHH inhibition is that it was unfeasible to test the wide range of SHH inhibitors that are available. I chose inhibitors that were commercially obtainable for research purposes and that acted on a range of nodes in the SHH pathway reflecting common therapeutic sites. SMO was an essential site due to the large number of available inhibitors that grew out of the discovery of cyclopamine. In addition, Gli inhibitors GANT-58, GANT-61, HPI1 and HPI4 were chosen to compare against the Gli targeted therapy, Gli1 and 2 ASO. These were unsuccessful in UM-UC-3 but GANT-61 and HPI1 were effective in 253J-BV over a period of up to 7 days (data not shown). I decided to continue experiments on SMO inhibitors because they were the only effective treatment in UM-UC-3. Unfortunately, I was not able to obtain GDE-0449 or LDE225

which are now the gold standard for SHH inhibition in medulloblastoma and the two compounds of the most interest when comparing the efficacy of our Gli2 ASO. Evaluation of these inhibitors in BCa would be the next step for this project.

Gli2 ASO was successful at reducing tumor growth *in vivo* but ASOs have previously failed to show improvement in clinical trials due to a range of complications. The first is nucleotide delivery to the tumor and to the nucleus of the cancer cell where it is required to bind pre-mRNA and induce RNase activity [179, 180]. Tumor delivery is uniquely efficacious in intravesical therapy where the tumor is in direct contact with the ASO solution. Effective oligonucleotide delivery to the nucleus requires that nucleotides escape endosomes after being endocytosed at the cell surface. The majority of nucleotides will remain in endosomes and associated vesicles before being broken down in the lysosome. At select points in vesical trafficking temporary lipid monolayers allow for nucleotide escape and once in the cytosol they can readily enter the nucleus [179]. Many nanoparticle carriers that increase membrane permeability have been developed for nucleotide treatment and these may potentially increase the efficacy of Gli2 ASO treatment. The second complication is that antisense oligonucleotides can elicit an innate immune response by triggering toll-like receptors [179]. Although this is a disadvantage for systemic treatment, intavesical therapy such as BCG already utilizes an immune response to treat tumors and may be an added benefit to ASO treatment. Intravesical therapy of BCa may be a niche in which ASOs can avoid systemic complications and provide clinically relevant outcomes.

5.5.3 Genetic variability

The variability found in SHH signaling between the two cell lines tested suggests that there is also a large amount of genetic variability in BCa cell lines. As mentioned in the previous sections, genetic variation is being quantified in patient sample of BCa but this research remains to be replicated in cell lines. Unpublished results of a large sampling of cell lines is currently being compiled by MD Anderson Cancer Centre (personal communication) but this information has not yet been released to the scientific community. It is interesting to consider that although UM-UC-3 and 253J-BV are both derived from MIBC and are both classified as a basal subtype (compared the alternative luminal subtype) the wide variety of classification systems suggests that these two lines may diverge in more stringent classifications [135]. The overall understanding from these studies is that BCa, like all other cancers, is highly individual and finding a common pathway amongst this variability will be an important challenge in the future. This signals the importance of personalized medicine in BCa or at the very least an understanding of which treatment modalities are the most probable for success. My therapy using Gli2 ASO is effective *in vitro* due to a common reliance on Gli2 in the two cell lines chosen but its efficacy in other cell lines and in patient samples remains to be seen. This therapy has yet to be confirmed in multiple cell lines *in vivo* as an animal model using 253J-BV could not be established but I predict that there would be a common reliance on Gli2 in this environment as well.

An important next step then is to evaluate Gli ASO in other cell lines, especially those in which Gli proteins are not present. I predict that without a strong dependence on SHH as evidenced by Gli protein presence it is unlikely that the ASO will be effective at reducing

growth or progression. It is possible that other cell lines are utilizing the SHH pathway but due to protein turnover the Gli levels are not as high as in the tested cells. More likely it is the importance of the SHH pathway temporally, especially during the transition from a non-invasive to invasive tumor, that will validate the use of SHH inhibition. Glis may not be constitutively elevated but are activated in order to increase EMT and establish an invasive phenotype [115-117]. This would mean that cell lines would not be the best way to evaluate Gli2 ASO but rather an animal model starting as a non-invasive tumor (will be discussed below). Alternatively, SHH is important in cancer stem cell signaling where it can initiate growth and drug resistance [85, 86, 89, 90]. Appropriate models are required to evaluate these other roles of SHH in cancer.

5.5.4 mio-hBC model

The mio-hBC model was developed to evaluate treatments on non-invasive tumors but the potential exists for the progression of these tumors to an invasive growth pattern or invasion into bladder wall. Preliminary analysis by immunohistochemical staining of these tumors at different time points throughout the 40 day period of the model were inconclusive (data not shown). A larger sample size and greater sectioning is needed to pinpoint the tumor location in the bladder and obtain a sagittal section through the invasive front. If these tumors invade, which I predict they will, SHH expression patterns can be measured over a time interval and the effects of Gli2 ASO on time to invasion, frequency of invasion, or invasion rate could be determined. This model may then be able to evaluate a tumor not only at the non-invasive stage but also at the transition point to a muscle invasive BCa.

Characteristics of the invasion process, such as regional signaling or genetic differences could also be elucidated and potentially interrupted, leading to a greater understanding of the triggers of disease progression.

This model may also be adapted to a patient derived xenograft (PDX) model. Currently PDX models for BCa involve implanting BCa patient samples obtained by transurethral resection under the renal capsule [181]. The advantage of this system is that therapies can be evaluated directly on the patient's own tumor and clinical outcomes can be predicted from the response. A disadvantage is that this model is not orthotopic and although the original genetic signatures of the patient tumor are retained, the microenvironment is much different than then bladder. The mio-hBC model may be adapted to PDXs by attaching samples surgically to the bladder lumen or using a non-invasive adhesive such as matrigel or a hydrogel bio-glue. These tumors can then be imaged with small animal ultrasound following local intravesical treatments for BCa as would occur in a clinical setting. This model has great promise for developing bladder PDXs and may be a helpful tool in the future of BCa research.

5.6 Conclusion

I have found that the high variability in SHH pathway function between two BCa cell lines, UM-UC-3 and 253J-BV, poses a significant challenge to the inhibition of this pathway. The most common form of inhibition, SMO inhibition with small molecules, is ineffective and I found that direct inhibition of Gli2 with an antisense oligonucleotide (ASO) is the

most effective treatment. In order to confirm this result *in vivo*, I developed a murine intravesical orthotopic human BCa (mio-hBC) model utilizing UM-UC-3 cells and a bladder pre-treatment of poly-L-lysine in athymic nude mice. Gli2 ASO was effective at reducing tumor growth in this model, validating the model and confirming the potential of Gli2 ASO therapy as a new treatment modality for BCa.

Bibliography

1. Rimkus, T.K., R.L. Carpenter, S. Qasem, M. Chan, and H.W. Lo, *Targeting the Sonic Hedgehog Signaling Pathway: Review of Smoothened and GLI Inhibitors.* Cancers (Basel), **2016**. 8(2).
2. Hadaschik, B.A., P.C. Black, J.C. Sea, A.R. Metwalli, L. Fazli, C.P. Dinney, M.E. Gleave, and A.I. So, *A validated mouse model for orthotopic bladder cancer using transurethral tumour inoculation and bioluminescence imaging.* BJU Int, **2007**. 100(6): p. 1377-84.
3. Statistics, C.C. *Urinary system cancer*. 2016 [cited 2017 April 4]; Available from: https://www.crs-src.ca/page.aspx?pid=1329.
4. Burger, M., J.W. Catto, G. Dalbagni, H.B. Grossman, H. Herr, P. Karakiewicz, W. Kassouf, L.A. Kiemeney, C. La Vecchia, S. Shariat, and Y. Lotan, *Epidemiology and risk factors of urothelial bladder cancer.* Eur Urol, **2013**. 63(2): p. 234-41.
5. Pignot, G., A. Vieillefond, S. Vacher, M. Zerbib, B. Debre, R. Lidereau, D. Amsellem-Ouazana, and I. Bieche, *Hedgehog pathway activation in human transitional cell carcinoma of the bladder.* Br J Cancer, **2012**. 106(6): p. 1177-86.
6. Botteman, M.F., C.L. Pashos, A. Redaelli, B. Laskin, and R. Hauser, *The health economics of bladder cancer: a comprehensive review of the published literature.* Pharmacoeconomics, **2003**. 21(18): p. 1315-30.
7. Noyes, K., E.A. Singer, and E.M. Messing, *Healthcare economics of bladder cancer: cost-enhancing and cost-reducing factors.* Curr Opin Urol, **2008**. 18(5): p. 533-9.

8. Standring, S. and N.R. Borley, *Gray's Anatomy: The Anatomical Basis of Clinical Practice*. 2008: Churchill Livingstone/Elsevier.

9. Brandt, W.D., W. Matsui, J.E. Rosenberg, X. He, S. Ling, E.M. Schaeffer, and D.M. Berman, *Urothelial carcinoma: stem cells on the edge.* Cancer Metastasis Rev, **2009**. 28(3-4): p. 291-304.

10. Weissman, I., *Stem cell research: paths to cancer therapies and regenerative medicine.* JAMA, **2005**. 294(11): p. 1359-66.

11. Kamat, A.M., M. Bagcioglu, and E. Huri, *What is new in non-muscle-invasive bladder cancer in 2016?* Turk J Urol, **2017**. 43(1): p. 9-13.

12. Sylvester, R.J., A.P. van der Meijden, W. Oosterlinck, J.A. Witjes, C. Bouffioux, L. Denis, D.W. Newling, and K. Kurth, *Predicting recurrence and progression in individual patients with stage Ta T1 bladder cancer using EORTC risk tables: a combined analysis of 2596 patients from seven EORTC trials.* Eur Urol, **2006**. 49(3): p. 466-5; discussion 475-7.

13. Mayr, R., M. May, T. Martini, M. Lodde, A. Pycha, E. Comploj, W.F. Wieland, S. Denzinger, W. Otto, M. Burger, and H.M. Fritsche, *Predictive capacity of four comorbidity indices estimating perioperative mortality after radical cystectomy for urothelial carcinoma of the bladder.* BJU Int, **2012**. 110(6 Pt B): p. E222-7.

14. Bokarica, P., A. Hrkac, and I. Gilja, *Re: J. Alfred Witjes, Thierry Lebret, Eva M. Comperat, et al. Updated 2016 EAU Guidelines on Muscle-invasive and Metastatic Bladder Cancer. Eur Urol 2017;71:462-75.* Eur Urol, **2017**. 72(2): p. e45.

15. Lindgren, D., A. Frigyesi, S. Gudjonsson, G. Sjodahl, C. Hallden, G. Chebil, S. Veerla, T. Ryden, W. Mansson, F. Liedberg, and M. Hoglund, *Combined gene*

expression and genomic profiling define two intrinsic molecular subtypes of urothelial carcinoma and gene signatures for molecular grading and outcome. Cancer Res, **2010**. 70(9): p. 3463-72.

16. Sjodahl, G., M. Lauss, K. Lovgren, G. Chebil, S. Gudjonsson, S. Veerla, O. Patschan, M. Aine, M. Ferno, M. Ringner, W. Mansson, F. Liedberg, D. Lindgren, and M. Hoglund, *A molecular taxonomy for urothelial carcinoma.* Clin Cancer Res, **2012**. 18(12): p. 3377-86.
17. Aine, M., P. Eriksson, F. Liedberg, G. Sjodahl, and M. Hoglund, *Biological determinants of bladder cancer gene expression subtypes.* Sci Rep, **2015**. 5: p. 10957.
18. Volkmer, J.P., D. Sahoo, R.K. Chin, P.L. Ho, C. Tang, A.V. Kurtova, S.B. Willingham, S.K. Pazhanisamy, H. Contreras-Trujillo, T.A. Storm, Y. Lotan, A.H. Beck, B.I. Chung, A.A. Alizadeh, G. Godoy, S.P. Lerner, M. van de Rijn, L.D. Shortliffe, I.L. Weissman, and K.S. Chan, *Three differentiation states risk-stratify bladder cancer into distinct subtypes.* Proc Natl Acad Sci U S A, **2012**. 109(6): p. 2078-83.
19. CGA, *Comprehensive molecular characterization of urothelial bladder carcinoma.* Nature, **2014**. 507(7492): p. 315-22.
20. Choi, W., S. Porten, S. Kim, D. Willis, E.R. Plimack, J. Hoffman-Censits, B. Roth, T. Cheng, M. Tran, I.L. Lee, J. Melquist, J. Bondaruk, T. Majewski, S. Zhang, S. Pretzsch, K. Baggerly, A. Siefker-Radtke, B. Czerniak, C.P. Dinney, and D.J. McConkey, *Identification of distinct basal and luminal subtypes of muscle-invasive*

bladder cancer with different sensitivities to frontline chemotherapy. Cancer Cell, **2014**. 25(2): p. 152-65.

21. Damrauer, J.S., K.A. Hoadley, D.D. Chism, C. Fan, C.J. Tiganelli, S.E. Wobker, J.J. Yeh, M.I. Milowsky, G. Iyer, J.S. Parker, and W.Y. Kim, *Intrinsic subtypes of high-grade bladder cancer reflect the hallmarks of breast cancer biology.* Proc Natl Acad Sci U S A, **2014**. 111(8): p. 3110-5.
22. Rebouissou, S., I. Bernard-Pierrot, A. de Reynies, M.L. Lepage, C. Krucker, E. Chapeaublanc, A. Herault, A. Kamoun, A. Caillault, E. Letouze, N. Elarouci, Y. Neuzillet, Y. Denoux, V. Molinie, D. Vordos, A. Laplanche, P. Maille, P. Soyeux, K. Ofualuka, F. Reyal, A. Biton, M. Sibony, X. Paoletti, J. Southgate, S. Benhamou, T. Lebret, Y. Allory, and F. Radvanyi, *EGFR as a potential therapeutic target for a subset of muscle-invasive bladder cancers presenting a basal-like phenotype.* Sci Transl Med, **2014**. 6(244): p. 244ra91.
23. Lerner, S.P., D.J. McConkey, K.A. Hoadley, K.S. Chan, W.Y. Kim, F. Radvanyi, M. Hoglund, and F.X. Real, *Bladder Cancer Molecular Taxonomy: Summary from a Consensus Meeting.* Bladder Cancer, **2016**. 2(1): p. 37-47.
24. Turati, F., C. Bosetti, J. Polesel, D. Serraino, M. Montella, M. Libra, G. Facchini, M. Ferraroni, A. Tavani, C. La Vecchia, and E. Negri, *Family history of cancer and the risk of bladder cancer: A case-control study from Italy.* Cancer Epidemiol, **2017**. 48: p. 29-35.
25. van der Post, R.S., L.A. Kiemeney, M.J. Ligtenberg, J.A. Witjes, C.A. Hulsbergen-van de Kaa, D. Bodmer, L. Schaap, C.M. Kets, J.H. van Krieken, and N. Hoogerbrugge, *Risk of urothelial bladder cancer in Lynch syndrome is increased,*

in particular among MSH2 mutation carriers. J Med Genet, **2010**. 47(7): p. 464-70.

26. Yee, D.S., N.M. Ishill, W.T. Lowrance, H.W. Herr, and E.B. Elkin, *Ethnic differences in bladder cancer survival.* Urology, **2011**. 78(3): p. 544-9.

27. Freedman, N.D., D.T. Silverman, A.R. Hollenbeck, A. Schatzkin, and C.C. Abnet, *Association between smoking and risk of bladder cancer among men and women.* JAMA, **2011**. 306(7): p. 737-45.

28. van Tong, H., P.J. Brindley, C.G. Meyer, and T.P. Velavan, *Parasite Infection, Carcinogenesis and Human Malignancy.* EBioMedicine, **2017**. 15: p. 12-23.

29. Szarvas, T., P. Nyirady, T. Kobayashi, O. Ogawa, C.J. Rosser, and H. Furuya, *Urinary Protein Markers for the Detection and Prognostication of Urothelial Carcinoma.* Methods Mol Biol, **2018**. 1655: p. 251-273.

30. Balci, M., A. Tuncel, T. Keten, O. Guzel, U. Lokman, E. Koseoglu, Y. Aslan, and A. Atan, *Comparison of Monopolar and Bipolar Transurethral Resection of Non-Muscle Invasive Bladder Cancer.* Urol Int, **2017**.

31. Hahn, R.G., *The transurethral resection syndrome.* Acta Anaesthesiol Scand, **1991**. 35(7): p. 557-67.

32. Zainfeld, D. and S. Daneshmand, *Transurethral Resection of Bladder Tumors: Improving Quality Through New Techniques and Technologies.* Curr Urol Rep, **2017**. 18(5): p. 34.

33. Boehm, B.E., J.E. Cornell, H. Wang, N. Mukherjee, J.S. Oppenheimer, and R.S. Svatek, *Efficacy of Bacillus Calmette-guerin Strains for the Treatment of non-*

muscle Invasive Bladder Cancer: a Systematic Review and Network Meta-analysis. J Urol, **2017**.

34. Kamat, A.M., M. Colombel, D. Sundi, D. Lamm, A. Boehle, M. Brausi, R. Buckley, R. Persad, J. Palou, M. Soloway, and J.A. Witjes, *BCG-unresponsive non-muscle-invasive bladder cancer: recommendations from the IBCG.* Nat Rev Urol, **2017**. 14(4): p. 244-255.

35. Nguyen, D.P. and G.N. Thalmann, *Contemporary update on neoadjuvant therapy for bladder cancer.* Nat Rev Urol, **2017**.

36. Baumann, B.C., P. Sargos, L.J. Eapen, J.A. Efstathiou, A. Choudhury, A. Bahl, V. Murthy, L.K. Ballas, V. Fonteyne, P.M. Richaud, M.S. Zaghloul, and J.P. Christodouleas, *The Rationale for Post-Operative Radiation in Localized Bladder Cancer.* Bladder Cancer, **2017**. 3(1): p. 19-30.

37. Herr, H.W. and A. Morales, *History of Bacillus Calmette-Guerin and Bladder Cancer: An Immunotherapy Success Story.* The Journal of Urology, **2008**. 179(1): p. 53-56.

38. Aydin, A.M., S.L. Woldu, R.C. Hutchinson, M. Boegemann, A. Bagrodia, Y. Lotan, V. Margulis, and L.M. Krabbe, *Spotlight on atezolizumab and its potential in the treatment of advanced urothelial bladder cancer.* Onco Targets Ther, **2017**. 10: p. 1487-1502.

39. Bellmunt, J., T. Powles, and N.J. Vogelzang, *A review on the evolution of PD-1/PD-L1 immunotherapy for bladder cancer: The future is now.* Cancer Treat Rev, **2017**. 54: p. 58-67.

40. Levine, J.J., R.A. Somer, H. Hosoya, and C. Squillante, *Atezolizumab-induced Encephalitis in Metastatic Bladder Cancer: A Case Report and Review of the Literature.* Clin Genitourin Cancer, **2017**.

41. Iyer, G., H. Al-Ahmadie, N. Schultz, A.J. Hanrahan, I. Ostrovnaya, A.V. Balar, P.H. Kim, O. Lin, N. Weinhold, C. Sander, E.C. Zabor, M. Janakiraman, I.R. Garcia-Grossman, A. Heguy, A. Viale, B.H. Bochner, V.E. Reuter, D.F. Bajorin, M.I. Milowsky, B.S. Taylor, and D.B. Solit, *Prevalence and co-occurrence of actionable genomic alterations in high-grade bladder cancer.* J Clin Oncol, **2013**. 31(25): p. 3133-40.

42. Mouw, K.W., *DNA Repair Pathway Alterations in Bladder Cancer*. Cancers (Basel), **2017**. 9(4).

43. Aragon-Ching, J.B. and D.L. Trump, *Targeted therapies in the treatment of urothelial cancers.* Urol Oncol, **2017**.

44. Briscoe, J. and P.P. Therond, *The mechanisms of Hedgehog signalling and its roles in development and disease.* Nat Rev Mol Cell Biol, **2013**. 14(7): p. 416-29.

45. Ingham, P.W., Y. Nakano, and C. Seger, *Mechanisms and functions of Hedgehog signalling across the metazoa.* Nat Rev Genet, **2011**. 12(6): p. 393-406.

46. McCabe, J.M. and D.J. Leahy, *Smoothened goes molecular: new pieces in the hedgehog signaling puzzle.* J Biol Chem, **2015**. 290(6): p. 3500-7.

47. Varjosalo, M. and J. Taipale, *Hedgehog: functions and mechanisms.* Genes Dev, **2008**. 22(18): p. 2454-72.

48. McMahon, A.P., P.W. Ingham, and C.J. Tabin, *Developmental roles and clinical significance of hedgehog signaling.* Curr Top Dev Biol, **2003**. 53: p. 1-114.

49. Stecca, B. and I.A.A. Ruiz, *Context-dependent regulation of the GLI code in cancer by HEDGEHOG and non-HEDGEHOG signals.* J Mol Cell Biol, **2010**. 2(2): p. 84-95.

50. Echelard, Y., D.J. Epstein, B. St-Jacques, L. Shen, J. Mohler, J.A. McMahon, and A.P. McMahon, *Sonic hedgehog, a member of a family of putative signaling molecules, is implicated in the regulation of CNS polarity.* Cell, **1993**. 75(7): p. 1417-30.

51. Nusslein-Volhard, C. and E. Wieschaus, *Mutations affecting segment number and polarity in Drosophila.* Nature, **1980**. 287(5785): p. 795-801.

52. Riddle, R.D., R.L. Johnson, E. Laufer, and C. Tabin, *Sonic hedgehog mediates the polarizing activity of the ZPA.* Cell, **1993**. 75(7): p. 1401-16.

53. Zhang, X.M., M. Ramalho-Santos, and A.P. McMahon, *Smoothened mutants reveal redundant roles for Shh and Ihh signaling including regulation of L/R asymmetry by the mouse node.* Cell, **2001**. 105(6): p. 781-92.

54. Chuang, P.T. and A.P. McMahon, *Vertebrate Hedgehog signalling modulated by induction of a Hedgehog-binding protein.* Nature, **1999**. 397(6720): p. 617-21.

55. Briscoe, J. and J. Ericson, *Specification of neuronal fates in the ventral neural tube.* Curr Opin Neurobiol, **2001**. 11(1): p. 43-9.

56. Taipale, J., M.K. Cooper, T. Maiti, and P.A. Beachy, *Patched acts catalytically to suppress the activity of Smoothened.* Nature, **2002**. 418(6900): p. 892-7.

57. DeSouza, K.R., M. Saha, A.R. Carpenter, M. Scott, and K.M. McHugh, *Analysis of the Sonic Hedgehog signaling pathway in normal and abnormal bladder development.* PLoS One, **2013**. 8(1): p. e53675.

58. Ng, J.M. and T. Curran, *The Hedgehog's tale: developing strategies for targeting cancer.* Nat Rev Cancer, **2011**. 11(7): p. 493-501.

59. Duman-Scheel, M., L. Weng, S. Xin, and W. Du, *Hedgehog regulates cell growth and proliferation by inducing Cyclin D and Cyclin E.* Nature, **2002**. 417(6886): p. 299-304.

60. Hui, C.C. and S. Angers, *Gli proteins in development and disease.* Annu Rev Cell Dev Biol, **2011**. 27: p. 513-37.

61. Scales, S.J. and F.J. de Sauvage, *Mechanisms of Hedgehog pathway activation in cancer and implications for therapy.* Trends Pharmacol Sci, **2009**. 30(6): p. 303-12.

62. Beachy, P.A., S.S. Karhadkar, and D.M. Berman, *Tissue repair and stem cell renewal in carcinogenesis.* Nature, **2004**. 432(7015): p. 324-31.

63. Hooper, J.E. and M.P. Scott, *Communicating with Hedgehogs.* Nat Rev Mol Cell Biol, **2005**. 6(4): p. 306-17.

64. Stecca, B. and A. Ruiz i Altaba, *A GLI1-p53 inhibitory loop controls neural stem cell and tumour cell numbers.* Embo j, **2009**. 28(6): p. 663-76.

65. Shin, K., J. Lee, N. Guo, J. Kim, A. Lim, L. Qu, I.U. Mysorekar, and P.A. Beachy, *Hedgehog/Wnt feedback supports regenerative proliferation of epithelial stem cells in bladder.* Nature, **2011**. 472(7341): p. 110-4.

66. Corcoran, R.B. and M.P. Scott, *Oxysterols stimulate Sonic hedgehog signal transduction and proliferation of medulloblastoma cells.* Proc Natl Acad Sci U S A, **2006**. 103(22): p. 8408-13.

67. Bijlsma, M.F., C.A. Spek, D. Zivkovic, S. van de Water, F. Rezaee, and M.P. Peppelenbosch, *Repression of smoothened by patched-dependent (pro-)vitamin D3 secretion.* PLoS Biol, **2006**. 4(8): p. e232.

68. Kogerman, P., T. Grimm, L. Kogerman, D. Krause, A.B. Unden, B. Sandstedt, R. Toftgard, and P.G. Zaphiropoulos, *Mammalian suppressor-of-fused modulates nuclear-cytoplasmic shuttling of Gli-1.* Nat Cell Biol, **1999**. 1(5): p. 312-9.

69. Mo, R., A.M. Freer, D.L. Zinyk, M.A. Crackower, J. Michaud, H.H. Heng, K.W. Chik, X.M. Shi, L.C. Tsui, S.H. Cheng, A.L. Joyner, and C. Hui, *Specific and redundant functions of Gli2 and Gli3 zinc finger genes in skeletal patterning and development.* Development, **1997**. 124(1): p. 113-23.

70. Park, H.L., C. Bai, K.A. Platt, M.P. Matise, A. Beeghly, C.C. Hui, M. Nakashima, and A.L. Joyner, *Mouse Gli1 mutants are viable but have defects in SHH signaling in combination with a Gli2 mutation.* Development, **2000**. 127(8): p. 1593-605.

71. Wang, B. and Y. Li, *Evidence for the direct involvement of {beta}TrCP in Gli3 protein processing.* Proc Natl Acad Sci U S A, **2006**. 103(1): p. 33-8.

72. Barnes, E.A., K.J. Heidtman, and D.J. Donoghue, *Constitutive activation of the shh-ptc1 pathway by a patched1 mutation identified in BCC.* Oncogene, **2005**. 24(5): p. 902-15.

73. Yam, P.T., S.D. Langlois, S. Morin, and F. Charron, *Sonic hedgehog guides axons through a noncanonical, Src-family-kinase-dependent signaling pathway.* Neuron, **2009**. 62(3): p. 349-62.

74. Polizio, A.H., P. Chinchilla, X. Chen, D.R. Manning, and N.A. Riobo, *Sonic Hedgehog activates the GTPases Rac1 and RhoA in a Gli-independent manner through coupling of smoothened to Gi proteins.* Sci Signal, **2011**. 4(200): p. pt7.

75. Mille, F., C. Thibert, J. Fombonne, N. Rama, C. Guix, H. Hayashi, V. Corset, J.C. Reed, and P. Mehlen, *The Patched dependence receptor triggers apoptosis through a DRAL-caspase-9 complex.* Nat Cell Biol, **2009**. 11(6): p. 739-46.

76. Varjosalo, M. and J. Taipale, *Hedgehog signaling.* J Cell Sci, **2007**. 120(Pt 1): p. 3-6.

77. Deng, W., D.B. Vanderbilt, C.C. Lin, K.H. Martin, K.M. Brundage, and J.M. Ruppert, *SOX9 inhibits beta-TrCP-mediated protein degradation to promote nuclear GLI1 expression and cancer stem cell properties.* J Cell Sci, **2015**. 128(6): p. 1123-38.

78. Ke, Z., S. Caiping, Z. Qing, and W. Xiaojing, *Sonic hedgehog-Gli1 signals promote epithelial-mesenchymal transition in ovarian cancer by mediating PI3K/AKT pathway.* Med Oncol, **2015**. 32(1): p. 368.

79. Rajurkar, M., W.E. De Jesus-Monge, D.R. Driscoll, V.A. Appleman, H. Huang, J.L. Cotton, D.S. Klimstra, L.J. Zhu, K. Simin, L. Xu, A.P. McMahon, B.C. Lewis, and J. Mao, *The activity of Gli transcription factors is essential for Kras-induced pancreatic tumorigenesis.* Proc Natl Acad Sci U S A, **2012**. 109(17): p. E1038-47.

80. Yoon, J.W., M. Lamm, S. Iannaccone, N. Higashiyama, K.F. Leong, P. Iannaccone, and D. Walterhouse, *p53 modulates the activity of the GLI1 oncogene through interactions with the shared coactivator TAF9.* DNA Repair (Amst), **2015**. 34: p. 9-17.

81. Teglund, S. and R. Toftgard, *Hedgehog beyond medulloblastoma and basal cell carcinoma.* Biochim Biophys Acta, **2010**. 1805(2): p. 181-208.

82. Gupta, S., N. Takebe, and P. Lorusso, *Targeting the Hedgehog pathway in cancer.* Ther Adv Med Oncol, **2010**. 2(4): p. 237-50.

83. Yauch, R.L., S.E. Gould, S.J. Scales, T. Tang, H. Tian, C.P. Ahn, D. Marshall, L. Fu, T. Januario, D. Kallop, M. Nannini-Pepe, K. Kotkow, J.C. Marsters, L.L. Rubin, and F.J. de Sauvage, *A paracrine requirement for hedgehog signalling in cancer.* Nature, **2008**. 455(7211): p. 406-10.

84. Theunissen, J.W. and F.J. de Sauvage, *Paracrine Hedgehog signaling in cancer.* Cancer Res, **2009**. 69(15): p. 6007-10.

85. Reya, T., S.J. Morrison, M.F. Clarke, and I.L. Weissman, *Stem cells, cancer, and cancer stem cells.* Nature, **2001**. 414(6859): p. 105-11.

86. Rubin, L.L. and F.J. de Sauvage, *Targeting the Hedgehog pathway in cancer.* Nat Rev Drug Discov, **2006**. 5(12): p. 1026-33.

87. Varnat, F., A. Duquet, M. Malerba, M. Zbinden, C. Mas, P. Gervaz, and A. Ruiz i Altaba, *Human colon cancer epithelial cells harbour active HEDGEHOG-GLI signalling that is essential for tumour growth, recurrence, metastasis and stem cell survival and expansion.* EMBO Mol Med, **2009**. 1(6-7): p. 338-51.

88. Rasheed, Z.A., J. Yang, Q. Wang, J. Kowalski, I. Freed, C. Murter, S.M. Hong, J.B. Koorstra, N.V. Rajeshkumar, X. He, M. Goggins, C. Iacobuzio-Donahue, D.M. Berman, D. Laheru, A. Jimeno, M. Hidalgo, A. Maitra, and W. Matsui, *Prognostic significance of tumorigenic cells with mesenchymal features in pancreatic adenocarcinoma.* J Natl Cancer Inst, **2010**. 102(5): p. 340-51.

89. Chen, Y.J., J. Sims-Mourtada, J. Izzo, and K.S. Chao, *Targeting the hedgehog pathway to mitigate treatment resistance.* Cell Cycle, **2007**. 6(15): p. 1826-30.

90. Sims-Mourtada, J., J.G. Izzo, J. Ajani, and K.S. Chao, *Sonic Hedgehog promotes multiple drug resistance by regulation of drug transport.* Oncogene, **2007**. 26(38): p. 5674-9.

91. Feldmann, G., S. Dhara, V. Fendrich, D. Bedja, R. Beaty, M. Mullendore, C. Karikari, H. Alvarez, C. Iacobuzio-Donahue, A. Jimeno, K.L. Gabrielson, W. Matsui, and A. Maitra, *Blockade of hedgehog signaling inhibits pancreatic cancer invasion and metastases: a new paradigm for combination therapy in solid cancers.* Cancer Res, **2007**. 67(5): p. 2187-96.

92. Karhadkar, S.S., G.S. Bova, N. Abdallah, S. Dhara, D. Gardner, A. Maitra, J.T. Isaacs, D.M. Berman, and P.A. Beachy, *Hedgehog signalling in prostate regeneration, neoplasia and metastasis.* Nature, **2004**. 431(7009): p. 707-12.

93. Syed, I.S., A. Pedram, and W.A. Farhat, *Role of Sonic Hedgehog (Shh) Signaling in Bladder Cancer Stemness and Tumorigenesis.* Curr Urol Rep, **2016**. 17(2): p. 11.

94. Cooper, M.K., J.A. Porter, K.E. Young, and P.A. Beachy, *Teratogen-mediated inhibition of target tissue response to Shh signaling.* Science, **1998**. 280(5369): p. 1603-7.

95. Robarge, K.D., S.A. Brunton, G.M. Castanedo, Y. Cui, M.S. Dina, R. Goldsmith, S.E. Gould, O. Guichert, J.L. Gunzner, J. Halladay, W. Jia, C. Khojasteh, M.F. Koehler, K. Kotkow, H. La, R.L. Lalonde, K. Lau, L. Lee, D. Marshall, J.C. Marsters, Jr., L.J. Murray, C. Qian, L.L. Rubin, L. Salphati, M.S. Stanley, J.H. Stibbard, D.P. Sutherlin, S. Ubhayaker, S. Wang, S. Wong, and M. Xie, *GDC-*

0449-a potent inhibitor of the hedgehog pathway. Bioorg Med Chem Lett, **2009**. 19(19): p. 5576-81.

96. Pan, S., X. Wu, J. Jiang, W. Gao, Y. Wan, D. Cheng, D. Han, J. Liu, N.P. Englund, Y. Wang, S. Peukert, K. Miller-Moslin, J. Yuan, R. Guo, M. Matsumoto, A. Vattay, Y. Jiang, J. Tsao, F. Sun, A.C. Pferdekamper, S. Dodd, T. Tuntland, W. Maniara, J.F. Kelleher, 3rd, Y.M. Yao, M. Warmuth, J. Williams, and M. Dorsch, *Discovery of NVP-LDE225, a Potent and Selective Smoothened Antagonist.* ACS Med Chem Lett, **2010**. 1(3): p. 130-4.

97. List, A., M. Beran, J. DiPersio, J. Slack, N. Vey, C.S. Rosenfeld, and P. Greenberg, *Opportunities for Trisenox (arsenic trioxide) in the treatment of myelodysplastic syndromes.* Leukemia, **2003**. 17(8): p. 1499-507.

98. Khatra, H., C. Bose, and S. Sinha, *Discovery of Hedgehog Antagonists for Cancer Therapy.* Curr Med Chem, **2017**. 24(19): p. 2033-2058.

99. Tang, S.N., J. Fu, D. Nall, M. Rodova, S. Shankar, and R.K. Srivastava, *Inhibition of sonic hedgehog pathway and pluripotency maintaining factors regulate human pancreatic cancer stem cell characteristics.* Int J Cancer, **2012**. 131(1): p. 30-40.

100. Kelley, R.I. and R.C. Hennekam, *The Smith-Lemli-Opitz syndrome.* J Med Genet, **2000**. 37(5): p. 321-35.

101. Dubourg, C., L. Lazaro, L. Pasquier, C. Bendavid, M. Blayau, F. Le Duff, M.R. Durou, S. Odent, and V. David, *Molecular screening of SHH, ZIC2, SIX3, and TGIF genes in patients with features of holoprosencephaly spectrum: Mutation review and genotype-phenotype correlations.* Hum Mutat, **2004**. 24(1): p. 43-51.

102. Johnston, J.J., I. Olivos-Glander, C. Killoran, E. Elson, J.T. Turner, K.F. Peters, M.H. Abbott, D.J. Aughton, A.S. Aylsworth, M.J. Bamshad, C. Booth, C.J. Curry, A. David, M.B. Dinulos, D.B. Flannery, M.A. Fox, J.M. Graham, D.K. Grange, A.E. Guttmacher, M.C. Hannibal, W. Henn, R.C. Hennekam, L.B. Holmes, H.E. Hoyme, K.A. Leppig, A.E. Lin, P. Macleod, D.K. Manchester, C. Marcelis, L. Mazzanti, E. McCann, M.T. McDonald, N.J. Mendelsohn, J.B. Moeschler, B. Moghaddam, G. Neri, R. Newbury-Ecob, R.A. Pagon, J.A. Phillips, L.S. Sadler, J.M. Stoler, D. Tilstra, C.M. Walsh Vockley, E.H. Zackai, T.M. Zadeh, L. Brueton, G.C. Black, and L.G. Biesecker, *Molecular and clinical analyses of Greig cephalopolysyndactyly and Pallister-Hall syndromes: robust phenotype prediction from the type and position of GLI3 mutations.* Am J Hum Genet, **2005**. 76(4): p. 609-22.

103. Shiroyanagi, Y., B. Liu, M. Cao, K. Agras, J. Li, M.H. Hsieh, E.J. Willingham, and L.S. Baskin, *Urothelial sonic hedgehog signaling plays an important role in bladder smooth muscle formation.* Differentiation, **2007**. 75(10): p. 968-77.

104. Jenkins, D., P.J. Winyard, and A.S. Woolf, *Immunohistochemical analysis of Sonic hedgehog signalling in normal human urinary tract development.* J Anat, **2007**. 211(5): p. 620-9.

105. Cheng, W., C.K. Yeung, Y.K. Ng, J.R. Zhang, C.C. Hui, and P.C. Kim, *Sonic Hedgehog mediator Gli2 regulates bladder mesenchymal patterning.* J Urol, **2008**. 180(4): p. 1543-50.

106. Haraguchi, R., D. Matsumaru, N. Nakagata, S. Miyagawa, K. Suzuki, S. Kitazawa, and G. Yamada, *The hedgehog signal induced modulation of bone morphogenetic*

protein signaling: an essential signaling relay for urinary tract morphogenesis. PLoS One, **2012**. 7(7): p. e42245.

107. Haraguchi, R., J. Motoyama, H. Sasaki, Y. Satoh, S. Miyagawa, N. Nakagata, A. Moon, and G. Yamada, *Molecular analysis of coordinated bladder and urogenital organ formation by Hedgehog signaling.* Development, **2007**. 134(3): p. 525-33.

108. Linnenbach, A.J., L.B. Pressler, B.A. Seng, B.S. Kimmel, J.E. Tomaszewski, and S.B. Malkowicz, *Characterization of chromosome 9 deletions in transitional cell carcinoma by microsatellite assay.* Hum Mol Genet, **1993**. 2(9): p. 1407-11.

109. Hamed, S., H. LaRue, H. Hovington, J. Girard, L. Jeannotte, E. Latulippe, and Y. Fradet, *Accelerated induction of bladder cancer in patched heterozygous mutant mice.* Cancer Res, **2004**. 64(6): p. 1938-42.

110. Thievessen, I., M. Wolter, A. Prior, H.H. Seifert, and W.A. Schulz, *Hedgehog signaling in normal urothelial cells and in urothelial carcinoma cell lines.* J Cell Physiol, **2005**. 203(2): p. 372-7.

111. Mechlin, C.W., M.J. Tanner, M. Chen, R. Buttyan, R.M. Levin, and B.M. Mian, *Gli2 expression and human bladder transitional carcinoma cell invasiveness.* J Urol, **2010**. 184(1): p. 344-51.

112. Fei, D.L., H. Li, C.D. Kozul, K.E. Black, S. Singh, J.A. Gosse, J. DiRenzo, K.A. Martin, B. Wang, J.W. Hamilton, M.R. Karagas, and D.J. Robbins, *Activation of Hedgehog signaling by the environmental toxicant arsenic may contribute to the etiology of arsenic-induced tumors.* Cancer Res, **2010**. 70(5): p. 1981-8.

113. Chen, M., M.A. Hildebrandt, J. Clague, A.M. Kamat, A. Picornell, J. Chang, X. Zhang, J. Izzo, H. Yang, J. Lin, J. Gu, S. Chanock, M. Kogevinas, N. Rothman,

D.T. Silverman, M. Garcia-Closas, H.B. Grossman, C.P. Dinney, N. Malats, and X. Wu, *Genetic variations in the sonic hedgehog pathway affect clinical outcomes in non-muscle-invasive bladder cancer.* Cancer Prev Res (Phila), **2010**. 3(10): p. 1235-45.

114. He, H.C., J.H. Chen, X.B. Chen, G.Q. Qin, C. Cai, Y.X. Liang, Z.D. Han, Q.S. Dai, Y.R. Chen, G.H. Zeng, J.G. Zhu, F.N. Jiang, and W.D. Zhong, *Expression of hedgehog pathway components is associated with bladder cancer progression and clinical outcome.* Pathol Oncol Res, **2012**. 18(2): p. 349-55.

115. Islam, S.S., R.B. Mokhtari, A.S. Noman, M. Uddin, M.Z. Rahman, M.A. Azadi, A. Zlotta, T. van der Kwast, H. Yeger, and W.A. Farhat, *Sonic hedgehog (Shh) signaling promotes tumorigenicity and stemness via activation of epithelial-to-mesenchymal transition (EMT) in bladder cancer.* Mol Carcinog, **2016**. 55(5): p. 537-51.

116. Shin, K., A. Lim, J.I. Odegaard, J.D. Honeycutt, S. Kawano, M.H. Hsieh, and P.A. Beachy, *Cellular origin of bladder neoplasia and tissue dynamics of its progression to invasive carcinoma.* Nat Cell Biol, **2014**. 16(5): p. 469-78.

117. Shin, K., A. Lim, C. Zhao, D. Sahoo, Y. Pan, E. Spiekerkoetter, J.C. Liao, and P.A. Beachy, *Hedgehog signaling restrains bladder cancer progression by eliciting stromal production of urothelial differentiation factors.* Cancer Cell, **2014**. 26(4): p. 521-33.

118. Seiler, R., H.Z. Oo, D. Tortora, T.M. Clausen, C.K. Wang, G. Kumar, M.A. Pereira, M.S. Orum-Madsen, M.O. Agerbaek, T. Gustavsson, M.A. Nordmaj, J.R. Rich, N. Lallous, L. Fazli, S.S. Lee, J. Douglas, T. Todenhofer, S. Esfandnia, D. Battsogt,

J.S. Babcook, N. Al-Nakouzi, S.J. Crabb, I. Moskalev, B. Kiss, E. Davicioni, G.N. Thalmann, P.S. Rennie, P.C. Black, A. Salanti, and M. Daugaard, *An Oncofetal Glycosaminoglycan Modification Provides Therapeutic Access to Cisplatin-resistant Bladder Cancer.* Eur Urol, **2017**. 72(1): p. 142-150.

119. Pipas, J.M., *SV40: Cell transformation and tumorigenesis.* Virology, **2009**. 384(2): p. 294-303.

120. Bangs, F. and K.V. Anderson, *Primary Cilia and Mammalian Hedgehog Signaling.* Cold Spring Harb Perspect Biol, **2017**. 9(5).

121. Goto, H., H. Inaba, and M. Inagaki, *Mechanisms of ciliogenesis suppression in dividing cells.* Cell Mol Life Sci, **2017**. 74(5): p. 881-890.

122. Yasar, B., K. Linton, C. Slater, and R. Byers, *Primary cilia are increased in number and demonstrate structural abnormalities in human cancer.* J Clin Pathol, **2016**.

123. Gerhardt, C., T. Leu, J.M. Lier, and U. Ruther, *The cilia-regulated proteasome and its role in the development of ciliopathies and cancer.* Cilia, **2016**. 5: p. 14.

124. So, A., P. Rocchi, and M. Gleave, *Antisense oligonucleotide therapy in the management of bladder cancer.* Curr Opin Urol, **2005**. 15(5): p. 320-7.

125. Masetti, R., S.N. Bertuccio, A. Astolfi, F. Chiarini, A. Lonetti, V. Indio, M. De Luca, J. Bandini, S. Serravalle, M. Franzoni, M. Pigazzi, A.M. Martelli, G. Basso, F. Locatelli, and A. Pession, *Hh/Gli antagonist in acute myeloid leukemia with CBFA2T3-GLIS2 fusion gene.* J Hematol Oncol, **2017**. 10(1): p. 26.

126. Ding, J., X.T. Zhou, H.Y. Zou, and J. Wu, *Hedgehog signaling pathway affects the sensitivity of hepatoma cells to drug therapy through the ABCC1 transporter.* Lab Invest, **2017**. 97(7): p. 819-832.

127. Yang, H., L. Hu, Z. Liu, Y. Qin, R. Li, G. Zhang, B. Zhao, C. Bi, Y. Lei, and Y. Bai, *Inhibition of Gli1-mediated prostate cancer cell proliferation by inhibiting the mTOR/S6K1 signaling pathway.* Oncol Lett, **2017**. 14(6): p. 7970-7976.

128. Ishiwata, T., S. Iwasawa, T. Ebata, M. Fan, Y. Tada, K. Tatsumi, and Y. Takiguchi, *Inhibition of Gli leads to antitumor growth and enhancement of cisplatin-induced cytotoxicity in large cell neuroendocrine carcinoma of the lung.* Oncol Rep, **2018**.

129. Tang, C.M., T.E. Lee, S.A. Syed, A.M. Burgoyne, S.Y. Leonard, F. Gao, J.C. Chan, E. Shi, J. Chmielecki, D. Morosini, K. Wang, J.S. Ross, M.L. Kendrick, M.R. Bardsley, M. Siena, J. Mao, O. Harismendy, T. Ordog, and J.K. Sicklick, *Hedgehog pathway dysregulation contributes to the pathogenesis of human gastrointestinal stromal tumors via GLI-mediated activation of KIT expression.* Oncotarget, **2016**. 7(48): p. 78226-78241.

130. Du, Z., F. Zhou, Z. Jia, B. Zheng, S. Han, J. Cheng, G. Zhu, and P. Huang, *The hedgehog/Gli-1 signaling pathways is involved in the inhibitory effect of resveratrol on human colorectal cancer HCT116 cells.* Iran J Basic Med Sci, **2016**. 19(11): p. 1171-1176.

131. Song, L., W. Wang, D. Liu, Y. Zhao, J. He, X. Wang, Z. Dai, H. Zhang, and X. Li, *Targeting of sonic hedgehog-Gli signaling: A potential therapeutic target for patients with breast cancer.* Oncol Lett, **2016**. 12(2): p. 1027-1033.

132. Vlckova, K., J. Reda, L. Ondrusova, M. Krayem, G. Ghanem, and J. Vachtenheim, *GLI inhibitor GANT61 kills melanoma cells and acts in synergy with obatoclax.* Int J Oncol, **2016**. 49(3): p. 953-60.

133. Arnhold, V., J. Boos, and C. Lanvers-Kaminsky, *Targeting hedgehog signaling pathway in pediatric tumors: in vitro evaluation of SMO and GLI inhibitors.* Cancer Chemother Pharmacol, **2016**. 77(3): p. 495-505.

134. Hagedorn, P.H., B.R. Hansen, T. Koch, and M. Lindow, *Managing the sequence-specificity of antisense oligonucleotides in drug discovery.* Nucleic Acids Res, **2017**. 45(5): p. 2262-2282.

135. Robertson, A.G., J. Kim, H. Al-Ahmadie, J. Bellmunt, G. Guo, A.D. Cherniack, T. Hinoue, P.W. Laird, K.A. Hoadley, R. Akbani, M.A.A. Castro, E.A. Gibb, R.S. Kanchi, D.A. Gordenin, S.A. Shukla, F. Sanchez-Vega, D.E. Hansel, B.A. Czerniak, V.E. Reuter, X. Su, B. de Sa Carvalho, V.S. Chagas, K.L. Mungall, S. Sadeghi, C.S. Pedamallu, Y. Lu, L.J. Klimczak, J. Zhang, C. Choo, A.I. Ojesina, S. Bullman, K.M. Leraas, T.M. Lichtenberg, C.J. Wu, N. Schultz, G. Getz, M. Meyerson, G.B. Mills, D.J. McConkey, J.N. Weinstein, D.J. Kwiatkowski, and S.P. Lerner, *Comprehensive Molecular Characterization of Muscle-Invasive Bladder Cancer.* Cell, **2017**. 171(3): p. 540-556.e25.

136. *Canadian Cancer Society's Advisory Committee on Cancer Statistics. Canadian Cancer Statistics.* p. 2016.

137. Schenk-Braat, E.A. and C.H. Bangma, *Immunotherapy for superficial bladder cancer.* Cancer Immunol Immunother, **2005**. 54(5): p. 414-23.

138. Vargo-Gogola, T. and J.M. Rosen, *Modelling breast cancer: one size does not fit all.* Nat Rev Cancer, **2007**. 7(9): p. 659-72.

139. Amstrong, E. and G. Bonser, *Epithelial tumors of the urinary bladder in mice induced by 2-acetylamino-fluorine.* Journal of Pathology, **1944**. 6: p. 506-512.

140. Lijinsky, W., *Species differences in nitrosamine carcinogenesis.* J Cancer Res Clin Oncol, **1984**. 108(1): p. 46-55.

141. Steinberg, G.D., C.B. Brendler, T. Ichikawa, R.A. Squire, and J.T. Isaacs, *Characterization of an N-methyl-N-nitrosourea-induced autochthonous rat bladder cancer model.* Cancer Res, **1990**. 50(20): p. 6668-74.

142. Arantes-Rodrigues, R., A. Colaco, R. Pinto-Leite, and P.A. Oliveira, *In vitro and in vivo experimental models as tools to investigate the efficacy of antineoplastic drugs on urinary bladder cancer.* Anticancer Res, **2013**. 33(4): p. 1273-96.

143. Rosenberg, M.P. and D. Bortner, *Why transgenic and knockout animal models should be used (for drug efficacy studies in cancer).* Cancer Metastasis Rev, **1998**. 17(3): p. 295-9.

144. Thomas, H. and F. Balkwill, *Assessing new anti-tumour agents and strategies in oncogene transgenic mice.* Cancer Metastasis Rev, **1995**. 14(2): p. 91-5.

145. Chan, E., A. Patel, W. Heston, and W. Larchian, *Mouse orthotopic models for bladder cancer research.* BJU Int, **2009**. 104(9): p. 1286-91.

146. Kubota, T., *Metastatic models of human cancer xenografted in the nude mouse: the importance of orthotopic transplantation.* J Cell Biochem, **1994**. 56(1): p. 4-8.

147. Jager, W., Y. Horiguchi, J. Shah, T. Hayashi, S. Awrey, K.M. Gust, B.A. Hadaschik, Y. Matsui, S. Anderson, R.H. Bell, S. Ettinger, A.I. So, M.E. Gleave, I.L. Lee, C.P. Dinney, M. Tachibana, D.J. McConkey, and P.C. Black, *Hiding in plain view: genetic profiling reveals decades old cross contamination of bladder cancer cell line KU7 with HeLa.* J Urol, **2013**. 190(4): p. 1404-9.

148. Livak, K.J. and T.D. Schmittgen, *Analysis of relative gene expression data using real-time quantitative PCR and the 2(-Delta Delta C(T)) Method.* Methods, **2001**. 25(4): p. 402-8.

149. Jager, W., I. Moskalev, C. Janssen, T. Hayashi, K.M. Gust, S. Awrey, and P.C. Black, *Minimally invasive establishment of murine orthotopic bladder xenografts.* J Vis Exp, **2014**(84): p. e51123.

150. Black, P.C., A. Shetty, G.A. Brown, E. Esparza-Coss, A.R. Metwalli, P.K. Agarwal, D.J. McConkey, J.D. Hazle, and C.P. Dinney, *Validating bladder cancer xenograft bioluminescence with magnetic resonance imaging: the significance of hypoxia and necrosis.* BJU Int, **2010**. 106(11): p. 1799-804.

151. Mangsbo, S.M., C. Ninalga, M. Essand, A. Loskog, and T.H. Totterman, *CpG therapy is superior to BCG in an orthotopic bladder cancer model and generates CD4+ T-cell immunity.* J Immunother, **2008**. 31(1): p. 34-42.

152. Chala, B., M.H. Choi, K.C. Moon, H.S. Kim, C. Kwak, and S.T. Hong, *Development of Urinary Bladder Pre-Neoplasia by Schistosoma haematobium Eggs and Chemical Carcinogen in Mice.* Korean J Parasitol, **2017**. 55(1): p. 21-29.

153. Saito, B., *[A study of BBN induced bladder cancer in mice. The time differences in changes of histopathology and nuclear DNA content].* Nihon Hinyokika Gakkai Zasshi, **1991**. 82(8): p. 1206-10.

154. Dobek, G.L. and W.T. Godbey, *An orthotopic model of murine bladder cancer.* J Vis Exp, **2011**(48).

155. Lin, T., A. Yuan, X. Zhao, H. Lian, J. Zhuang, W. Chen, Q. Zhang, G. Liu, S. Zhang, W. Chen, W. Cao, C. Zhang, J. Wu, Y. Hu, and H. Guo, *Self-assembled*

tumor-targeting hyaluronic acid nanoparticles for photothermal ablation in orthotopic bladder cancer. Acta Biomater, **2017**.

156. Seo, H.K., S.P. Shin, N.R. Jung, W.A. Kwon, K.C. Jeong, and S.J. Lee, *The establishment of a growth-controllable orthotopic bladder cancer model through the down-regulation of c-myc expression.* Oncotarget, **2016**.

157. Horiguchi, Y., W.A. Larchian, R. Kaplinsky, W.R. Fair, and W.D. Heston, *Intravesical liposome-mediated interleukin-2 gene therapy in orthotopic murine bladder cancer model.* Gene Ther, **2000**. 7(10): p. 844-51.

158. Nakamura, T., M. Fukiage, Y. Suzuki, I. Yano, J. Miyazaki, H. Nishiyama, H. Akaza, and H. Harashima, *Mechanism responsible for the antitumor effect of BCG-CWS using the LEEL method in a mouse bladder cancer model.* J Control Release, **2014**. 196: p. 161-7.

159. Fazel, J., S. Rotzer, C. Seidl, B. Feuerecker, M. Autenrieth, G. Weirich, F. Bruchertseifer, A. Morgenstern, and R. Senekowitsch-Schmidtke, *Fractionated intravesical radioimmunotherapy with (213)Bi-anti-EGFR-MAb is effective without toxic side-effects in a nude mouse model of advanced human bladder carcinoma.* Cancer Biol Ther, **2015**. 16(10): p. 1526-34.

160. Yang, X.H., L.S. Ren, G.P. Wang, L.L. Zhao, H. Zhang, Z.G. Mi, and X. Bai, *A new method of establishing orthotopic bladder transplantable tumor in mice.* Cancer Biol Med, **2012**. 9(4): p. 261-5.

161. Cui, M., J.L. Au, M.G. Wientjes, M.A. O'Donnell, K.R. Loughlin, and Z. Lu, *Intravenous siRNA Silencing of Survivin Enhances Activity of Mitomycin C in Human Bladder RT4 Xenografts.* J Urol, **2015**. 194(1): p. 230-7.

162. Liu, Z., N.N. Yokoyama, C.A. Blair, X. Li, D. Avizonis, X.R. Wu, E. Uchio, R. Youssef, M. McClelland, M. Pollak, and X. Zi, *High Sensitivity of an Ha-RAS Transgenic Model of Superficial Bladder Cancer to Metformin Is Associated with approximately 240-Fold Higher Drug Concentration in Urine than Serum.* Mol Cancer Ther, **2016**. 15(3): p. 430-8.

163. Gong, Z., H. Xu, Y. Su, W. Wu, L. Hao, and C. Han, *Establishment of a Novel Bladder Cancer Xenograft Model in Humanized Immunodeficient Mice.* Cell Physiol Biochem, **2015**. 37(4): p. 1355-68.

164. John, B.A., T. Xu, S. Ripp, and H.R. Wang, *A Real-Time Non-invasive Auto-bioluminescent Urinary Bladder Cancer Xenograft Model.* Mol Imaging Biol, **2017**. 19(1): p. 10-14.

165. Yang, R., M. Liu, H. Liang, S. Guo, X. Guo, M. Yuan, H. Lian, X. Yan, S. Zhang, X. Chen, F. Fang, H. Guo, and C. Zhang, *miR-138-5p contributes to cell proliferation and invasion by targeting Survivin in bladder cancer cells.* Mol Cancer, **2016**. 15(1): p. 82.

166. Wan, W., K. Peng, M. Li, L. Qin, Z. Tong, J. Yan, B. Shen, and C. Yu, *Histone demethylase JMJD1A promotes urinary bladder cancer progression by enhancing glycolysis through coactivation of hypoxia inducible factor 1alpha.* Oncogene, **2017**.

167. Cui, X., D. Shen, C. Kong, Z. Zhang, Y. Zeng, X. Lin, and X. Liu, *NF-kappaB suppresses apoptosis and promotes bladder cancer cell proliferation by upregulating survivin expression in vitro and in vivo.* Sci Rep, **2017**. 7: p. 40723.

168. Madka, V., A. Mohammed, Q. Li, Y. Zhang, G. Kumar, S. Lightfoot, X. Wu, V. Steele, L. Kopelovich, and C.V. Rao, *TP53 modulating agent, CP-31398 enhances antitumor effects of ODC inhibitor in mouse model of urinary bladder transitional cell carcinoma.* Am J Cancer Res, **2015**. 5(10): p. 3030-41.

169. Santos, M., M. Martinez-Fernandez, M. Duenas, R. Garcia-Escudero, B. Alfaya, F. Villacampa, C. Saiz-Ladera, C. Costa, M. Oteo, J. Duarte, V. Martinez, M.J. Gomez-Rodriguez, M.L. Martin, M. Fernandez, P. Viatour, M.A. Morcillo, J. Sage, D. Castellano, J.L. Rodriguez-Peralto, F. de la Rosa, and J.M. Paramio, *In vivo disruption of an Rb-E2F-Ezh2 signaling loop causes bladder cancer.* Cancer Res, **2014**. 74(22): p. 6565-77.

170. Watanabe, T., N. Shinohara, A. Sazawa, T. Harabayashi, Y. Ogiso, T. Koyanagi, M. Takiguchi, A. Hashimoto, N. Kuzumaki, M. Yamashita, M. Tanaka, H.B. Grossman, and W.F. Benedict, *An improved intravesical model using human bladder cancer cell lines to optimize gene and other therapies.* Cancer Gene Ther, **2000**. 7(12): p. 1575-80.

171. Kang, M.R., G. Yang, K. Charisse, H. Epstein-Barash, M. Manoharan, and L.C. Li, *An orthotopic bladder tumor model and the evaluation of intravesical saRNA treatment.* J Vis Exp, **2012**(65).

172. Yu, D.S., C.F. Lee, and S.Y. Chang, *Immunotherapy for orthotopic murine bladder cancer using bacillus Calmette-Guerin recombinant protein Mpt-64.* J Urol, **2007**. 177(2): p. 738-42.

173. DeGraff, D.J., V.L. Robinson, J.B. Shah, W.D. Brandt, G. Sonpavde, Y. Kang, M. Liebert, X.R. Wu, and J.A. Taylor, 3rd, *Current preclinical models for the*

advancement of translational bladder cancer research. Mol Cancer Ther, **2013**. 12(2): p. 121-30.

174. Jager, W., I. Moskalev, P. Raven, A. Goriki, S. Bidnur, and P.C. Black, *Orthotopic Mouse Models of Urothelial Cancer.* Methods Mol Biol, **2018**. 1655: p. 177-197.

175. Zhu, J. and S. Mackem, *John Saunders' ZPA, Sonic hedgehog and digit identity - How does it really all work?* Dev Biol, **2017**. 429(2): p. 391-400.

176. Shigemura, K. and M. Fujisawa, *Hedgehog signaling and urological cancers.* Curr Drug Targets, **2015**. 16(3): p. 258-71.

177. Zhang, L.C., X. Jin, Z. Huang, Z.N. Yan, P.B. Li, R.F. Duan, H. Feng, J.H. Jiang, H. Peng, and W. Liu, *Protective effects of choline against hypoxia-induced injuries of vessels and endothelial cells.* Exp Ther Med, **2017**. 13(5): p. 2316-2324.

178. Vishnoi, K., S. Mahata, A. Tyagi, A. Pandey, G. Verma, M. Jadli, T. Singh, S.M. Singh, and A.C. Bharti, *Cross-talk between Human Papillomavirus Oncoproteins and Hedgehog Signaling Synergistically Promotes Stemness in Cervical Cancer Cells.* Sci Rep, **2016**. 6: p. 34377.

179. Juliano, R.L., *The delivery of therapeutic oligonucleotides.* Nucleic Acids Res, **2016**. 44(14): p. 6518-48.

180. Mahato, R.I., *Biomaterials for delivery and targeting of proteins and nucleic acids*. 2004: CRC Press.

181. Inoue, T., N. Terada, T. Kobayashi, and O. Ogawa, *Patient-derived xenografts as in vivo models for research in urological malignancies.* Nat Rev Urol, **2017**. 14(5): p. 267-283.